

Supporting information

Direct transformation of coumarins into orange-red emitting rhodols

Kateryna V. Vygranenko,^a Yevgen M. Poronik,^a Manon H. E. Bousquet,^b Olena Vakuliuk,^a Denis Jacquemin^{*b} and Daniel T. Gryko^{*a}

- a. Institute of Organic Chemistry, Polish Academy of Sciences, Kasprzaka 44/52, 01-224 Warsaw, Poland.
E-mail: dtgryko@icho.edu.pl.
- b. CEISAM Lab—UMR 6230, CNRS, University of Nantes, Nantes, France. E-mail : Denis.Jacquemin@univ-nantes.fr

Table of Contents

Instrumentation and Materials	S1
Optimization of reaction conditions for the rhodol synthesis	S2
Experimental Part.....	S5
¹ H and ¹³ C NMR Spectra	S20
X-Ray data for compounds 12 and 13	S48
Absorption and emission spectra of compounds 4-13	S71
Photostability measurements	S74
Theoretical methods	S76
Notes and references	S79

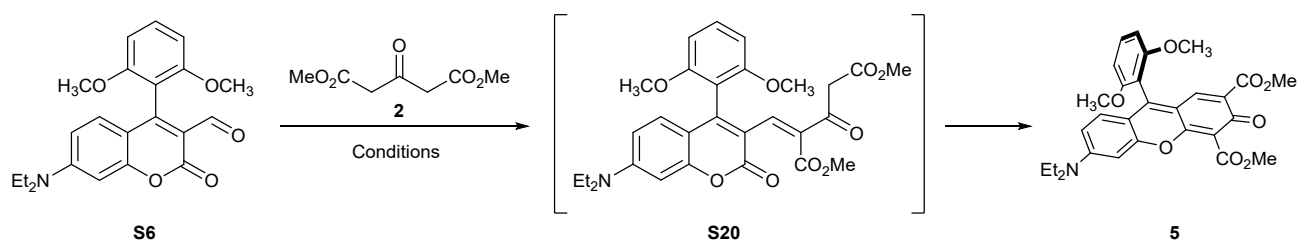
Instrumentation and Materials

All chemicals were used as received unless otherwise noted. All reported ¹H and ¹³C NMR spectra were collected using 500 MHz and 600 MHz spectrometers. Chemical shifts (δ ppm) were determined with TMS as the internal reference; J values are given in Hz. Chromatography was performed on silicagel (230-400 mesh). Preparative thin layer chromatography (TLC) was carried out using Merck PLC Silica gel 60 F₂₅₄ 1 mm plates. The mass spectra were obtained via electron ionization (EI-MS) or electrospray ionization (ESI-MS). All photophysical studies have been performed with freshly-prepared air-equilibrated solutions at room temperature (298 K).

A Shimadzu UV-3600i Plus spectrophotometer and an Edinburgh Instruments Spectrofluorometer FS5 equipped with Hamamatsu R13456 PMT were used to acquire the absorption and emission spectra. Spectrophotometric grade solvents were used without further purification. Fluorescence quantum yields were determined in CH_2Cl_2 and DMSO using Rhodamine 6G in EtOH and sulforhodamine SR101 (for measurements of compounds **8-11** in DMSO) as standards. Photostability was determined using an Asahi Spectra Max-350 as a light source and Shimadzu UV-3600i Plus spectrophotometer.

Optimization of reaction conditions for the rhodol synthesis

As a model reaction we chose the formation of rhodol **5** from coumarin aldehyde **S6** through intermediate **S20** (**Scheme S2**)



Scheme S1. The formation rhodol **5** from coumarin aldehyde **S6**.

Optical absorption measurement was chosen as a convenient instrumental method for the rhodol formation. The samples of coumarin aldehyde substrate were weighed with a 10^{-2} mg precision, that allows keeping the concentration of the substrate within the same range for all optimization experiments. First we determined molar absorptivity (ε) of coumarin aldehyde substrate, the intermediate and the rhodol product (Fig. S1). The concentration (c) of the substrate and the reaction product was calculated based on the Beer–Lambert law (Eq. 1), where A is absorbance and l is optical path length in cm:

$$A = \varepsilon lc \quad (1)$$

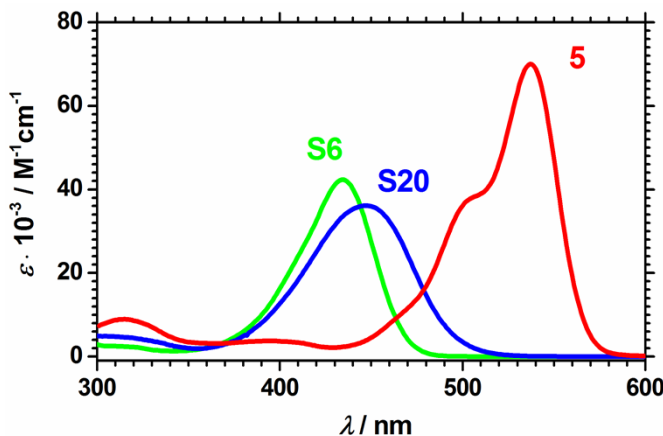


Figure S1. The absorption spectrum for **S6**, **S20** and **5** in CH_2Cl_2 .

The standard procedure for all optimization experiments was chosen as follows:

Coumarin aldehyde (1mg) was dissolved in 1 mL of an appropriate solvent with a certain excess of **2** in the presence of basic catalyst at certain conditions. To check the concentration an 20 μL aliquot was taken from the reaction mixture and diluted to 5 mL with CH_2Cl_2 . The absorption at the maxima was taken into account to calculate the concentration and the reaction yield of rhodol. Before the experiment started the exact amount of coumarin substrate was determined. In course of the reaction the concentrations of coumarin substrate and rhodol were monitored at equal time periods specified for each experiments. A dependence of the reaction yield on time allowed us finding optimal conditions for this type of transformation (Fig. S2).

To eliminate misinterpretations in the analysis of experiments we consider both spectroscopic data and TLC as in a number of experiments side reaction occurred that distorted the absorption data. For instance, all experiments in acetic anhydride as a solvent led to a formation of side products that has absorption in the same range as rhodol **5**, though rhodol formed very fast. We observed the similar situation for tests performed in pyridine or quinoline. The reactions were not efficient, besides that side products formed.

Studying model reaction in methanol in the presence of 1 eq. of piperidine we found that the use of 10eq. of dimethylacetondicarboxylate **2** leads to efficient conversion towards rhodol **5** with a minimum of side reactions, though due to the presence of little amount of side products having absorption at the spectral range of rhodol the reaction yield was overestimated (Fig. S2).

Using this method we have studied other rhodol formation to find the standard synthetic procedure. The chosen examples of the dependencies are shown in Fig. S2.

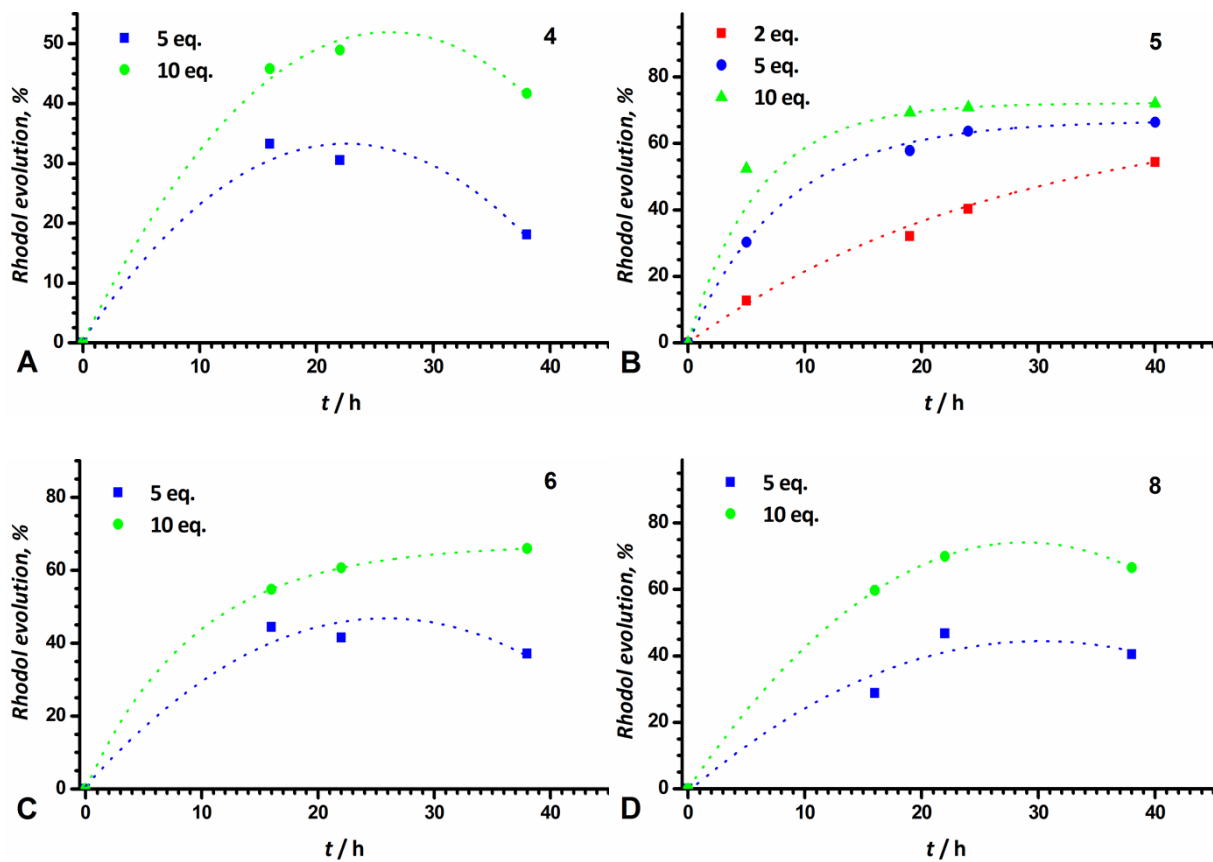
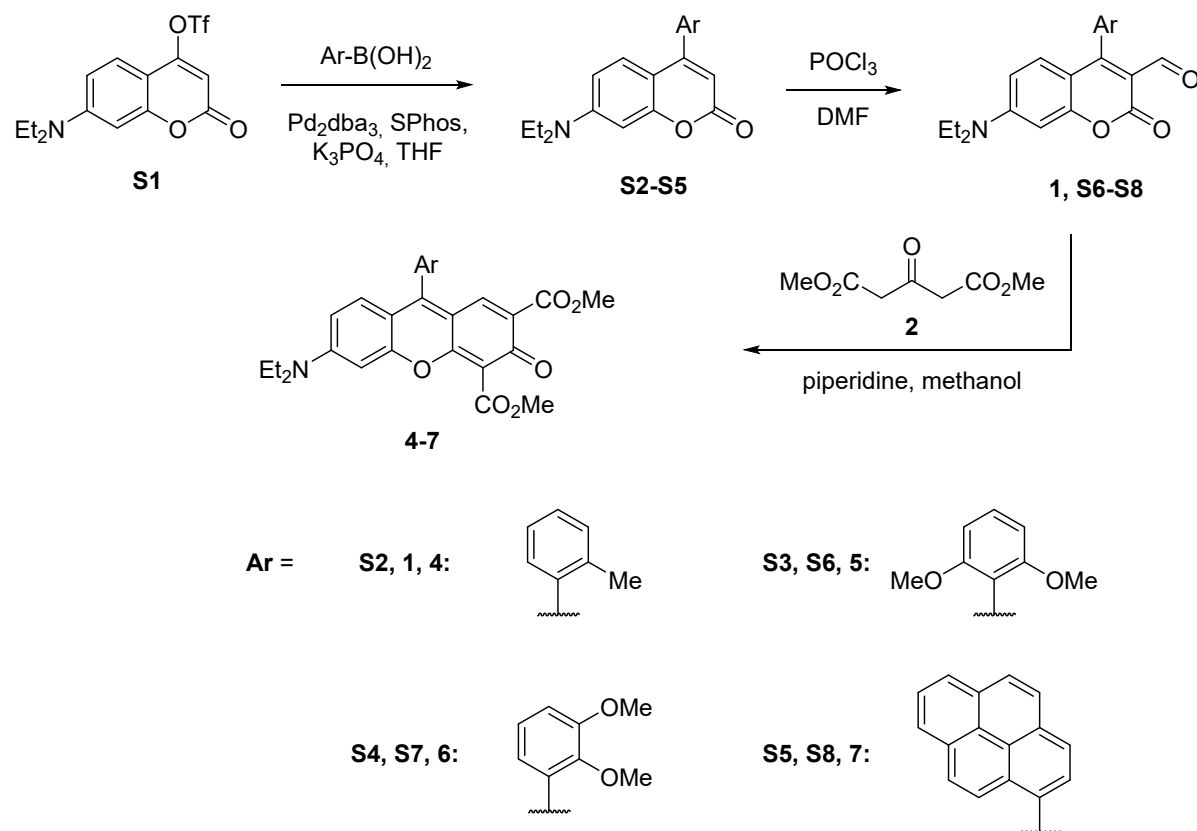


Figure S2. The optimization for the rhodols synthesis (A: Rhodol **4**; B: Rhodol **5**; C: Rhodol **6**; D: Rhodol **8**). The rhodol evolution at using different excess of **2** based on the absorption at the correspondent absorption maxima. The intensity of rhodol signal is overestimated due to residual absorption of contaminants in this region.

Experimental part

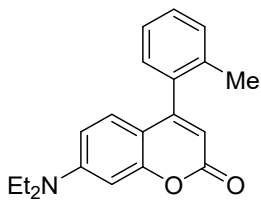


Scheme S2. Synthetic route from coumarin **S1** to rhodols **4-7**.

General procedure for the preparation of compounds **S2-S5**.

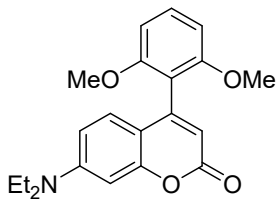
Compound **S1** (10 mmol), arylboronic acid (15 mmol), bis(dibenzylideneacetone)-palladium(0) (0,25 mmol), 2-dicyclohexylphosphino-2',6'-dimethoxybiphenyl (SPhos) (0,75 mmol) and tribasic potassium phosphate (40 mmol) were placed under Ar in a flame-dried Schlenk flask. Dry and degassed THF (50 ml) was added and the reaction mixture was stirred at 70°C for 4h under inert atmosphere. After the reaction was complete the mixture was diluted with DCM, filtered through celite and washed with NaHCO₃ solution (3 × 150 ml). The organic layer was dried over Na₂SO₄ and concentrated under vacuo. The residue was purified using column chromatography (hexane : EtOAc 1:1 + 1% AcOH).

Compound **S2**. Yield 97%. M.p. 95-96°C



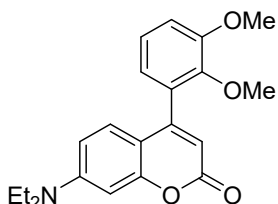
¹H NMR (500 MHz, CDCl₃) δ 7.35 (m, 1H, H-Ar), 7.32 – 7.27 (m, 2H, H-Ar), 7.16 (dd, J = 7.5, 1.5 Hz, 1H, H-Ar), 6.82 (d, J = 9.0 Hz, 1H, H-Ar), 6.56 (d, J = 2.6 Hz, 1H, H-Ar), 6.45 (dd, J = 9.0, 2.6 Hz, 1H, H-Ar), 5.94 (s, 1H, C-H), 3.40 (q, J = 7.1 Hz, 4H, CH₂), 2.18 (s, 3H, CH₃-Ar), 1.20 (t, J = 7.1 Hz, 6H, CH₃); ¹³C NMR (126 MHz, CDCl₃) δ 162.2, 156.4 (2), 150.7, 135.8, 135.3, 130.3, 128.7, 128.3, 127.8, 125.8, 108.8, 108.6, 108.5, 97.6, 44.7, 19.7, 12.4; HRMS (ESI) calc. for C₂₀H₂₁NO₂Na 330.1470 [M + Na]⁺, found 330.1465.

Compound **S3**. Yield 76%. M.p. 136-138°C



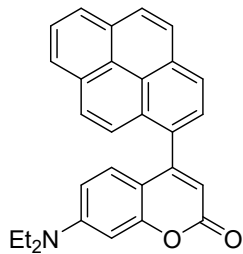
¹H NMR (500 MHz, CDCl₃) δ 7.36 (t, J = 8.4 Hz, 1H, H-Ar), 6.85 (d, J = 8.9 Hz, 1H, H-Ar), 6.66 (d, J = 8.4 Hz, 2H, H-Ar), 6.55 (d, J = 2.5 Hz, 1H, H-Ar), 6.45 (d, J = 8.9 Hz, 1H, H-Ar), 5.98 (s, 1H, C-H), 3.71 (s, 6H, OCH₃), 3.39 (q, J = 7.1 Hz, 4H, CH₂), 1.19 (t, J = 7.1 Hz, 6H, CH₃); ¹³C NMR (126 MHz, CDCl₃) δ 162.6, 157.6, 156.3, 150.4, 130.3, 127.4, 113.5, 111.0, 109.2, 108.3, 104.0, 99.7, 55.9, 44.8, 12.5; HRMS (ESI) calc. for C₂₁H₂₃NO₄Na 376.1525 [M + Na]⁺, found 376.1535.

Compound **S4**. Yield 92%. M.p. 123-124°C



¹H NMR (500 MHz, CDCl₃) δ 7.14 (t, J = 7.9 Hz, 1H, Ar), 7.05 – 6.98 (m, 2H, Ar), 6.81 (dd, J = 7.6, 1.6 Hz, 1H, Ar), 6.58 (d, J = 2.5 Hz, 1H, Ar), 6.53 – 6.47 (m, 1H, Ar), 6.04 (s, 1H, C-H), 3.93 (s, 3H, OCH₃), 3.67 (s, 3H, OCH₃), 3.40 (q, J = 7.1 Hz, 4H, CH₂), 1.20 (t, J = 7.1 Hz, 6H, CH₃); ¹³C NMR (126 MHz, CDCl₃) δ 162.2, 156.3, 153.7, 152.9, 150.6, 146.3, 130.6, 128.9, 124.2, 121.6, 113.1, 109.1, 108.5, 108.4, 97.4, 61.3, 55.9, 44.7, 12.4; HRMS (ESI) calc. for C₂₁H₂₃NO₄Na 376.1525 [M + Na]⁺, found 376.1532.

Compound **S5**. Yield 86%. M.p. 130-131°C

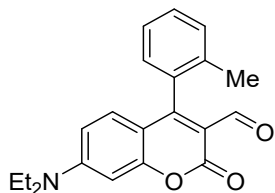


¹H NMR (500 MHz, CDCl₃) δ 8.28 – 8.22 (m, 2H, Ar), 8.19 (dd, *J* = 7.6, 1.2 Hz, 1H, Ar), 8.18 – 8.10 (m, 2H, Ar), 8.07 – 7.99 (m, 2H, Ar), 7.95 – 7.89 (m, 2H, Ar), 6.75 (d, *J* = 9.1 Hz, 1H, Ar), 6.64 (d, *J* = 2.6 Hz, 1H, Ar), 6.33 (dd, *J* = 9.1, 2.6 Hz, 1H, Ar), 6.24 (s, 1H, C-H), 3.39 (q, *J* = 7.1 Hz, 4H, CH₂), 1.19 (t, *J* = 7.1 Hz, 6H, CH₃); ¹³C NMR (126 MHz, CDCl₃) δ 162.1, 156.5, 155.9, 150.8, 131.7, 131.3, 130.8, 128.6, 128.5, 128.2, 127.2, 126.3 (2), 125.7, 125.5, 124.7, 124.6 (2), 110.4, 109.5, 108.6, 97.6, 44.8, 12.4; HRMS (ESI) calc. for C₂₉H₂₃NO₂Na 440.1626 [M + Na]⁺, found 440.1613.

General procedure for the preparation of compounds **1**, **S6-S8**.

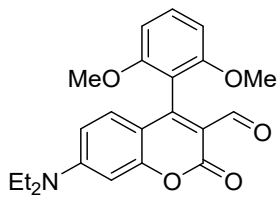
Phosphorus oxychloride (7.7 mmol) was added dropwise to a solution of 7-diethylamino-4-aryl-coumarin (**S2-S5**) (5 mmol) in DMF (15 ml) upon cooling on ice. The reaction mixture was allowed to stir at 50°C for 24h. The solution then was cooled to room temperature, poured into NaHCO₃ aqueous solution (20 g in 100 ml H₂O) with 300 ml of crashed ice. The precipitate which formed was filtered, washed with distilled water, dried under vacuum and purified via recrystallization from hexane + 2-propanol.

Compound **1**. Yield 60%. M.p. 160-161°C



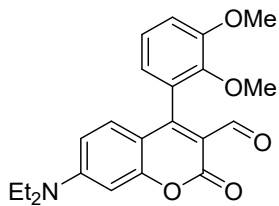
¹H NMR (500 MHz, CDCl₃) δ 9.83 (s, 1H, CHO), 7.39 (td, *J* = 7.5, 1.4 Hz, 1H, H-Ar), 7.35 – 7.26 (m, 2H, H-Ar), 7.06 (dd, *J* = 7.5, 1.4 Hz, 1H, H-Ar), 6.80 (d, *J* = 9.2 Hz, 1H, H-Ar), 6.52 (d, *J* = 2.6 Hz, 1H, H-Ar), 6.48 (dd, *J* = 9.2, 2.6 Hz, 1H, H-Ar), 3.45 (q, *J* = 7.1 Hz, 4H, CH₂), 2.10 (s, *J* = 2.4 Hz, 3H, CH₃-Ar), 1.23 (t, *J* = 7.1 Hz, 6H, CH₃); ¹³C NMR (126 MHz, CDCl₃) δ 188.2, 162.0, 160.0, 157.8, 153.2, 135.1, 133.0, 130.5, 130.1, 128.9, 127.6, 125.8, 112.2, 109.8, 108.7, 97.0, 45.1, 19.4, 12.4; HRMS (ESI) calc. for C₂₁H₂₁NO₃Na 358.1419 [M + Na]⁺, found 358.1415.

Compound **S6**. Yield 50%. M.p. 213-215°C



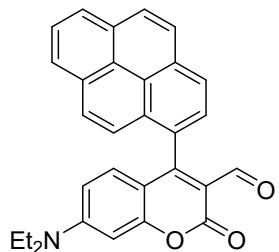
¹H NMR (500 MHz, CDCl₃) δ 9.81 (s, 1H, CHO), 7.41 (t, J = 8.4 Hz, 1H, H-Ar), 6.92 (d, J = 9.1 Hz, 1H, H-Ar), 6.67 (d, J = 8.4 Hz, 2H, H-Ar), 6.52 – 6.44 (m, 2H, H-Ar), 3.69 (s, 6H, OCH₃), 3.43 (q, J = 7.1 Hz, 4H, CH₂), 1.22 (t, J = 7.1 Hz, 6H, CH₃); ¹³C NMR (126 MHz, CDCl₃) δ 188.7, 160.2, 157.7, 157.4, 157.1, 152.9, 130.9, 129.9, 113.4, 110.3, 109.4, 109.0, 103.9, 96.9, 55.9, 45.0, 12.5; HRMS (ESI) calc. for C₂₂H₂₃NO₅Na 404.1474 [M + Na]⁺, found 404.1486.

Compound **S7**. Yield 28%. M.p. 163-164°C



¹H NMR (500 MHz, CDCl₃) δ 9.98 (s, 1H, CHO), 7.16 (t, J = 7.9 Hz, 1H, H-Ar), 7.05 (d, J = 8.2 Hz, 1H, H-Ar), 6.93 (d, J = 9.1 Hz, 1H, H-Ar), 6.66 (d, J = 7.6 Hz, 1H, H-Ar), 6.53 – 6.45 (m, 2H, H-Ar), 3.94 (s, 3H, OCH₃), 3.67 (s, 3H, OCH₃), 3.43 (q, J = 7.1 Hz, 4H, CH₂), 1.22 (t, J = 7.1 Hz, 6H, CH₃); ¹³C NMR (126 MHz, CDCl₃) δ 188.4, 160.5, 158.8, 157.6, 153.0, 152.7, 145.7, 130.9, 128.0, 124.2, 120.7, 113.1, 112.5, 109.7, 109.2, 97.0, 60.9, 55.8, 45.1, 12.4; HRMS (ESI) calc. for C₂₂H₂₃NO₅Na 404.1474 [M + Na]⁺, found 404.1479.

Compound **S8**. Yield 80%. M.p. 169-171°C

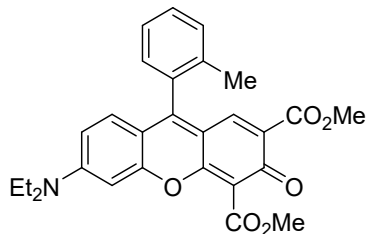


¹H NMR (500 MHz, CDCl₃) δ 9.79 (s, 1H, CHO), 8.30 - 8.22 (m, 2H, H-Ar), 8.21 – 8.12 (m, 3H, H-Ar), 8.04 (t, J = 7.6 Hz, 1H, H-Ar), 8.01 (d, J = 9.1 Hz, 1H, H-Ar), 7.83 (d, J = 7.8 Hz, 1H, H-Ar), 7.72 (d, J = 9.1 Hz, 1H, H-Ar), 6.63 – 6.55 (m, 2H, H-Ar), 6.30 (dd, J = 9.3, 2.6 Hz, 1H, H-Ar), 3.41 (q, J = 7.1 Hz, 4H, CH₂), 1.19 (t, J = 7.1 Hz, 6H, CH₃); ¹³C NMR (126 MHz, CDCl₃) δ 188.0, 161.4, 160.0, 157.8, 153.2, 131.8, 131.3, 131.2, 130.8, 128.8, 128.7, 128.3, 128.0, 127.3, 126.4, 125.9 (2), 125.7, 124.5 (3), 124.1, 113.6, 109.9, 109.8, 97.0, 45.2, 12.4; HRMS (ESI) calc. for C₃₀H₂₄NO₃ 446.1756 [M + H]⁺, found 446.1761.

General procedure for the preparation of compounds **4-7**.

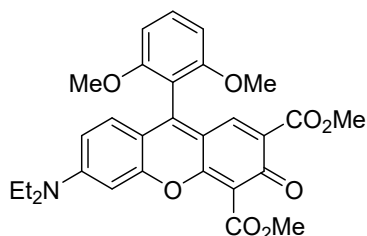
Aldehyde (**1**, **S6-S8**) (1 mmol), dimethyl-1,3-acetonedicarboxylate (**2**) (10 mmol) and piperidine (1 mmol) were dissolved in methanol (3 ml) and allowed to stir at 60°C for 20h. The solvent was evaporated and the residue was washed with diethyl ether. The crude product was purified via column chromatography (CH_2Cl_2 : MeOH 93:7).

Compound **4**. Yield 28%. M.p. 258-260°C



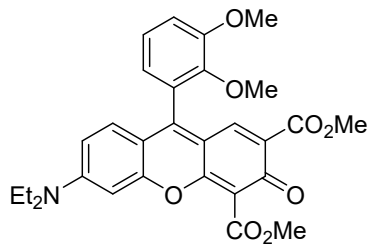
^1H NMR (500 MHz, CDCl_3) δ 7.52 (s, 1H, H-Ar), 7.45 (td, J = 7.6, 1.4 Hz, 1H, H-Ar), 7.4 – 7.33 (m, 2H, H-Ar), 7.12 (d, J = 7.5 Hz, 1H, H-Ar), 6.90 (d, J = 9.1 Hz, 1H, H-Ar), 6.62 – 6.55 (m, 2H, H-Ar), 4.01 (s, 3H, OCH₃), 3.81 (s, 3H, OCH₃), 3.50 (q, J = 7.3 Hz, 4H, CH₂), 2.06 (s, 3H, CH₃ - Ar), 1.26 (t, J = 7.1 Hz, 6H, CH₃); ^{13}C NMR (126 MHz, CDCl_3) δ 176.7, 167.1, 166.4, 156.2, 155.6, 155.3, 153.6, 136.0, 135.1, 132.1, 130.7 (2), 129.7, 129.0, 128.2, 126.1, 113.0, 112.1, 111.1, 110.9, 96.9, 52.3, 52.2, 45.3, 19.6, 12.6; HRMS (ESI) calc. for $\text{C}_{28}\text{H}_{28}\text{NO}_6$ 474.1917 [M + H]⁺, found 474.1903.

Compound **5**. Yield 21%. M.p. 217-218°C



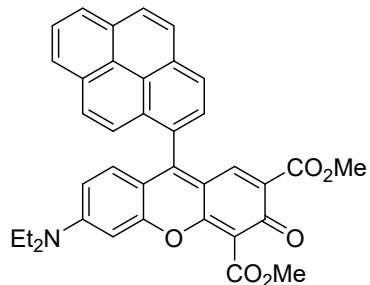
^1H NMR (500 MHz, CDCl_3) δ 7.61 (s, 1H, H-Ar), 7.51 – 7.41 (t, J = 8.4 Hz, 1H, H-Ar), 7.02 – 6.96 (m, 1H, H-Ar), 6.73 – 6.67 (m, 2H, H-Ar), 6.59 – 6.53 (m, 2H, H-Ar), 4.00 (s, 3H, OCH₃), 3.82 (s, 3H, OCH₃), 3.66 (s, 6H, OCH₃), 3.48 (q, J = 7.1 Hz, 4H, CH₂), 1.25 (t, J = 7.1 Hz, 6H, CH₃); ^{13}C NMR (126 MHz, CDCl_3) δ 176.8, 167.5, 166.7, 157.7, 156.3, 156.0, 153.4, 151.3, 135.8, 131.6, 130.4, 127.5, 113.3, 112.5, 111.5, 110.8, 109.5, 104.1, 96.7, 55.9, 52.2, 52.0, 45.1, 12.6; HRMS (ESI) calc. for $\text{C}_{29}\text{H}_{30}\text{NO}_8$ 520.1971 [M + H]⁺, found 520.1978.

Compound **6**. Yield 13%. M.p. 210-211°C

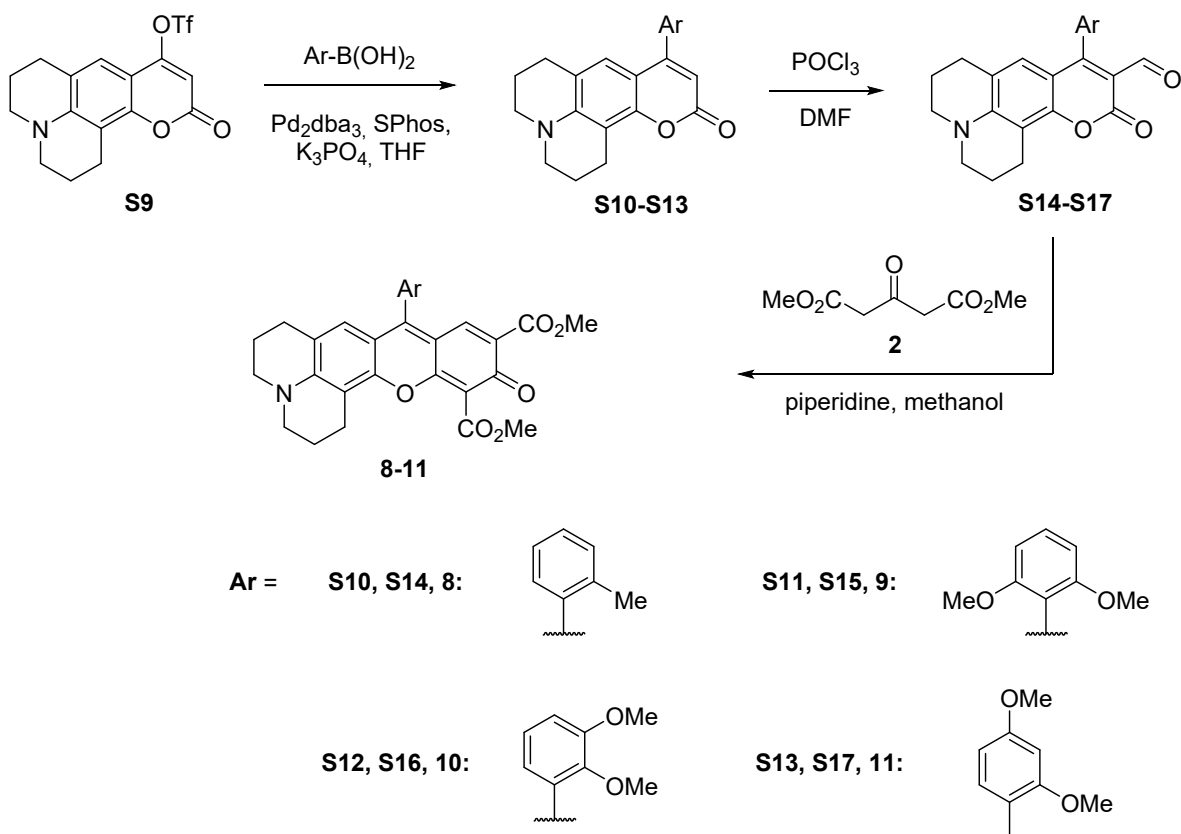


¹H NMR (500 MHz, CDCl₃) δ 7.70 (s, 1H, H-Ar), 7.21 (t, J = 7.9 Hz, 1H, H-Ar), 7.11 (dd, J = 8.3, 1.5 Hz, 1H, H-Ar), 7.06 – 7.01 (m, 1H, H-Ar), 6.73 (dd, J = 7.7, 1.5 Hz, 1H, H-Ar), 6.61 – 6.55 (m, 2H, H-Ar), 4.01 (s, 3H, OCH₃), 3.96 (s, 3H, OCH₃), 3.82 (s, 3H, OCH₃), 3.61 (s, 3H, OCH₃), 3.49 (q, J = 7.2 Hz, 4H, CH₂), 1.25 (t, J = 7.1 Hz, 6H, CH₃); ¹³C NMR (126 MHz, CDCl₃) δ 176.6, 167.1, 166.4, 156.1, 155.6, 153.6, 152.9, 152.8, 146.5, 135.4, 131.0, 127.7, 126.7, 124.4, 121.8, 113.8, 112.8, 112.4, 111.2, 110.9, 96.7, 61.2, 55.8, 52.2, 52.0, 45.2, 12.5; HRMS (ESI) calc. for C₂₉H₃₀NO₈ 520.1977 [M + H]⁺, found 520.1978.

Compound 7. Yield 23%. M.p. 211–213°C



¹H NMR (500 MHz, CDCl₃) δ 8.33 (d, J = 7.8 Hz, 1H, H-Ar), 8.29 (d, J = 7.7 Hz, 1H, H-Ar), 8.25 – 8.15 (m, 3H, H-Ar), 8.07 (t, J = 7.6 Hz, 1H, H-Ar), 8.01 (d, J = 9.1 Hz, 1H, H-Ar), 7.86 (d, J = 7.8 Hz, 1H, H-Ar), 7.61 (d, J = 9.1 Hz, 1H, H-Ar), 7.43 (s, 1H, H-Ar), 6.73 (d, J = 9.4 Hz, 1H, H-Ar), 6.67 (d, J = 2.5 Hz, 1H, H-Ar), 6.41 (dd, J = 9.4, 2.5 Hz, 1H, H-Ar), 4.05 (s, 3H, OCH₃), 3.64 (s, 3H, OCH₃), 3.47 (q, J = 7.2 Hz, 4H, CH₂), 1.24 (t, J = 7.1 Hz, 6H, CH₃); ¹³C NMR (126 MHz, CDCl₃) δ 176.7, 166.8, 166.4, 156.1, 155.6, 154.7, 153.6, 135.3, 132.3, 131.3, 130.8, 129.5, 129.1, 128.8, 128.3, 127.2, 126.9, 126.8, 126.6, 126.2, 126.0, 124.6 (2), 124.4, 124.1, 113.6, 113.0, 112.1, 111.1, 96.9, 52.4, 52.0, 45.3, 12.6; HRMS (ESI) calc. for C₃₇H₃₀NO₆ 584.2073 [M + H]⁺, found 584.2075.

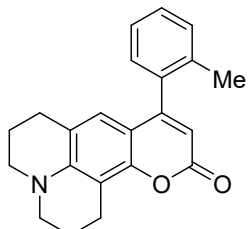


Scheme S3. Synthetic route from coumarin **S9** to rhodols **8-11**.

General procedure for the preparation of compounds **S10-S13**.

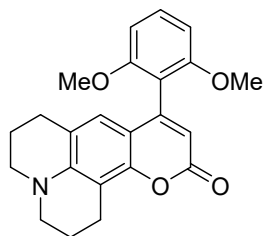
Compound **S9** (10 mmol), arylboronic acid (15 mmol), bis(dibenzylideneacetone)-palladium(0) (0.25 mmol), 2-dicyclohexylphosphino-2',6'-dimethoxybiphenyl (SPhos) (0.75 mmol) and tribasic potassium phosphate (40 mmol) were placed under Ar in a flame-dried Schlenk flask. Dry and degassed THF (75 ml) was added and the reaction mixture was stirred at 70°C for 7h under inert atmosphere. After the reaction was complete the mixture was diluted with DCM, filtered through celite and washed with NaHCO_3 solution (3 × 150 ml). The organic layer was dried over Na_2SO_4 and concentrated under vacuo. The residue was recrystallized from methanol.

Compound **S10**. Yield 90%. M.p. 166-167°C



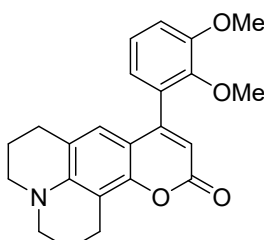
¹H NMR (600 MHz, CDCl₃) δ 7.37 – 7.34 (m, 1H, H-Ar), 7.32 – 7.26 (m, 2H, H-Ar), 7.14 (dd, *J* = 7.6, 1.4 Hz, 1H, H-Ar), 6.39 (s, 1H, H-Ar), 5.89 (s, 1H, C-H), 3.29 – 3.21 (m, 4H, CH₂), 2.95 (t, *J* = 6.5 Hz, 2H, CH₂), 2.60 (t, *J* = 6.5 Hz, 2H, CH₂), 2.17 (s, 3H, CH₃-Ar), 2.02 – 1.97 (m, 2H, CH₂), 1.93 – 1.88 (m, *J* = 7.9, 5.5 Hz, 2H, CH₂); ¹³C NMR (151 MHz, CDCl₃) δ 162.5, 156.6, 151.4, 145.9, 136.2, 135.3, 130.2, 128.5, 128.4, 125.7, 123.8, 118.2, 108.3, 108.2, 106.8, 49.9, 49.5, 27.5, 21.5, 20.6, 20.5, 19.7; HRMS (ESI) calc. for C₂₂H₂₁NO₂Na 354.1470 [M + Na]⁺, found 354.1469.

Compound **S11**. Yield 94%.



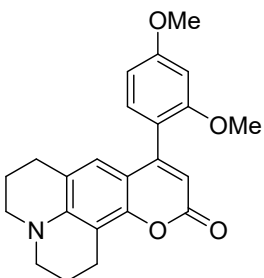
¹H NMR (500 MHz, CDCl₃) δ 7.36 (t, *J* = 8.4 Hz, 1H, H-Ar), 6.66 (d, *J* = 8.4 Hz, 2H, H-Ar), 6.43 (s, 1H, H-Ar), 5.92 (s, 1H, C-H), 3.70 (s, 6H, OCH₃), 3.23 – 3.19 (m, 4H, CH₂), 2.94 (t, *J* = 6.6 Hz, 2H, CH₂), 2.62 (t, *J* = 6.4 Hz, 2H, CH₂), 2.02 – 1.99 (m, 2H, CH₂), 1.97 – 1.93 (m, 2H, CH₂); ¹³C NMR (126 MHz, CDCl₃) δ 162.9, 157.6, 151.4, 150.7, 145.6, 130.1, 123.4, 117.9, 114.0, 110.3, 109.0, 106.7, 104.1, 56.0, 50.0, 49.6, 27.5, 21.6, 20.8, 20.6; HRMS (ESI) calc. for C₂₃H₂₃NO₄Na 400.1525 [M + Na]⁺, found 400.1529.

Compound **S12**. Yield 89%. M.p. 208-210°C



¹H NMR (500 MHz, CDCl₃) δ 7.13 (t, *J* = 7.9 Hz, 1H, H-Ar), 7.02 (dd, *J* = 8.3, 1.5 Hz, 1H, H-Ar), 6.78 (dd, *J* = 7.7, 1.5 Hz, 1H, H-Ar), 6.56 (s, 1H, H-Ar), 5.97 (s, 1H, C-H), 3.93 (s, 3H, OCH₃), 3.67 (s, 3H, OCH₃), 3.27 – 3.20 (m, 4H, CH₂), 2.94 (t, *J* = 6.5 Hz, 2H, CH₂), 2.69 – 2.55 (m, 2H, CH₂), 2.02 – 1.96 (m, 2H, CH₂), 1.92 – 1.87 (m, 2H, CH₂); ¹³C NMR (126 MHz, CDCl₃) δ 162.5, 153.9, 152.8, 151.3, 146.2, 145.9, 131.0, 124.2, 124.1, 121.6, 118.1, 112.8, 108.4, 108.4, 106.6, 61.3, 55.8, 50.0, 49.5, 27.5, 21.5, 20.7, 20.5; HRMS (ESI) calc. for C₂₃H₂₃NO₄Na 400.1525 [M + Na]⁺, found 400.1522.

Compound **S13**. Yield 84%. M.p. 201-203°C

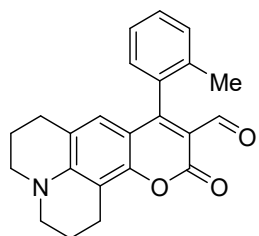


¹H NMR (500 MHz, CDCl₃) δ 7.13 – 7.08 (m, 1H, H-Ar), 6.59 – 6.57 (m, 3H, H-Ar), 5.95 (s, 1H, C-H), 3.87 (s, 3H, OCH₃), 3.73 (s, 3H, OCH₃), 3.23 (t, J = 5.8 Hz, 4H, CH₂), 2.93 (t, J = 6.5 Hz, 2H, CH₂), 2.64 (t, J = 6.4 Hz, 2H, CH₂), 2.01 - 1.96 (m, J = 6.2 Hz, 2H, CH₂), 1.94 – 1.89 (d, J = 6.0 Hz, 2H, CH₂); ¹³C NMR (126 MHz, CDCl₃) δ 162.8, 161.5, 157.6, 153.9, 151.3, 145.6, 130.8, 124.2, 118.3, 117.8, 109.2, 108.8, 106.7, 104.5, 99.0, 55.6, 55.5, 49.9, 49.6, 27.6, 21.6, 20.8, 20.5; HRMS (ESI) calc. for C₂₃H₂₃NO₄Na 400.1525 [M + Na]⁺, found 400.1530.

General procedure for the preparation of compounds **S14-S17**.

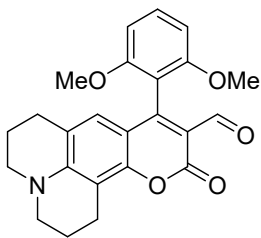
Phosphorus oxychloride (7.7 mmol) was added dropwise to a solution of 7-diethylamino-4-aryl-coumarin (**S10-S13**) (5 mmol) in DMF (15 ml) upon cooling on ice. The reaction mixture was allowed to stir at 50°C for 24h. The solution then was cooled to room temperature, poured into NaHCO₃ aqueous solution (20 g in 100 ml H₂O) with 300 ml of crashed ice. The precipitate which formed was filtered, washed with distilled water and methanol, dried under vacuo and purified via recrystallization from MeOH/CH₂Cl₂.

Compound **S14**. Yield 84%. M.p. 201-203°C



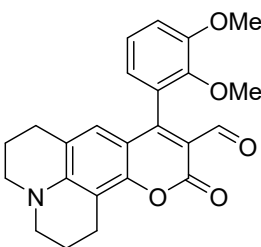
¹H NMR (500 MHz, CDCl₃) δ 9.80 (s, 1H, CHO), 7.38 (t, J = 7.5 Hz, 1H, H-Ar), 7.33 – 7.24 (m, 2H, H-Ar), 7.03 (d, J = 7.5 Hz, 1H, H-Ar), 6.35 (s, 1H, H-Ar), 3.36 – 3.32 (m, 4H, CH₂), 2.94 (t, J = 6.4 Hz, 2H, CH₂), 2.57 (t, J = 6.2 Hz, 2H, CH₂), 2.08 (s, 3H, CH₃-Ar), 2.00 (quint, J = 6.2 Hz, 2H, CH₂), 1.90 (quint, J = 6.3 Hz, 2H, CH₂); ¹³C NMR (126 MHz, CDCl₃) δ 188.4, 161.6, 160.3, 152.9, 149.0, 135.2, 133.5, 130.0, 128.7, 127.8, 126.1, 125.7, 119.5, 111.3, 108.4, 106.0, 50.3, 49.9, 27.5, 21.1, 20.2, 20.2, 19.5; HRMS (ESI) calc. for C₂₃H₂₂NO₃ 360.1600 [M + H]⁺, found 360.1588.

Compound **S15**. Yield 87%. M.p. 263-265°C



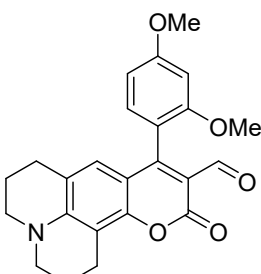
¹H NMR (500 MHz, CDCl₃) δ 9.77 (s, 1H, CHO), 7.41 (t, J = 8.4 Hz, 1H, H-Ar), 6.66 (d, J = 8.4 Hz, 2H, H-Ar), 6.49 (s, 1H, H-Ar), 3.68 (s, 6H, OCH₃), 3.34 – 3.28 (m, 4H, CH₂), 2.92 (t, J = 6.4 Hz, 2H, CH₂), 2.60 (t, J = 6.3 Hz, 2H, CH₂), 1.97 (quint, J = 6.1 Hz, 2H, CH₂), 1.91 (quint, J = 6.1 Hz, 2H, CH₂); ¹³C NMR (126 MHz, CDCl₃) δ 188.8, 160.4, 157.3, 157.1, 152.8, 148.7, 130.7, 125.5, 119.1, 112.3, 110.8, 108.7, 105.8, 103.9, 56.0, 50.2, 49.9, 49.6, 27.5, 21.1, 20.3 (2); HRMS (ESI) calc. for C₂₄H₂₃NO₅Na 428.1474 [M + Na]⁺, found 428.1472.

Compound **S16**. Yield 86%. M.p. 242-244°C



¹H NMR (500 MHz, CDCl₃) δ 9.89 (s, 1H, CHO), 7.15 (t, J = 7.9 Hz, 1H, H-Ar), 7.06 (d, J = 8.2 Hz, 1H, H-Ar), 6.64 (d, J = 7.6 Hz, 1H, H-Ar), 6.50 (s, 1H, H-Ar), 3.94 (s, 3H, OCH₃), 3.66 (s, 3H, OCH₃), 3.36 – 3.32 (m, 4H, CH₂), 2.91 (t, J = 6.4 Hz, 2H, CH₂), 2.59 (t, J = 6.4 Hz, 2H, CH₂), 1.97 (quint, J = 6.2 Hz, 2H, CH₂), 1.89 (quint, J = 6.0 Hz, 2H, CH₂); ¹³C NMR (126 MHz, CDCl₃) δ 188.0, 160.1, 158.4, 152.3, 152.2, 148.7, 145.2, 127.8, 126.0, 123.7, 120.3, 119.2, 112.6, 110.6, 108.3, 105.3, 60.4, 55.4, 49.9, 49.4, 27.0, 20.5, 19.7 (2); HRMS (ESI) calc. for C₂₄H₂₃NO₅Na 428.1474 [M + Na]⁺, found 428.1481.

Compound **S17**. Yield 32%. M.p. 210-211°C



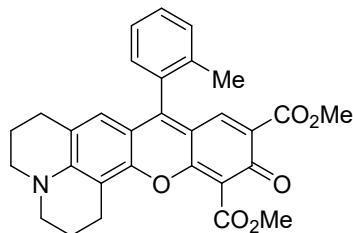
¹H NMR (500 MHz, CDCl₃) δ 9.80 (s, 1H, CHO), 6.97 (d, J = 8.3 Hz, 1H, H-Ar), 6.60 (dd, J = 8.3, 2.3 Hz, 1H, H-Ar), 6.57-6.56 (m, 2H, H-Ar), 3.88 (s, 3H, OCH₃), 3.70 (s, 3H, OCH₃), 3.35 – 3.29 (m, 4H, CH₂), 2.92 (t,

$J = 6.4$ Hz, 2H, CH₂), 2.64 – 2.58 (m, 2H, CH₂), 2.02 – 1.95 (m, 2H, CH₂), 1.93 – 1.88 (m, 2H, CH₂); ¹³C NMR (126 MHz, CDCl₃) δ 188.9, 161.7, 160.3, 159.1, 157.7, 152.9, 148.6, 130.3, 126.3, 119.1, 114.8, 112.1, 109.1, 106.0, 104.5, 98.7, 55.7, 55.5, 50.2, 49.9, 27.5, 21.1, 20.3 (2); HRMS (ESI) calc. for C₂₄H₂₃NO₅Na 428.1474 [M + Na]⁺, found 428.1472.

General procedure for the preparation of compounds **8-11**.

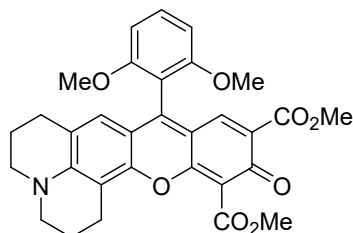
3-formyl coumarin (**S14-S17**) (1 mmol), dimethyl-1,3-acetonedicarboxylate (**2**) (10 mmol) and piperidine (1 mmol) were dissolved in methanol (5 ml) and allowed to stir at 60°C for 20h. The solvent was evaporated and the residue was washed with diethyl ether. The crude product was purified via column chromatography (CH₂Cl₂ : MeOH 9:1).

Compound **8**. Yield 19%. M.p. 265-266°C



¹H NMR (500 MHz, CDCl₃) δ 7.49 – 7.41 (m, 2H, H-Ar), 7.38 – 7.33 (m, 2H, H-Ar), 7.10 – 7.08 (m, 1H, H-Ar), 6.47 (s, 1H, H-Ar), 3.98 (s, 3H, OCH₃), 3.80 (s, 3H, OCH₃), 3.41 – 3.37 (m, 4H, CH₂), 2.95 – 2.91 (m, 2H, CH₂), 2.63 (t, $J = 6.2$ Hz, 2H, CH₂), 2.08 – 1.99 (m, 5H, CH₃-Ar, CH₂), 1.98 – 1.89 (m, 2H, CH₂); ¹³C NMR (126 MHz, CDCl₃) δ 176.2, 167.4, 166.6, 155.8, 155.0, 151.1, 149.7, 136.0, 134.8, 132.5, 130.6, 129.5, 129.0, 127.8, 126.1, 126.0, 121.2, 112.2, 111.1, 110.8, 105.8, 52.2, 52.1, 50.5, 50.2, 27.5, 20.9, 20.0, 19.8, 19.6; HRMS (ESI) calc. for C₃₀H₂₈NO₆ 498.1917 [M + H]⁺, found 498.1921.

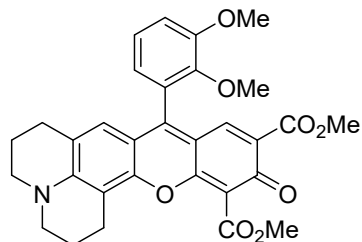
Compound **9**. Yield 28%. M.p. 260-262°C



¹H NMR (500 MHz, CDCl₃) δ 7.57 (s, 1H, H-Ar), 7.46 (t, $J = 8.4$ Hz, 1H, H-Ar), 6.70 (d, $J = 8.4$ Hz, 2H, H-Ar), 6.57 (s, 1H, H-Ar), 3.98 (s, 3H, OCH₃), 3.82 (s, 3H, OCH₃), 3.65 (s, 6H, OCH₃), 3.41 – 3.34 (m, 4H, CH₂), 2.93 (t, $J = 6.4$ Hz, 2H, CH₂), 2.65 (t, $J = 6.2$ Hz, 2H, CH₂), 2.03 – 1.98 (m, 2H, CH₂), 1.97 – 1.92 (m, 2H, CH₂); ¹³C NMR (126 MHz, CDCl₃) δ 176.4, 167.9, 166.9, 157.7, 156.3, 151.3, 151.0, 149.6, 135.5,

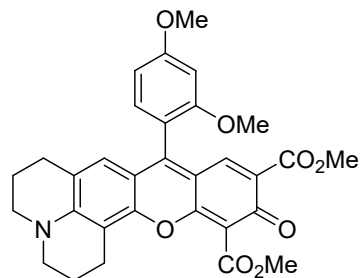
131.5, 127.0, 126.1, 120.9, 112.1, 111.8, 111.5, 109.9, 105.5, 104.1, 56.0, 52.1, 52.0, 50.5, 50.2, 27.6, 21.1, 20.2, 19.8; HRMS (ESI) calc. for $C_{31}H_{30}NO_8$ 544.1971 [M + H]⁺, found 544.1970.

Compound **10**. Yield 28%. M.p. 200°C (dec.)



¹H NMR (500 MHz, CDCl₃) δ 7.66 (s, 1H, H-Ar), 7.21 (t, *J* = 7.9 Hz, 1H, H-Ar), 7.10 (d, *J* = 8.2 Hz, 1H, H-Ar), 6.74 – 6.68 (m, 1H, H-Ar), 6.60 (s, 1H, H-Ar), 3.98 (s, 3H, OCH₃), 3.97 (s, 3H, OCH₃), 3.81 (s, 3H, OCH₃), 3.59 (s, 3H, OCH₃), 3.41 – 3.37 (m, 4H, CH₂), 2.92 (t, *J* = 6.4 Hz, 2H, CH₂), 2.65 – 2.62 (m, 2H, CH₂), 2.03 – 2.00 (m, 2H, CH₂), 1.95 – 1.90 (m, 2H, CH₂); ¹³C NMR (126 MHz, CDCl₃) δ 176.2, 167.6, 166.6, 152.9, 146.5, 135.3, 127.1 (2), 126.6, 124.3, 121.9, 113.6, 111.4, 105.6, 61.2, 55.8, 52.1, 52.0, 50.5, 50.2, 27.5, 20.9, 20.1, 19.8; HRMS (ESI) calc. for $C_{31}H_{30}NO_8$ 544.1971 [M + H]⁺, found 544.1974.

Compound **11**. Yield 16%. M.p. 181°C (dec.)

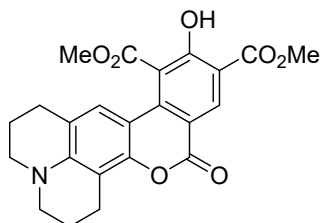


¹H NMR (500 MHz, CDCl₃) δ 7.64 (s, 1H, H-Ar), 7.02 (d, *J* = 8.3 Hz, 1H, H-Ar), 6.68 – 6.60 (m, 3H, H-Ar), 3.97 (s, 3H, OCH₃), 3.91 (s, 3H, OCH₃), 3.82 (s, 3H, OCH₃), 3.68 (s, 3H, OCH₃), 3.40 – 3.36 (m, 4H, CH₂), 2.92 (t, *J* = 6.3 Hz, 2H, CH₂), 2.66 (t, *J* = 6.3 Hz, 2H, CH₂), 2.01 (quint, *J* = 6.2 Hz, 2H, CH₂), 1.99 – 1.90 (m, 2H, CH₂); ¹³C NMR (126 MHz, CDCl₃) δ 176.2, 167.7, 166.7, 162.2, 158.0, 156.1, 153.1, 151.3, 149.5, 135.8, 131.4, 127.1, 126.6, 120.8, 114.0, 112.0, 111.9, 111.5, 105.6, 104.9, 99.1, 55.7, 55.5, 52.1, 52.0, 50.5, 50.2, 27.6, 21.0, 20.1, 19.8; HRMS (ESI) calc. for $C_{31}H_{30}NO_8$ 544.1971 [M + H]⁺, found 544.1975.

General procedure for the preparation of compounds **12**, **13**.

3-formyl coumarin (**S18, S19**) (1 mmol), dimethyl-1,3-acetonedicarboxylate (**2**) (10 mmol) and piperidine (1 mmol) were dissolved in methanol (5 ml) and allowed to stir at 60°C for 20h. The precipitate which formed was filtered and recrystallized from MeOH/CH₂Cl₂.

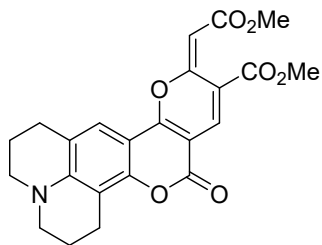
Compound **12**. Yield 21%. M.p. M.p. 250°C(dec.)



Starting compound **S18** was synthesized following a procedure described in the literature.¹

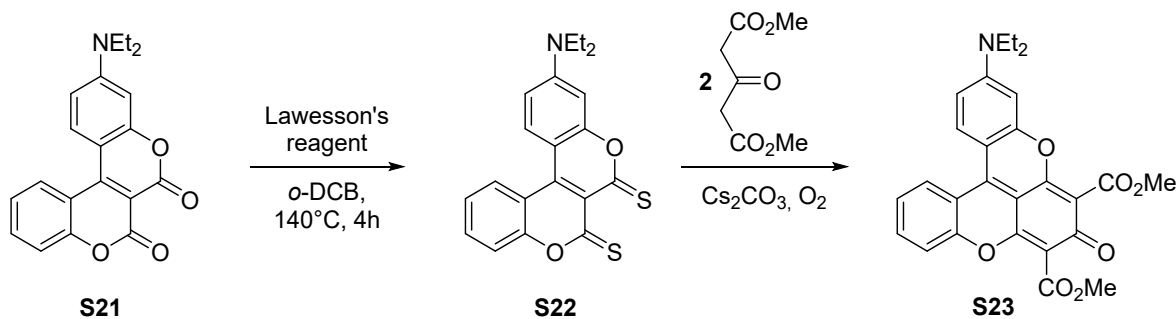
¹H NMR (500 MHz, CDCl₃) δ 11.66 (s, 1H, OH), 8.92 (s, 1H, H-Ar), 7.09 (s, 1H, H-Ar), 4.01 (s, 3H, OCH₃), 3.99 (s, 3H, OCH₃), 3.28 – 3.24 (m, 4H, CH₂), 2.89 (t, J = 6.5 Hz, 2H, CH₂), 2.74 (t, J = 6.3 Hz, 2H, CH₂), 1.98 (quint, J = 6.1 Hz, 4H, CH₂); ¹³C NMR (126 MHz, CDCl₃) δ 169.5, 168.4, 162.6, 160.8, 149.4, 146.1, 139.0, 135.6, 122.9, 117.9, 115.6, 111.7, 110.5, 107.4, 103.4, 52.9, 52.7, 49.9, 49.3, 27.9, 21.5, 20.7, 20.6; HRMS (EI) calc. for C₂₃H₂₁NO₇ 423.1318 M⁺, found 423.1302.

Compound **30**. Yield 60%. M.p. 288-289°C



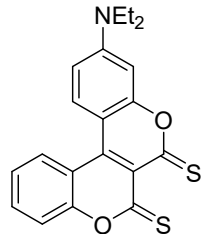
Starting compound **S19** was synthesized following a procedure described in the literature.²

¹H NMR (500 MHz, 1,1,2,2-CD₂Cl₄) δ 8.04 (s, 1H), 7.58 (s, 1H), 6.38 (s, 1H), 3.82 (s, 3H, OCH₃), 3.76 (s, 3H, OCH₃), 3.37 – 3.32 (m, 4H, CH₂), 2.85 – 2.82 (m, 4H, CH₂), 1.99 – 1.94 (m, 4H, CH₂); ¹³C NMR (500 MHz, 1,1,2,2- CD₂Cl₄) δ 165.6, 163.4, 161.6, 159.6, 154.6, 151.9, 149.0, 136.9, 121.6, 119.9, 113.3, 106.0, 99.8, 95.8, 94.6, 52.2, 51.0, 50.2, 49.7, 27.7, 20.9, 20.1, 19.9; HRMS (ESI) calc. for C₂₃H₂₁NO₇Na 446.1216 [M + Na]⁺, found 446.1218.



Scheme S4. Transformation of bis-coumarins into V-shaped rhodols.

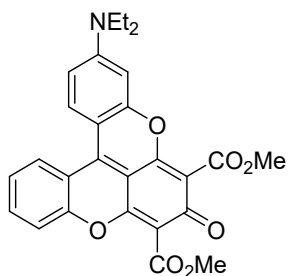
Compound **S22**. Yield 18%. M.p. 170-171°C



The starting compound **S21** was synthesized according to the literature procedure.³ The bis-coumarin **S21** (1 mmol) together with Lawesson's reagent (1,25 mmol) were dissolved in 25 ml of dry *o*-DCB and the reaction was heated at 140°C for 4 hours. After the solvent was evaporated under the vacuo, the residue was filtered through a silica pad, washed with mixture of hexane and CH₂Cl₂ (1:1) and concentrated under vacuo. The product was next purified via DCVC (CH₂Cl₂ : hexane 1:2) followed by the recrystallization from the mixture of hexane and CH₂Cl₂.

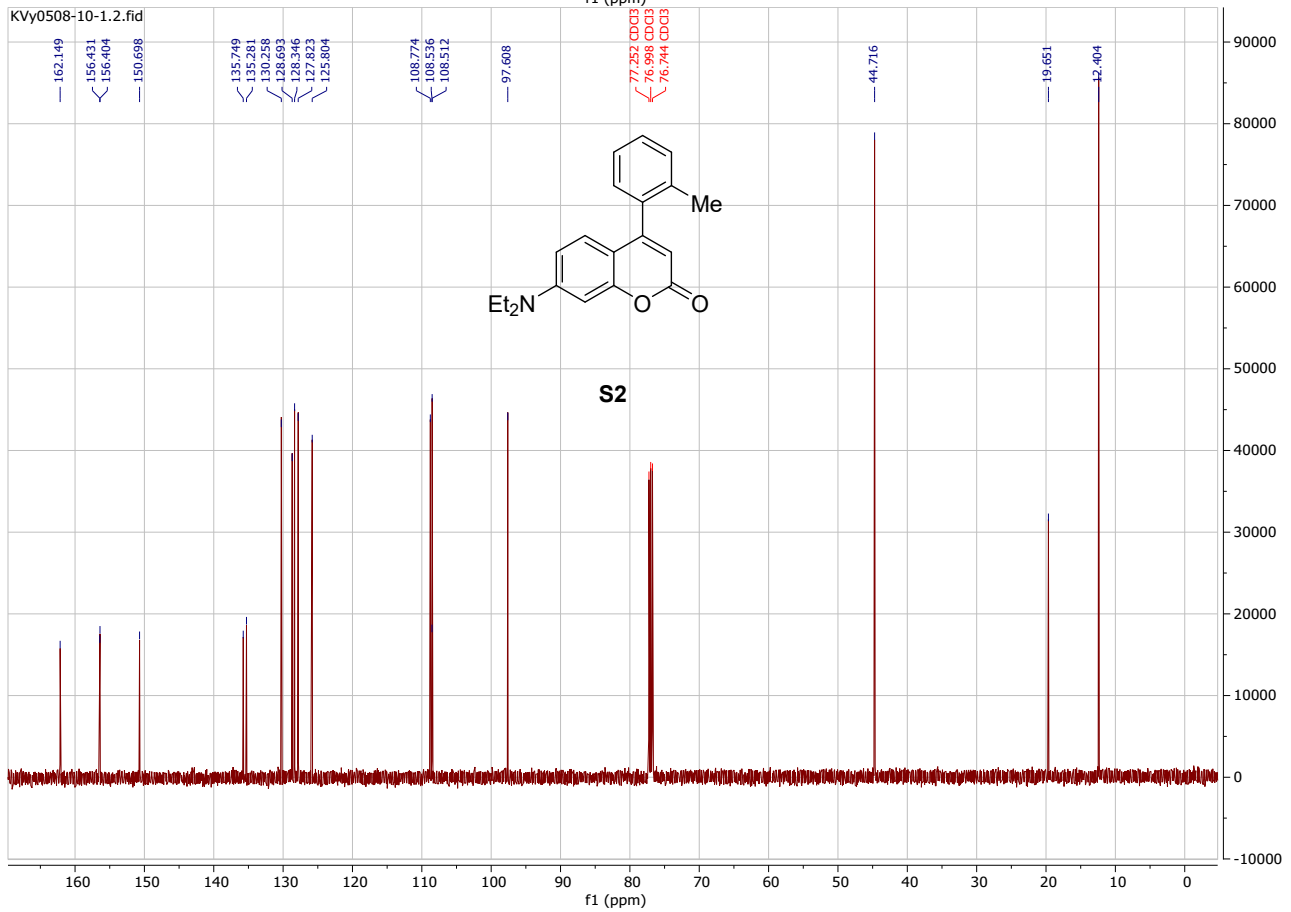
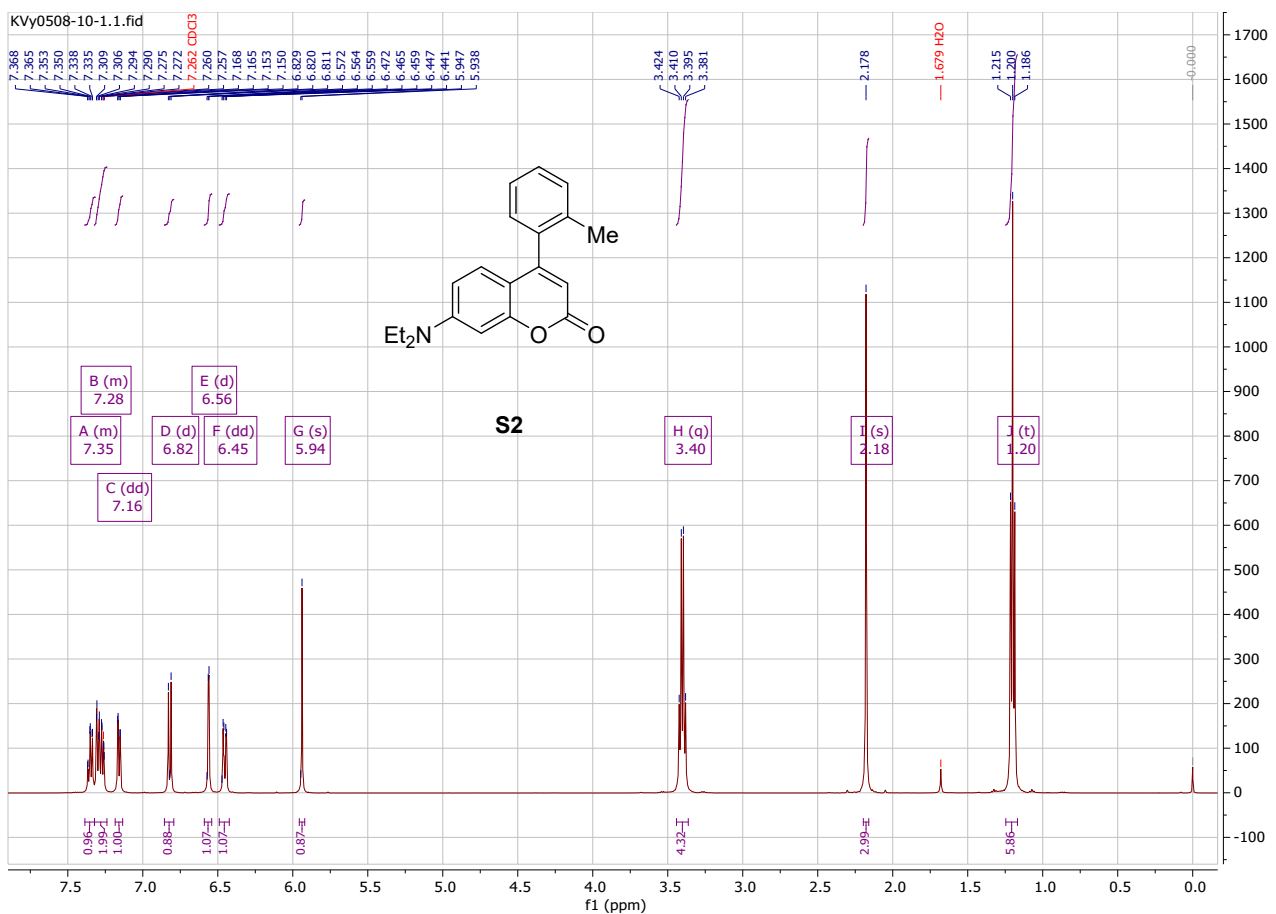
¹H NMR (500 MHz, CDCl₃) δ 8.07 (dd, *J* = 8.1, 1.5 Hz, 1H, H-Ar), 7.96 (d, *J* = 9.3 Hz, 1H, H-Ar), 7.66 (ddd, *J* = 8.5, 7.2, 1.5 Hz, 1H, H-Ar), 7.42 (dd, *J* = 8.4, 1.2 Hz, 1H, H-Ar), 7.35 (ddd, *J* = 8.3, 7.3, 1.3 Hz, 1H, H-Ar), 6.75 (dd, *J* = 9.4, 2.7 Hz, 1H, H-Ar), 6.60 (d, *J* = 2.6 Hz, 1H, H-Ar), 3.50 (q, *J* = 7.2 Hz, 4H, CH₂), 1.28 (t, *J* = 7.2 Hz, 6H, CH₃); ¹³C NMR (126 MHz, CDCl₃) δ 190.6, 190.5, 158.6, 155.2, 153.3, 139.8, 134.1, 131.0, 129.2, 124.8, 121.1, 117.3, 117.0, 111.3, 105.6, 97.0, 45.4, 12.5; HRMS (EI) calc. for C₂₀H₁₇NO₂S₂ 367.0701 M⁺, found 367.0706.

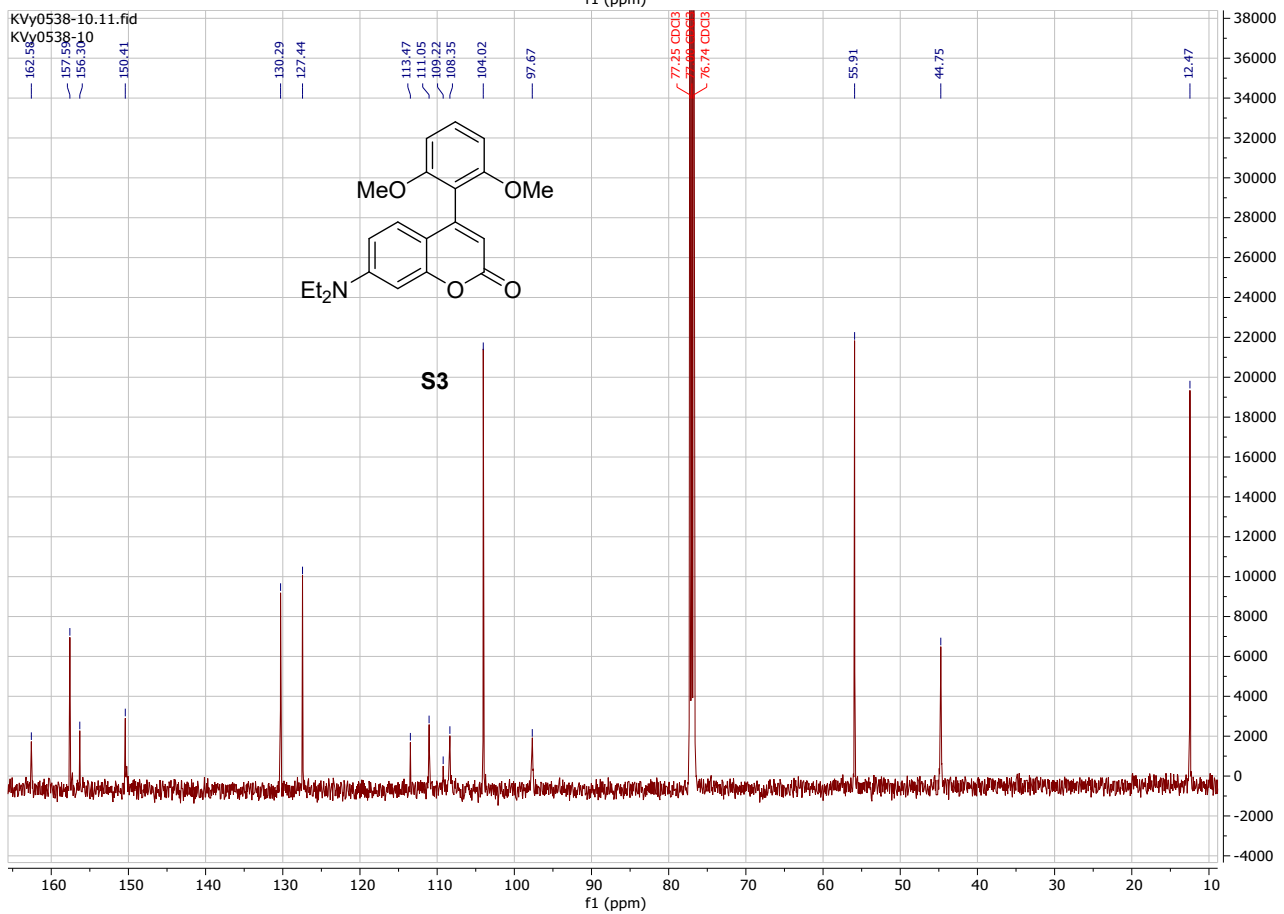
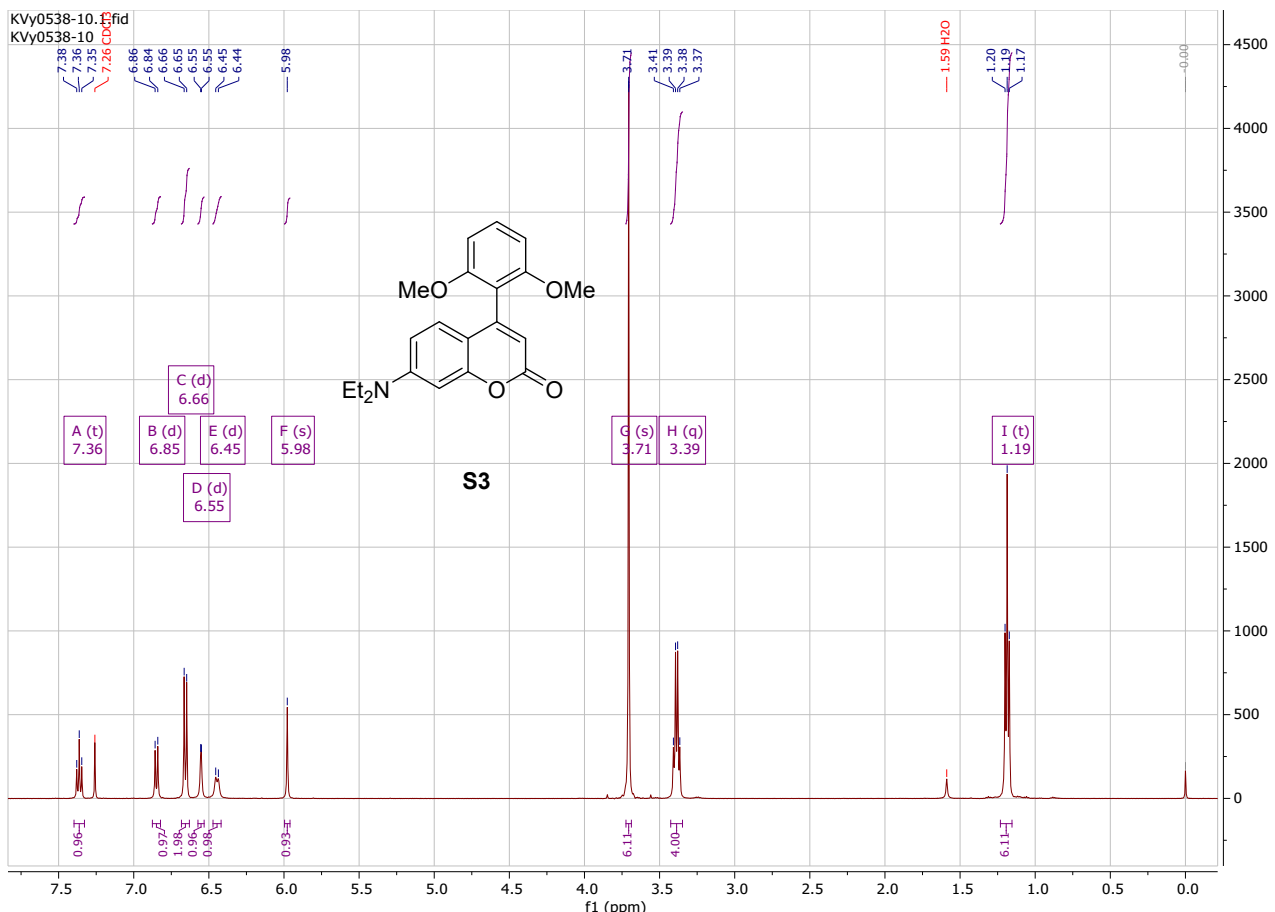
Compound **S23**. Yield 30%. M.p. 294-295°C

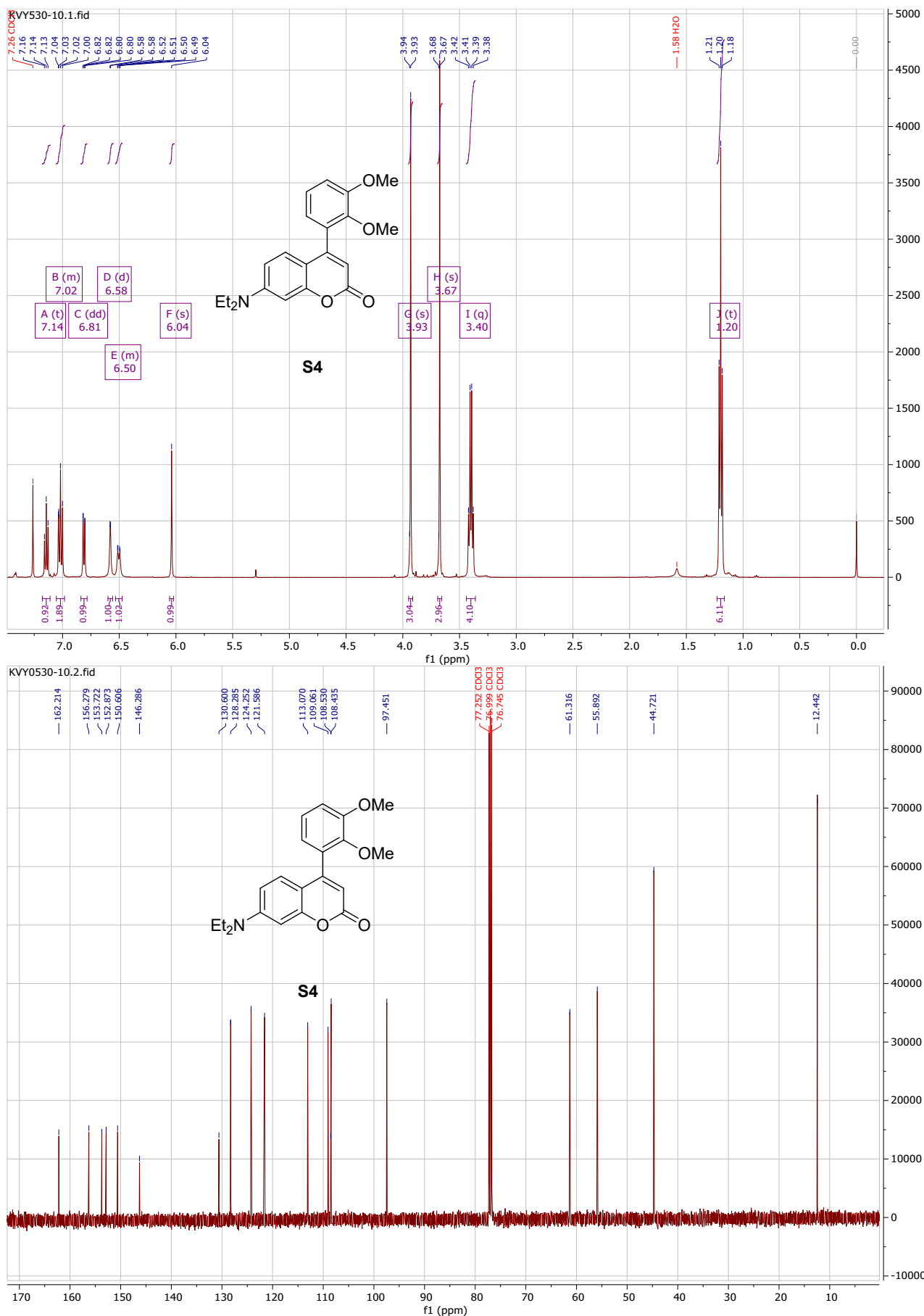


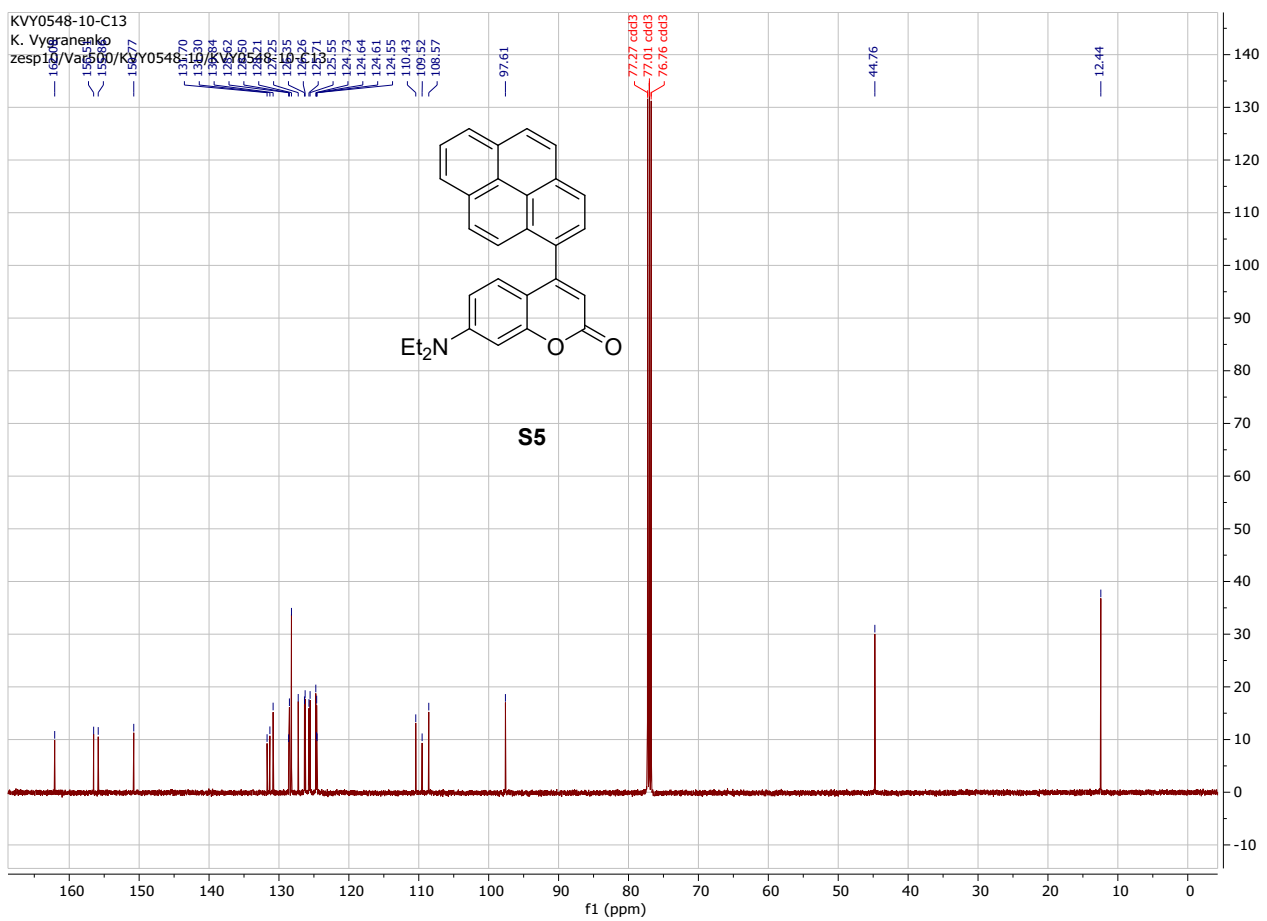
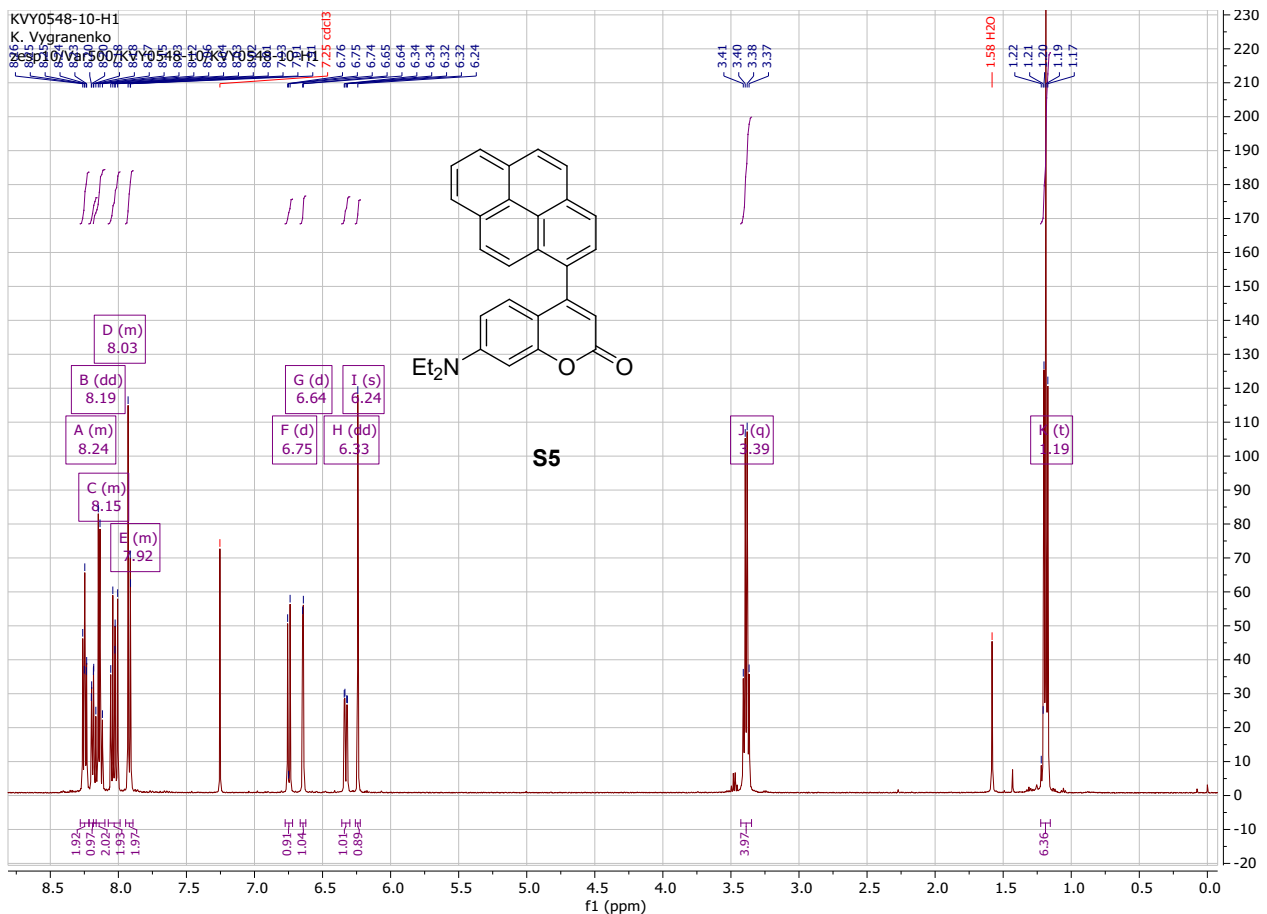
0,03 mmol of compound **S22**, 0,072 mmol of Cs₂CO₃ and 0,3 mmol od dimethyl 1,3-acetonedicarboxylate were mixed together in 2 ml of CH₃CN and were allowed to stir at r.t. overnight. The solvent was evaporated and the residue was purified using DCVC (0,1-2% MeOH in CH₂Cl₂).

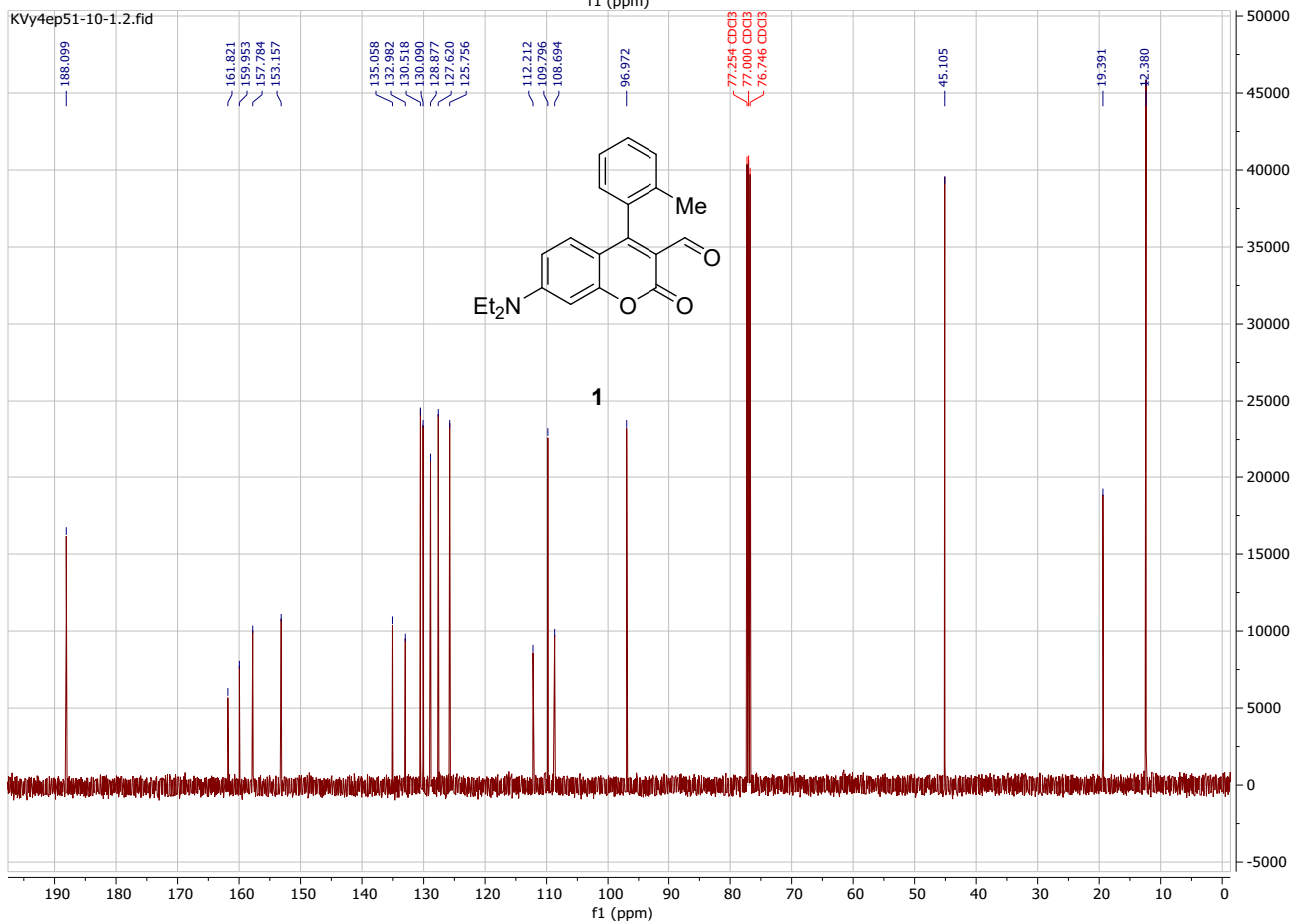
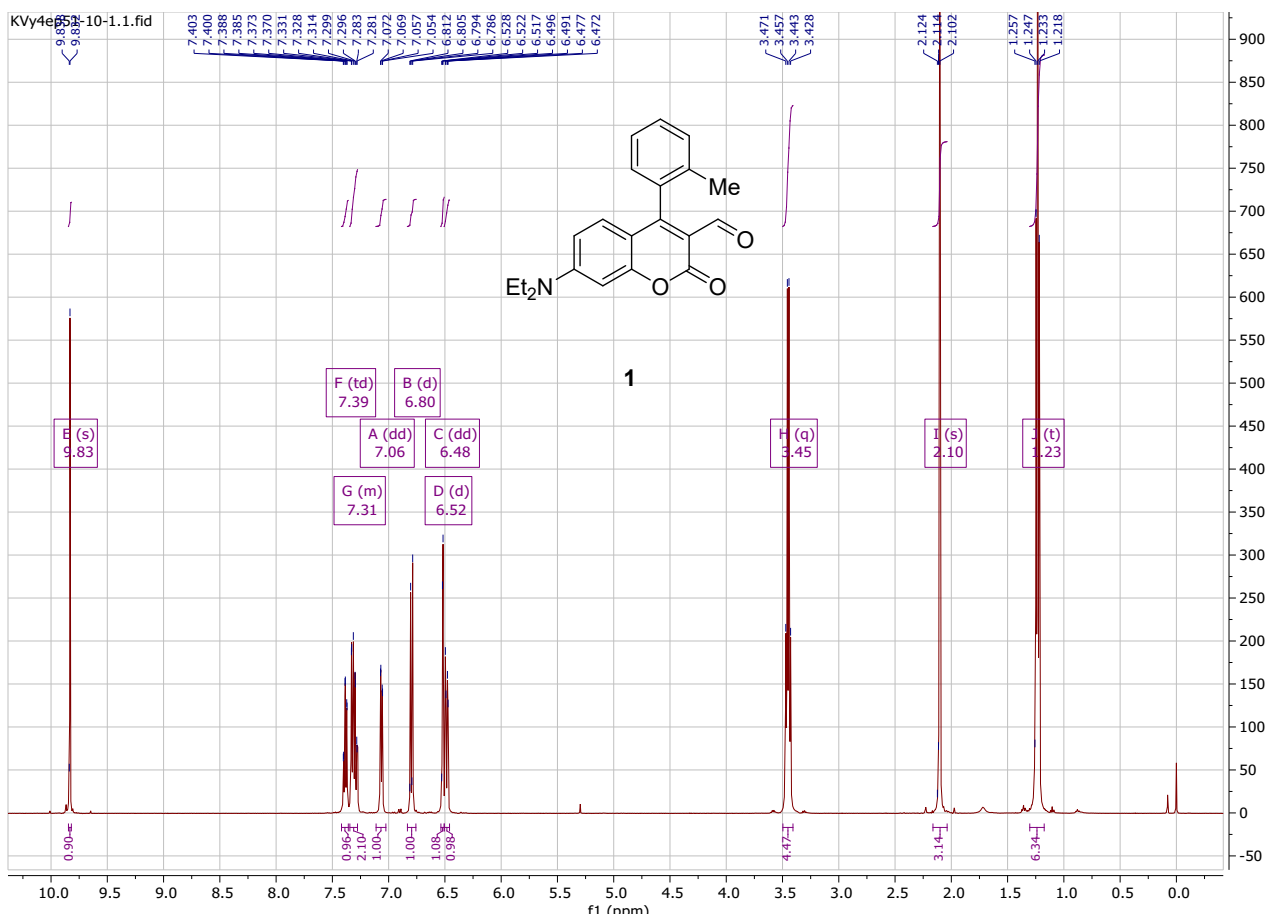
¹H NMR (500 MHz, CDCl₃) δ 8.27 (d, *J* = 8.1 Hz, 1H, H-Ar), 8.14 (d, *J* = 9.4 Hz, 1H, H-Ar), 7.65 (t, *J* = 7.8 Hz, 1H, H-Ar), 7.46 (d, *J* = 8.3 Hz, 1H, H-Ar), 7.37 (t, *J* = 7.7 Hz, 1H, H-Ar), 6.74 (dd, *J* = 9.4, 2.7 Hz, 1H, H-Ar), 6.55 (d, *J* = 2.6 Hz, 1H, H-Ar), 3.98 (d, *J* = 7.1 Hz, 6H, OCH₃), 3.51 (q, *J* = 7.1 Hz, 4H, CH₂), 1.29 (t, *J* = 7.1 Hz, 6H, CH₃); ¹³C NMR (126 MHz, CDCl₃) δ 175.4, 165.6, 165.4, 157.3, 154.2, 152.8, 151.3, 150.7, 140.1, 134.0, 129.7, 128.2, 124.5, 118.8, 116.3, 110.5, 105.4, 105.1, 98.1, 52.3, 52.3, 45.1, 12.6; HRMS (EI) calc. for C₂₇H₂₃NO₇ 473.1457 M⁺, found 473.1470.

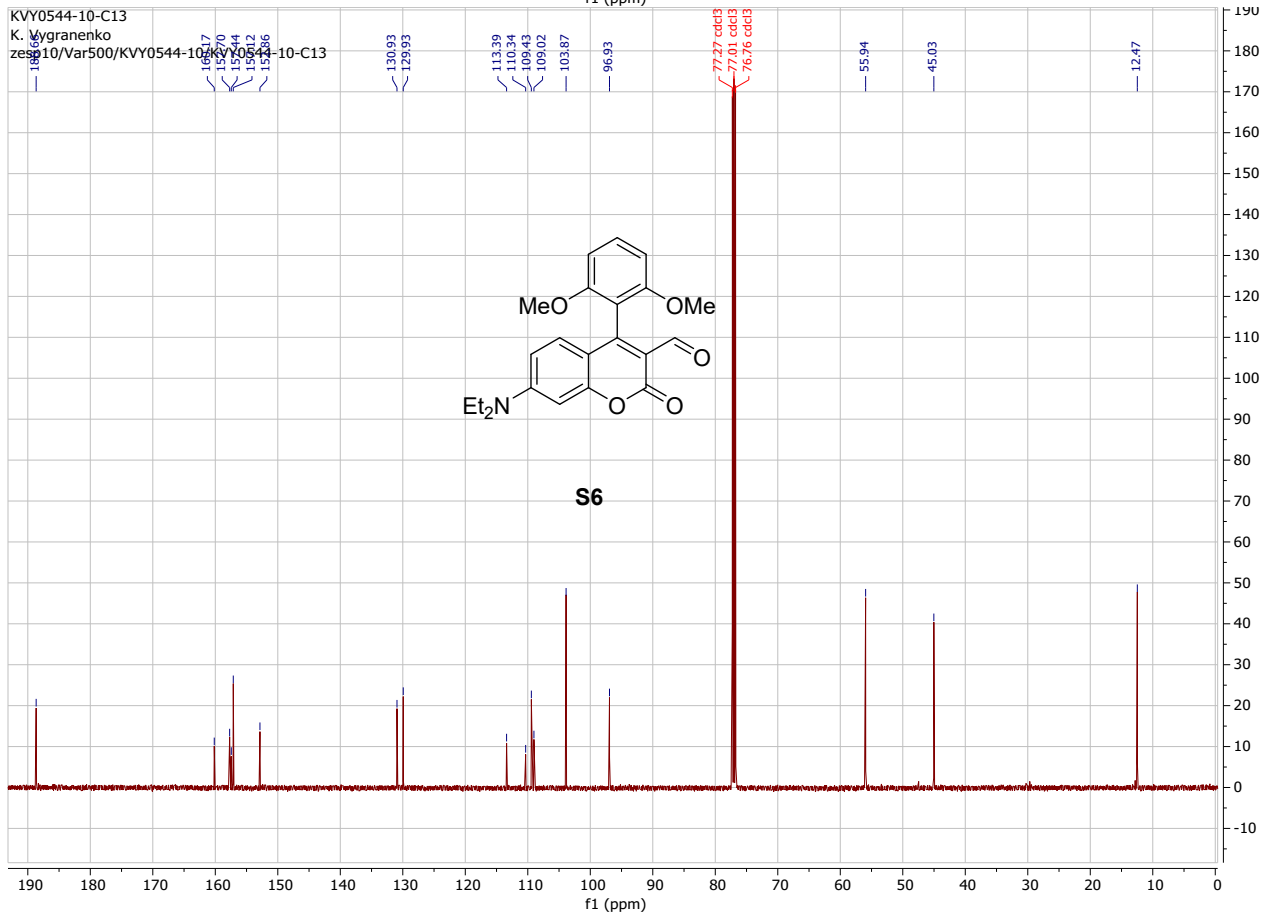
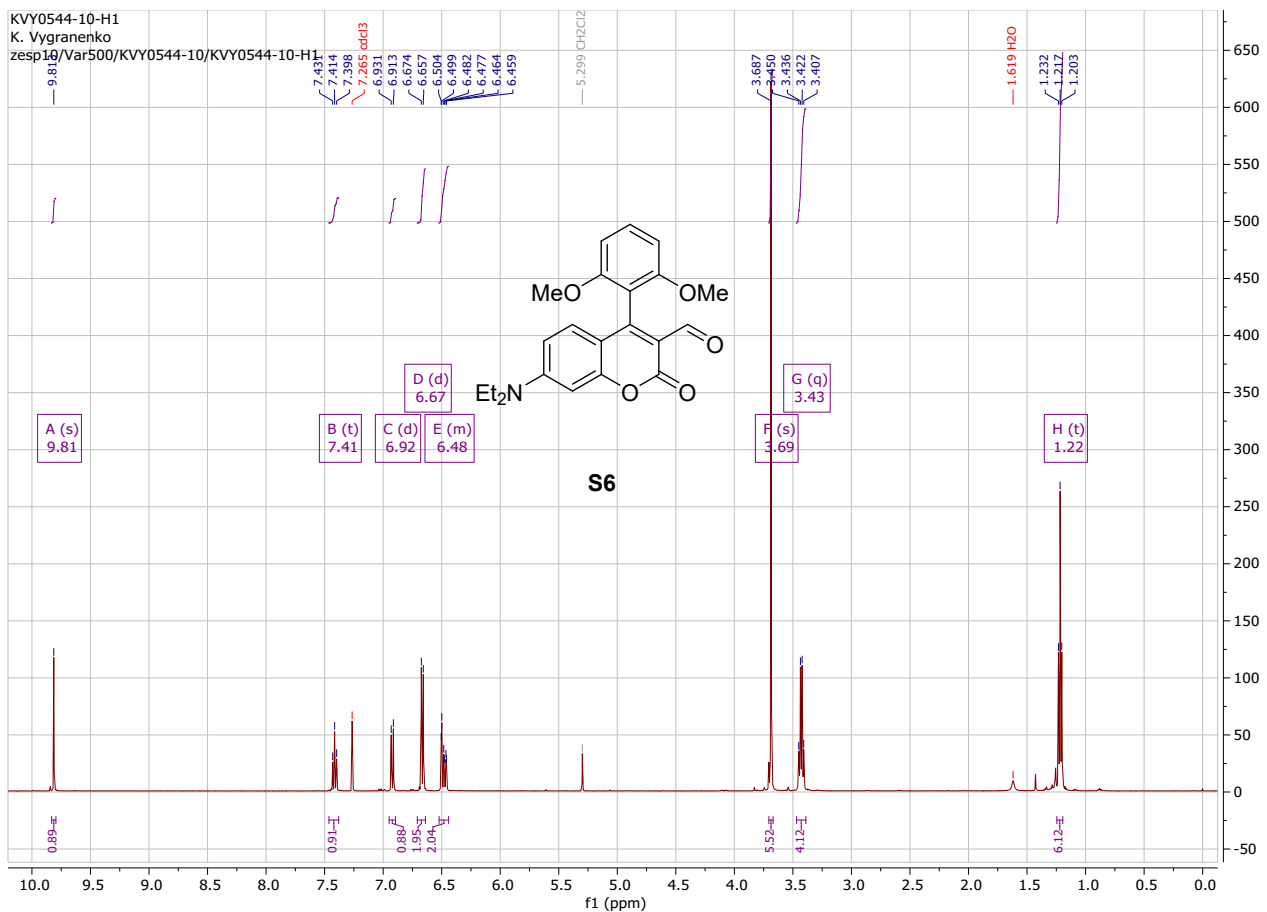


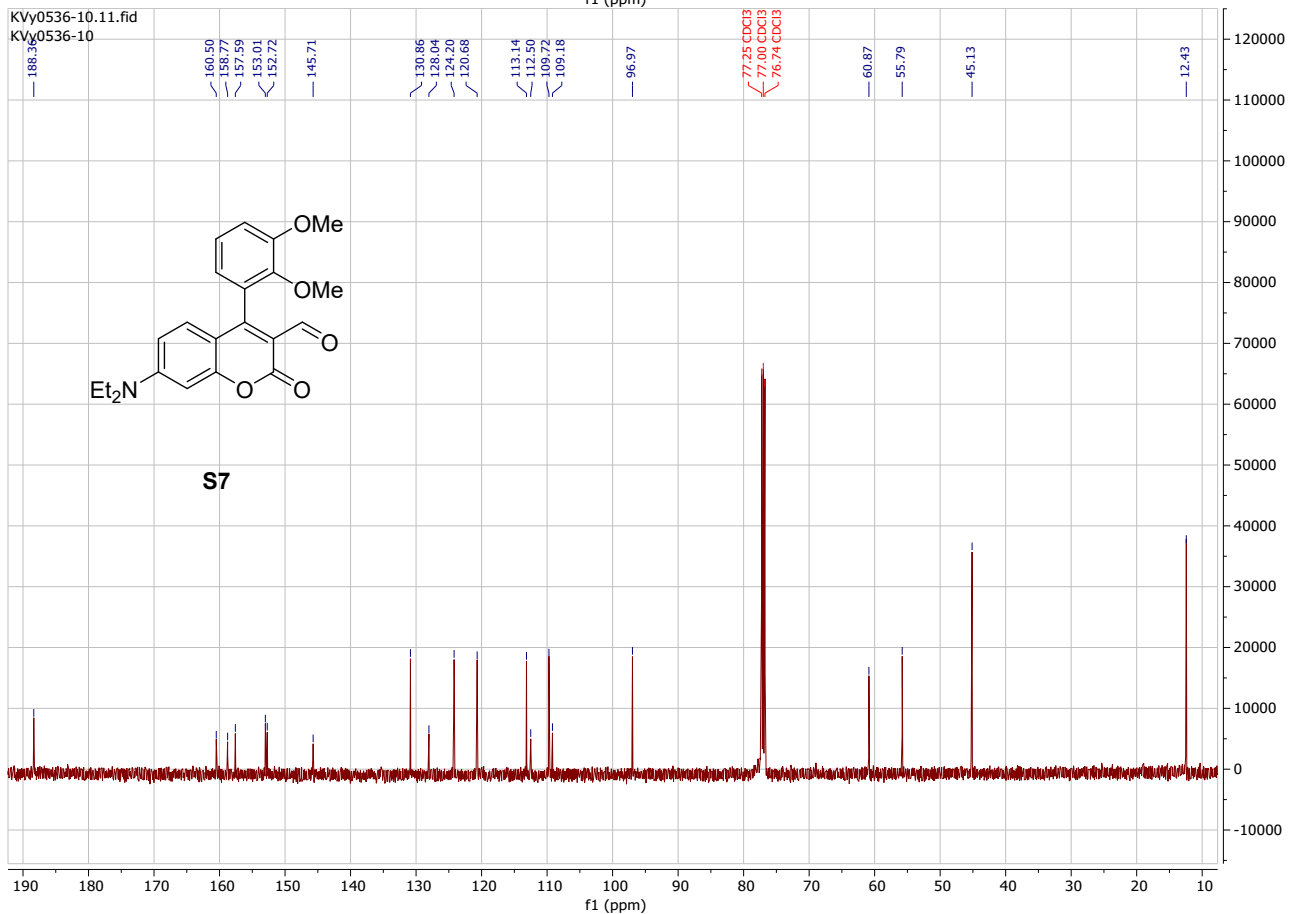
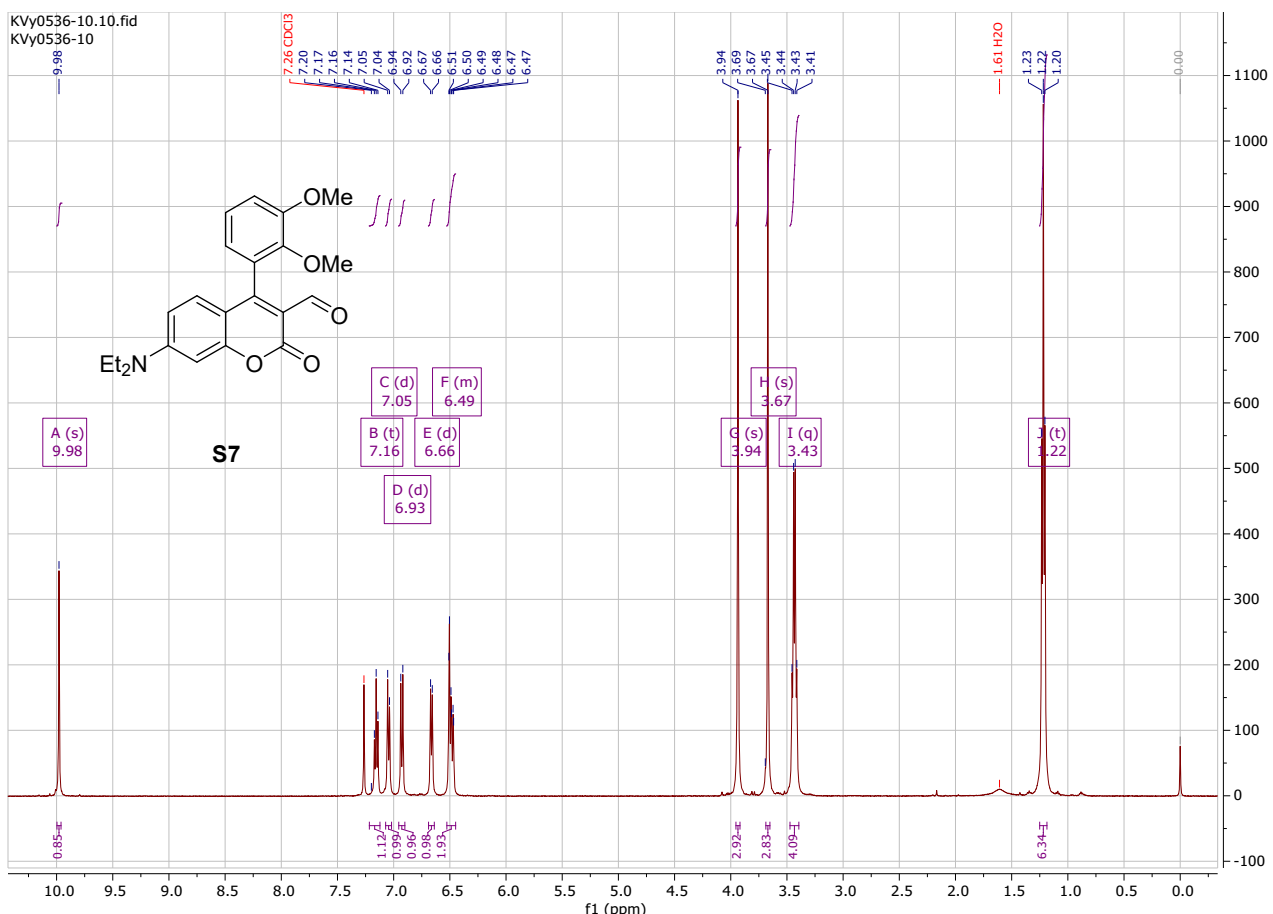


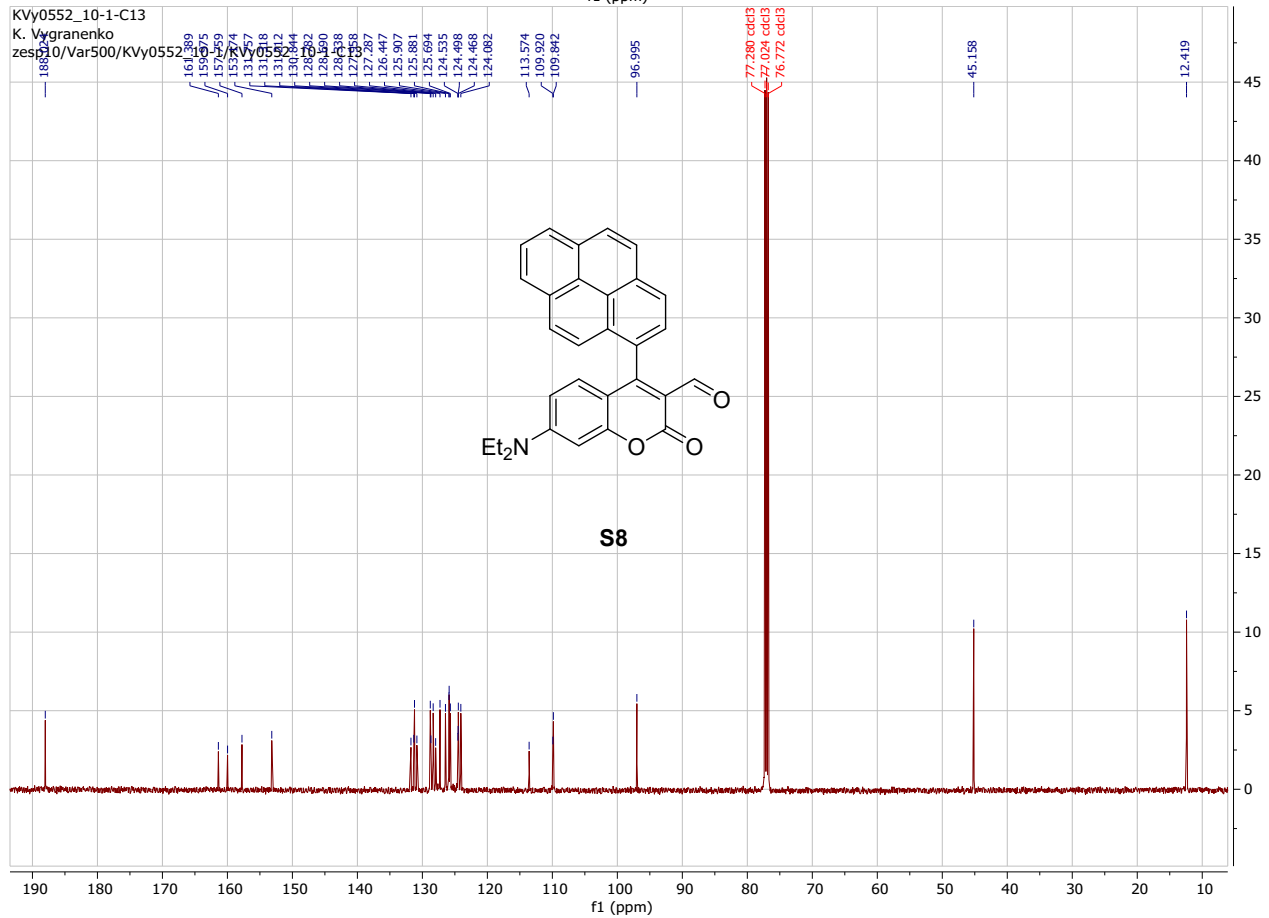
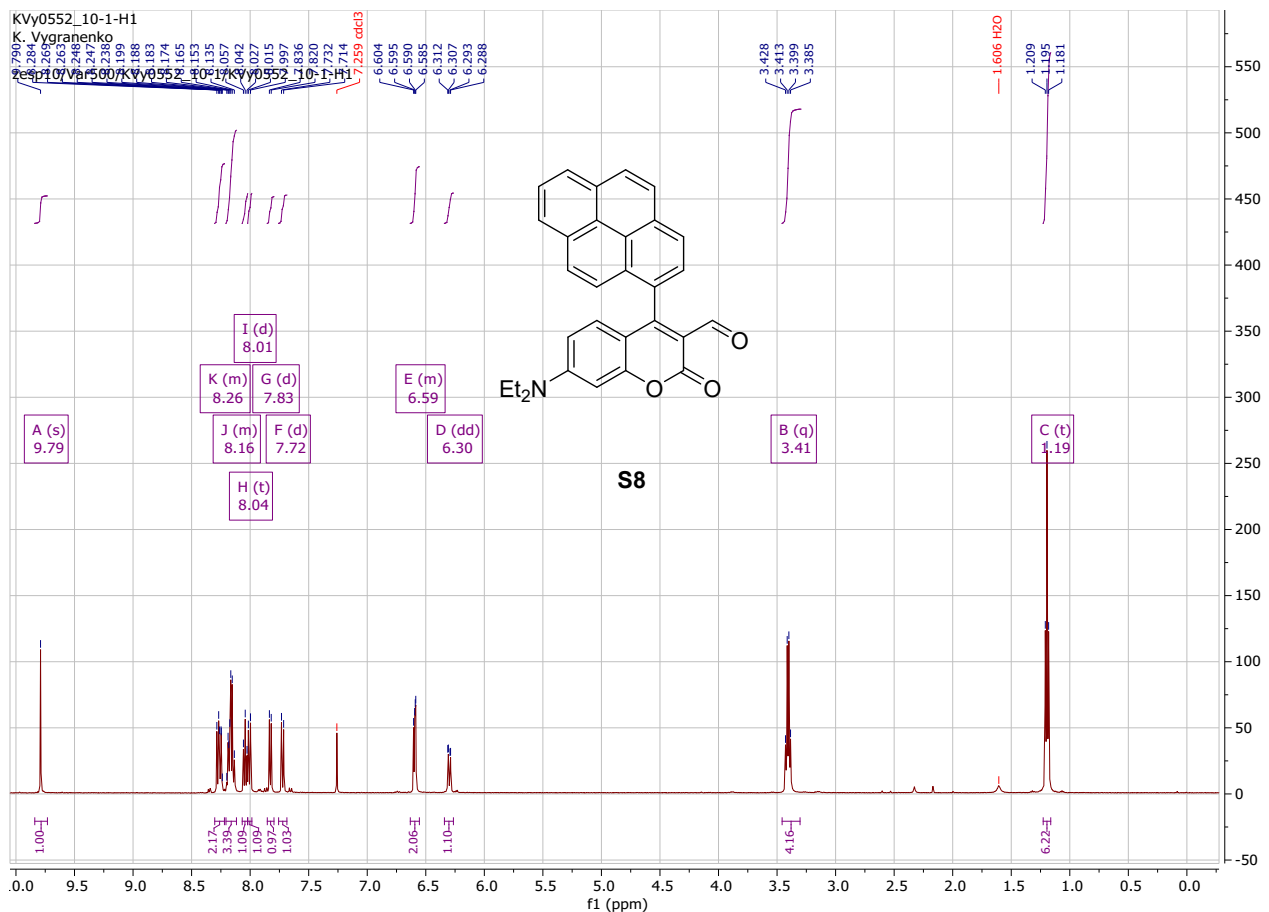


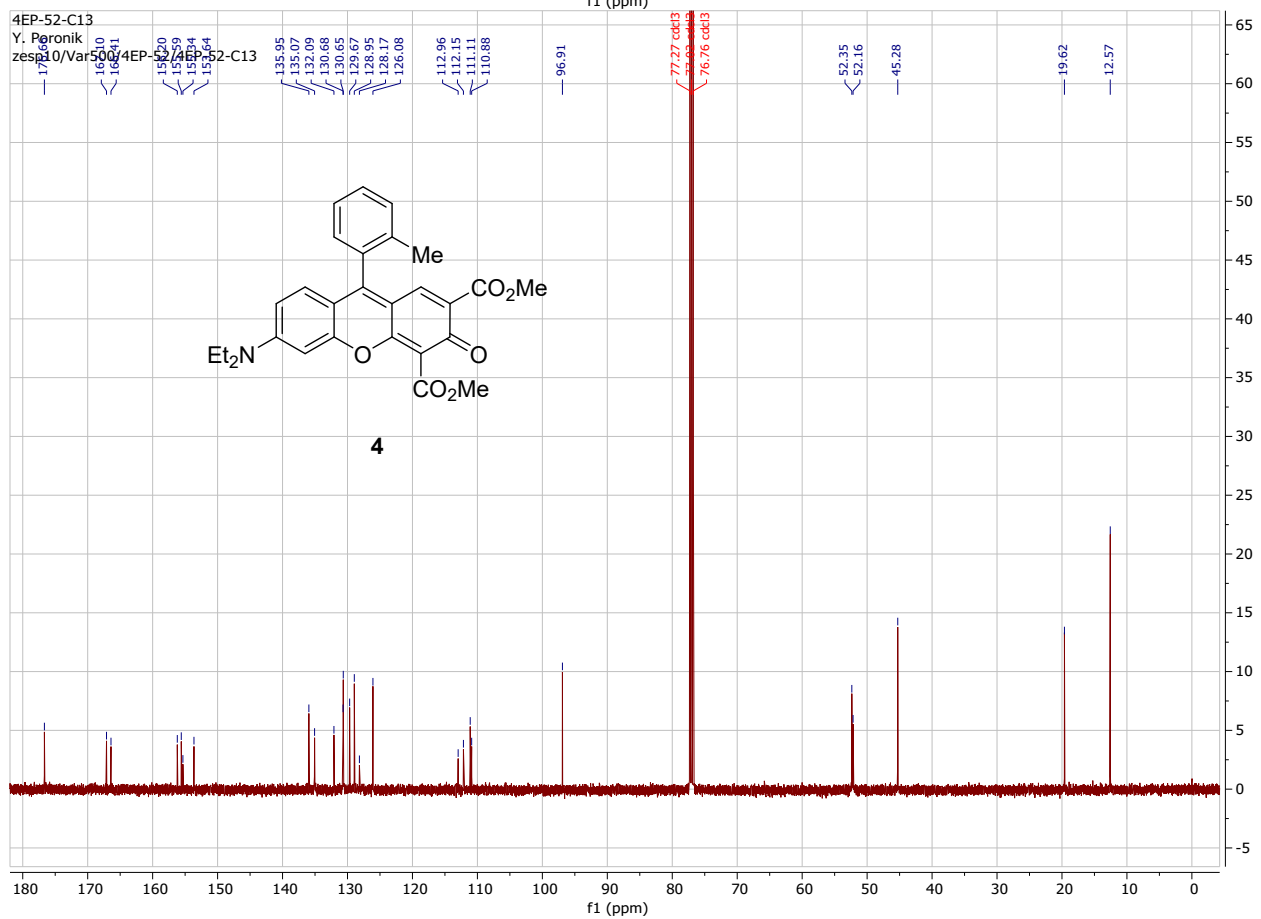
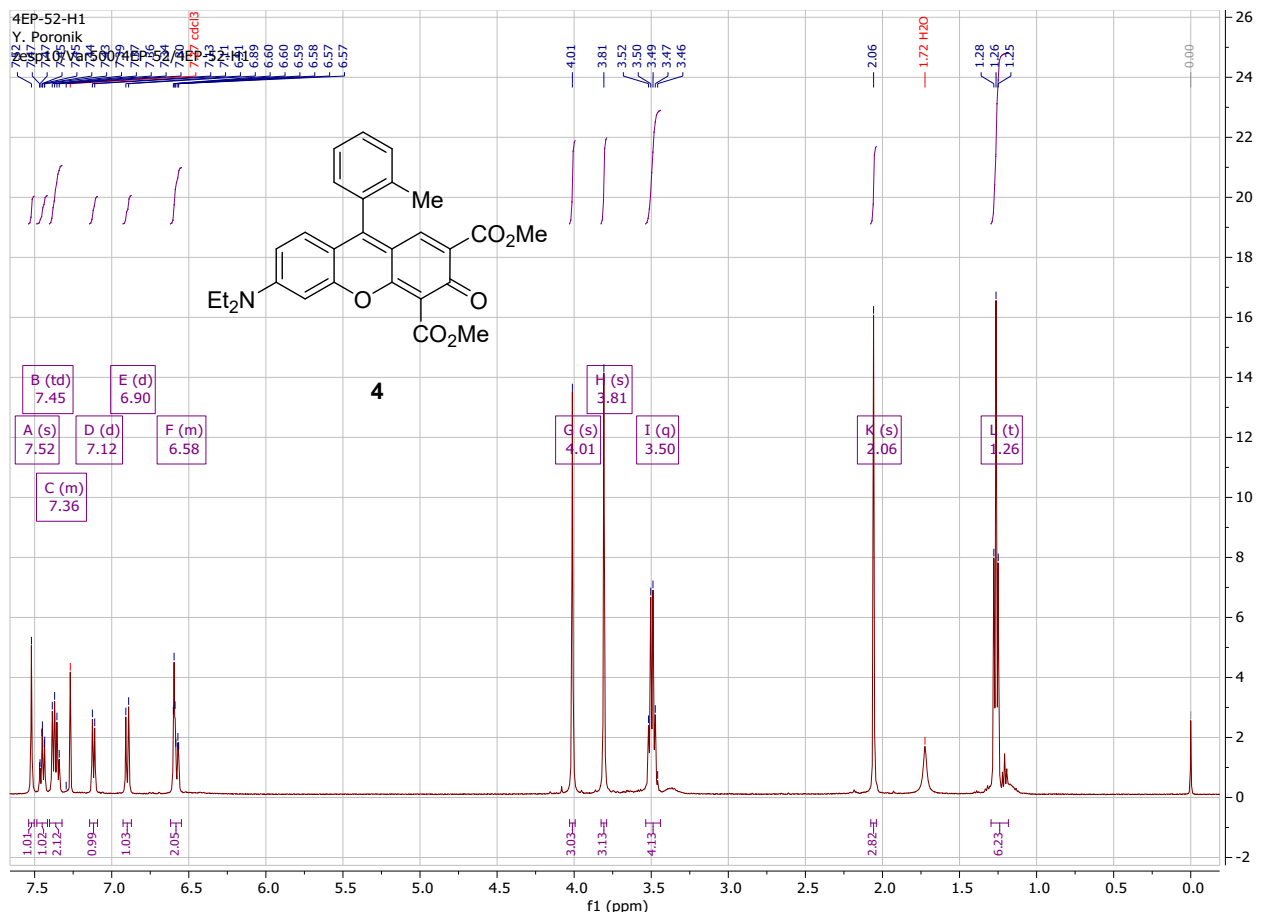


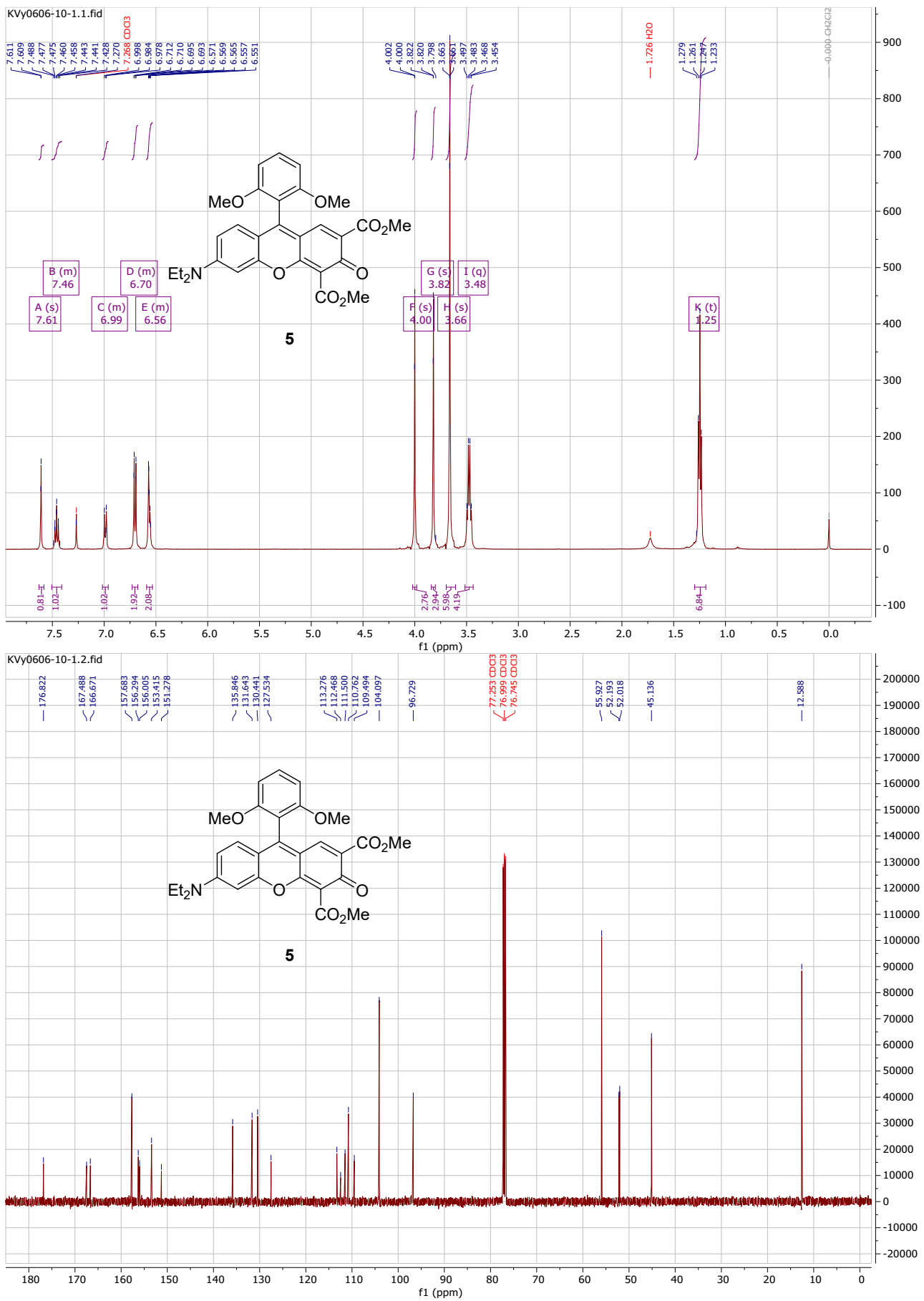


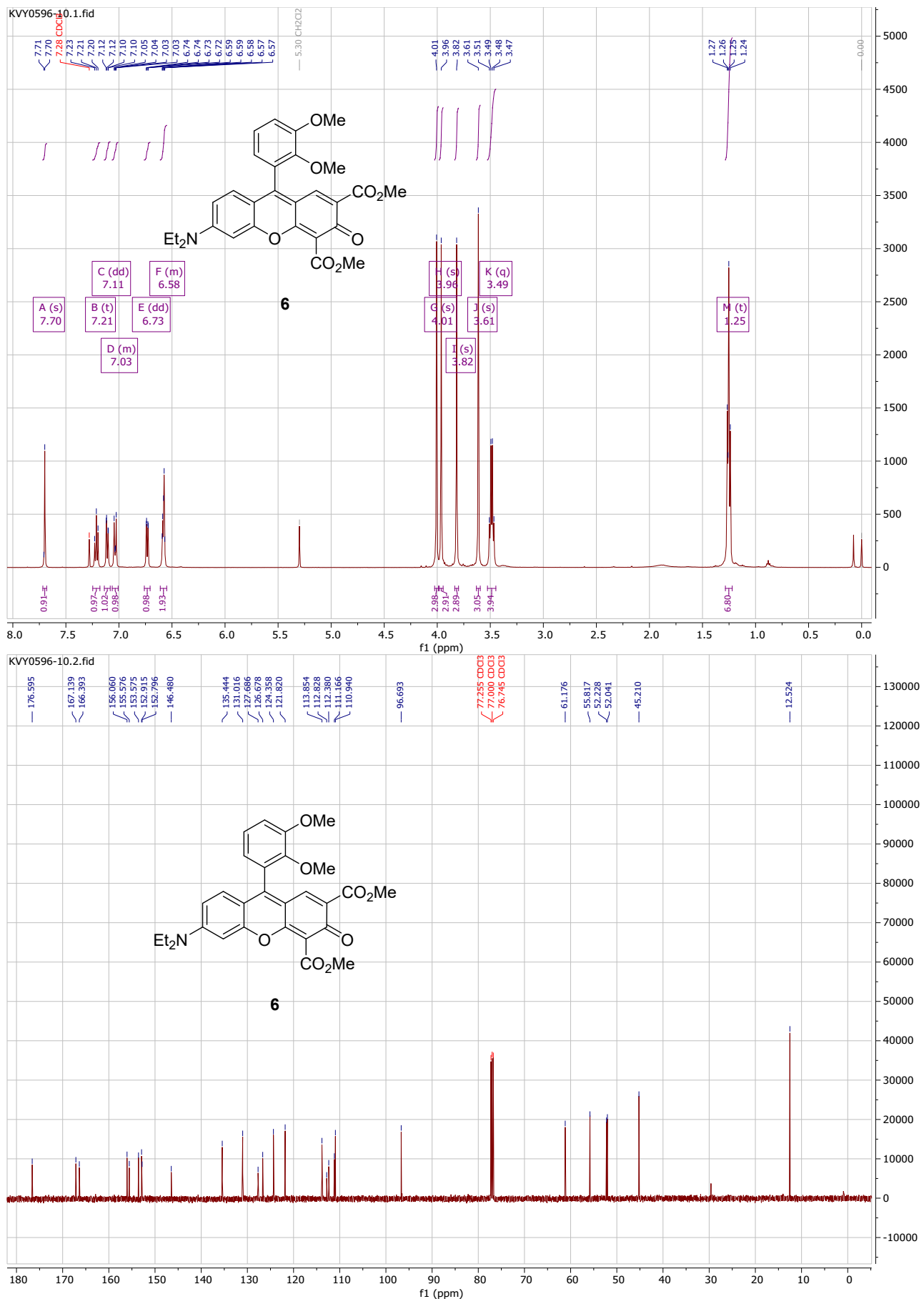


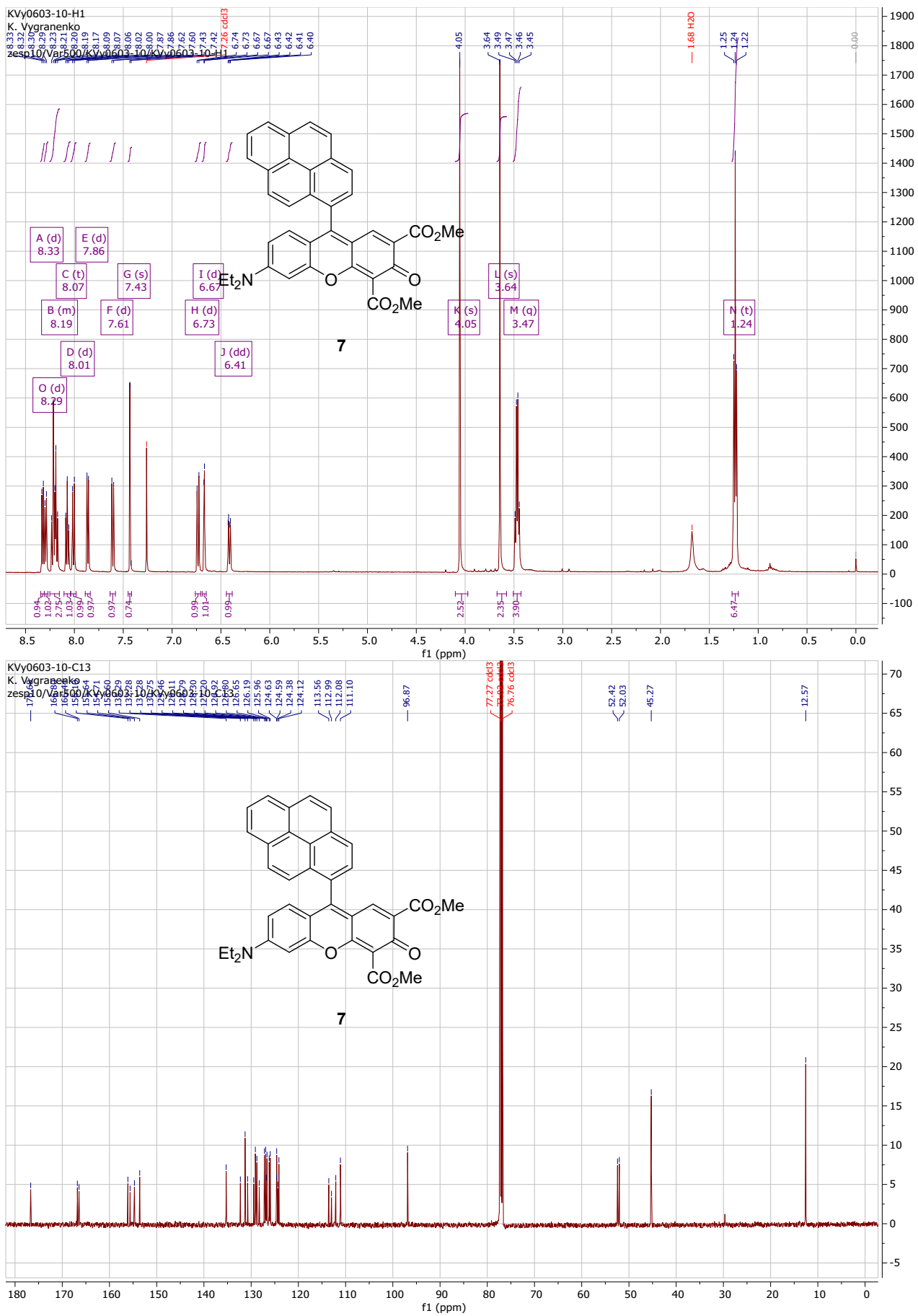


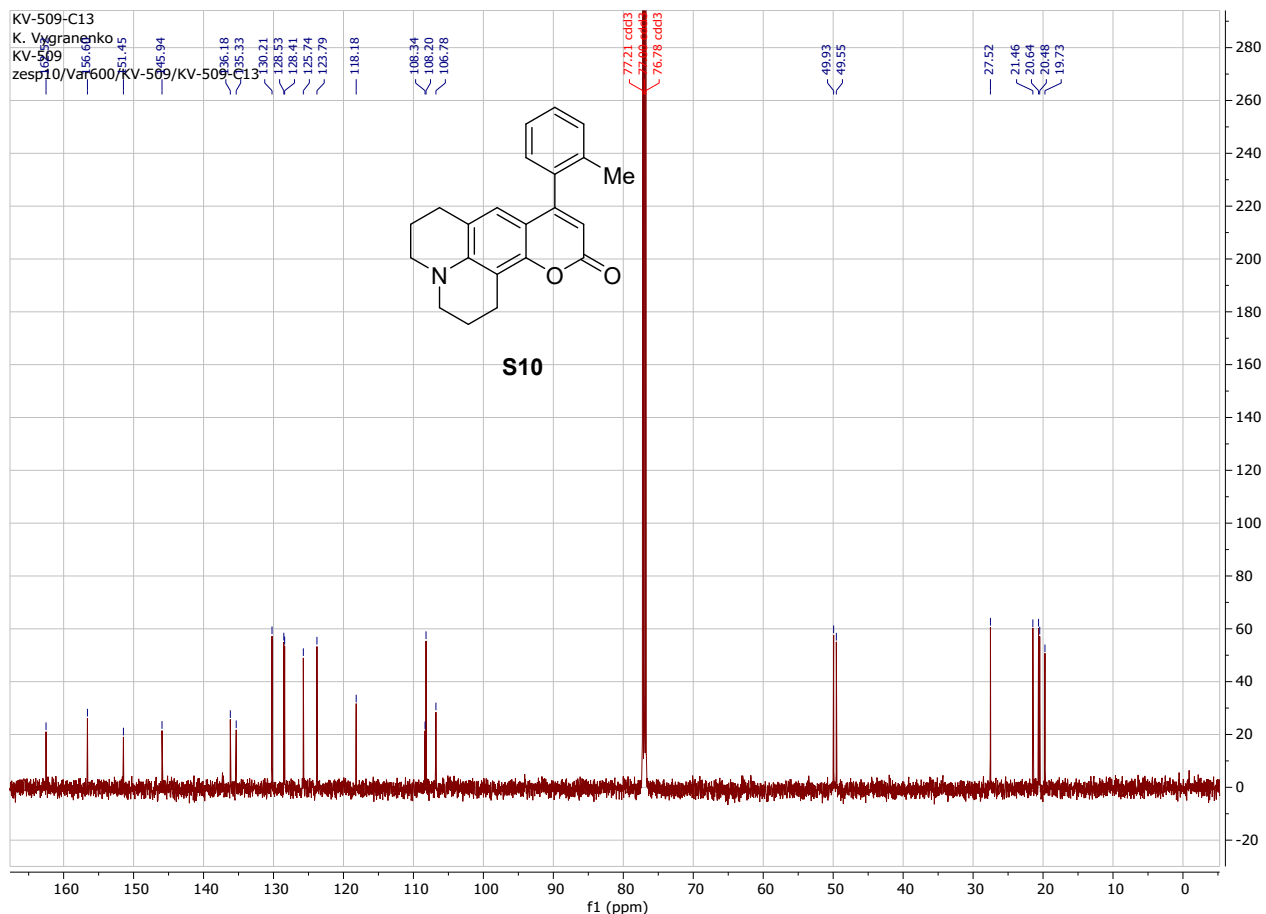
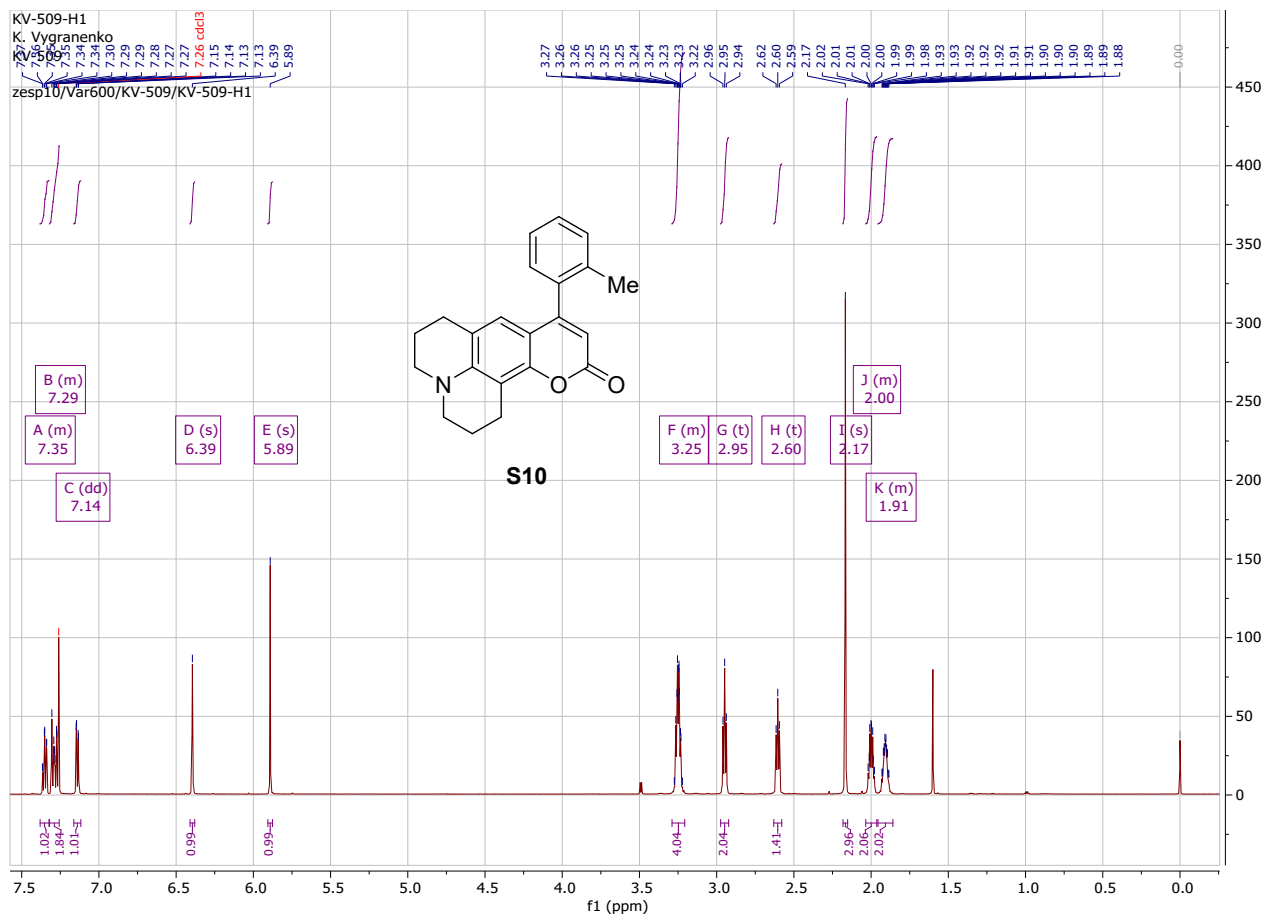


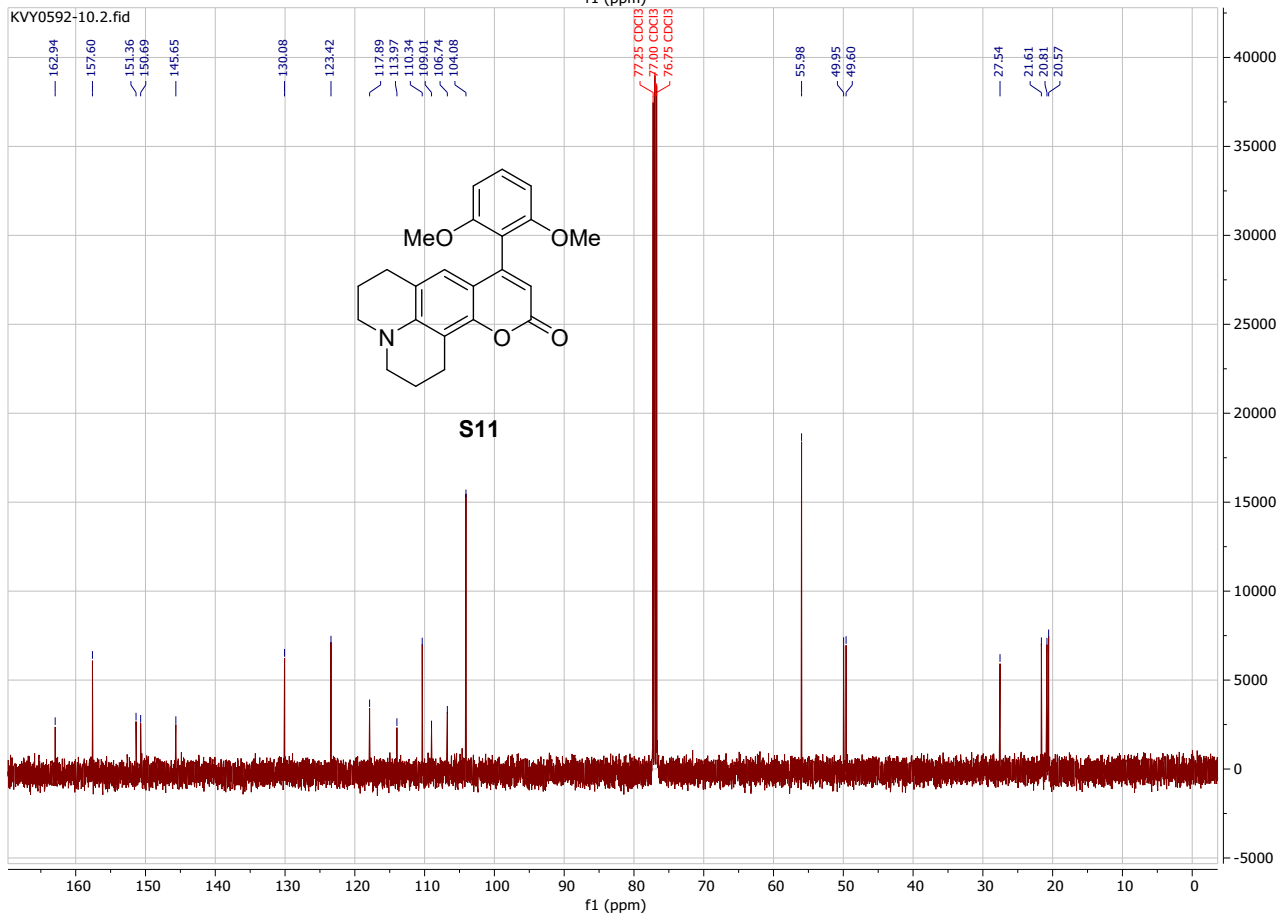
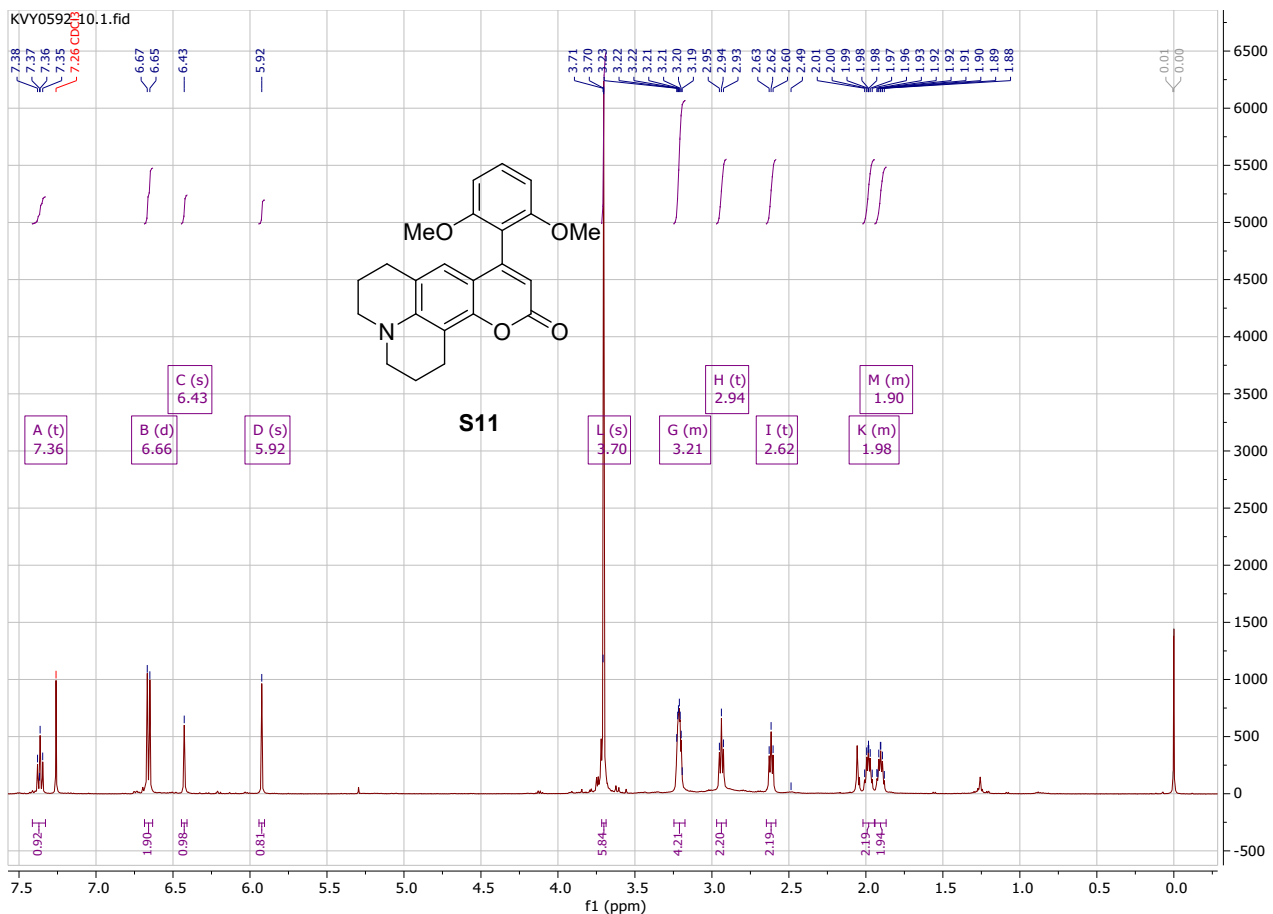


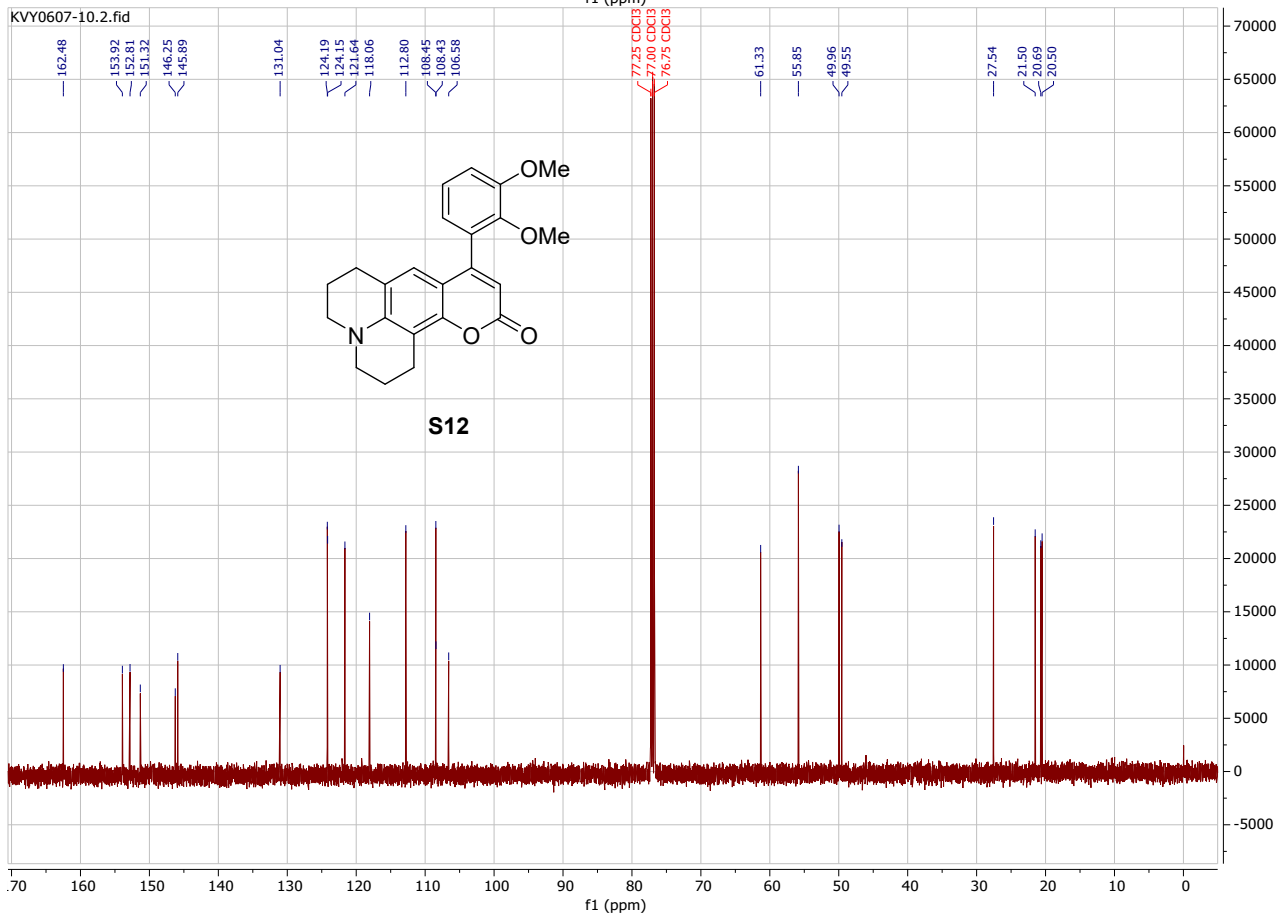
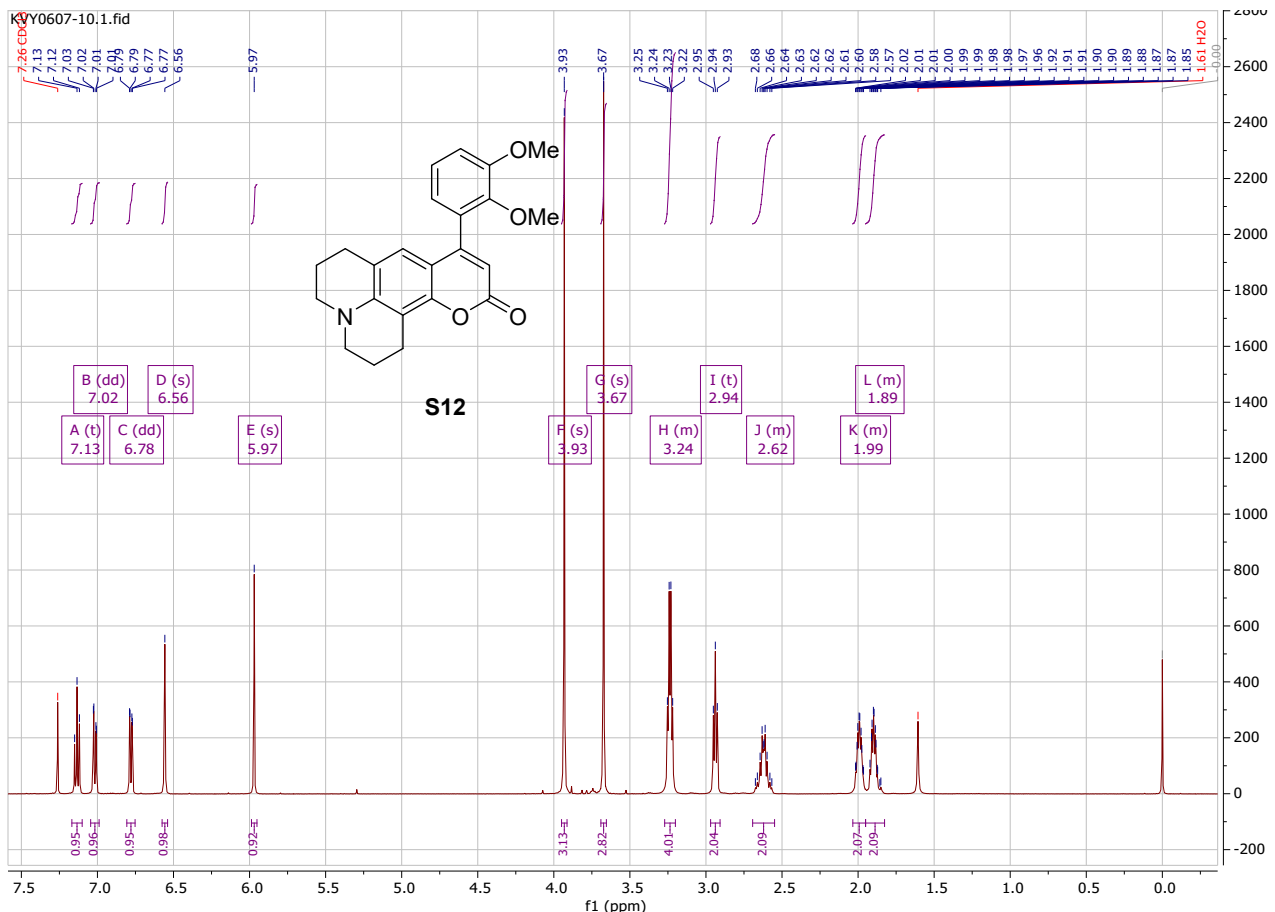


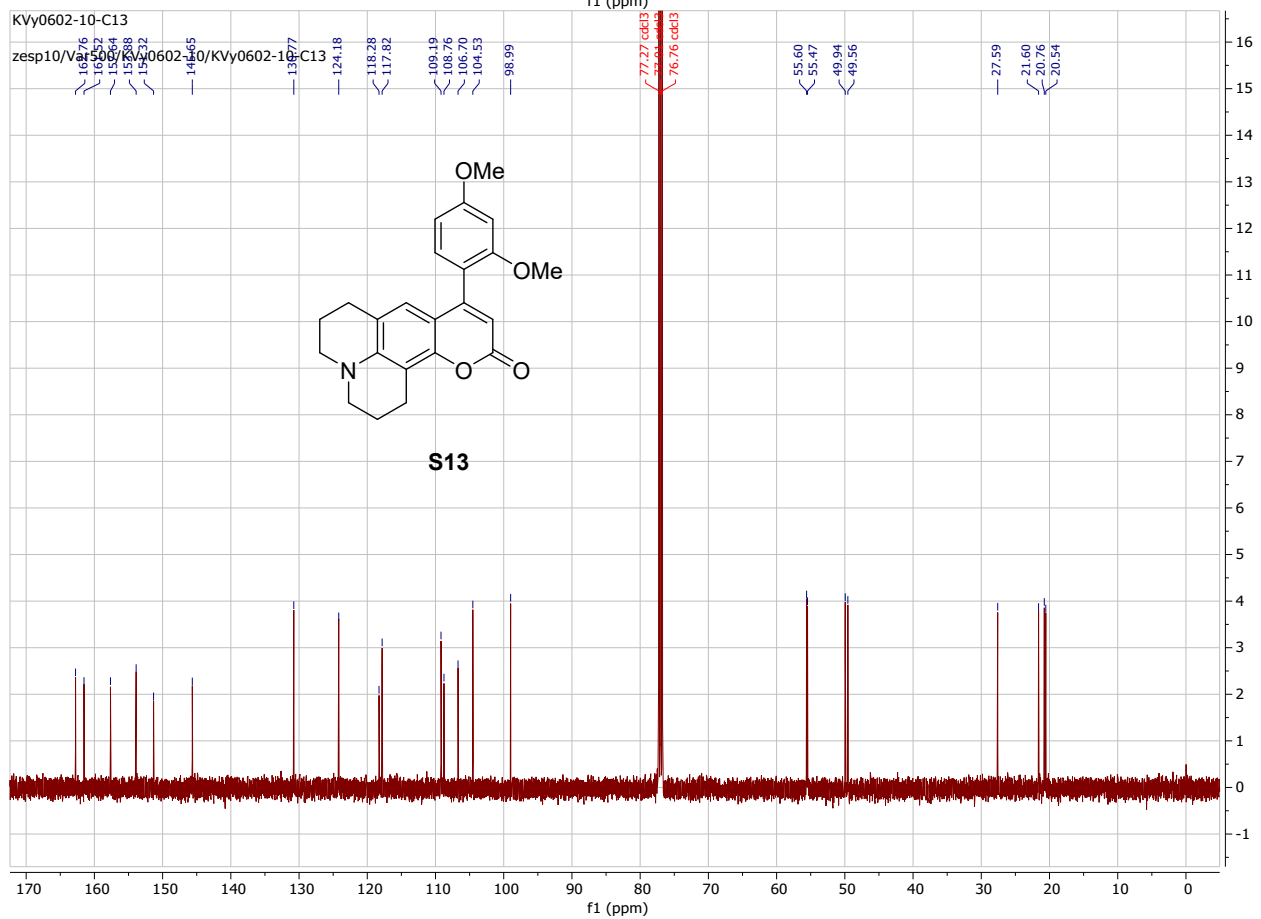
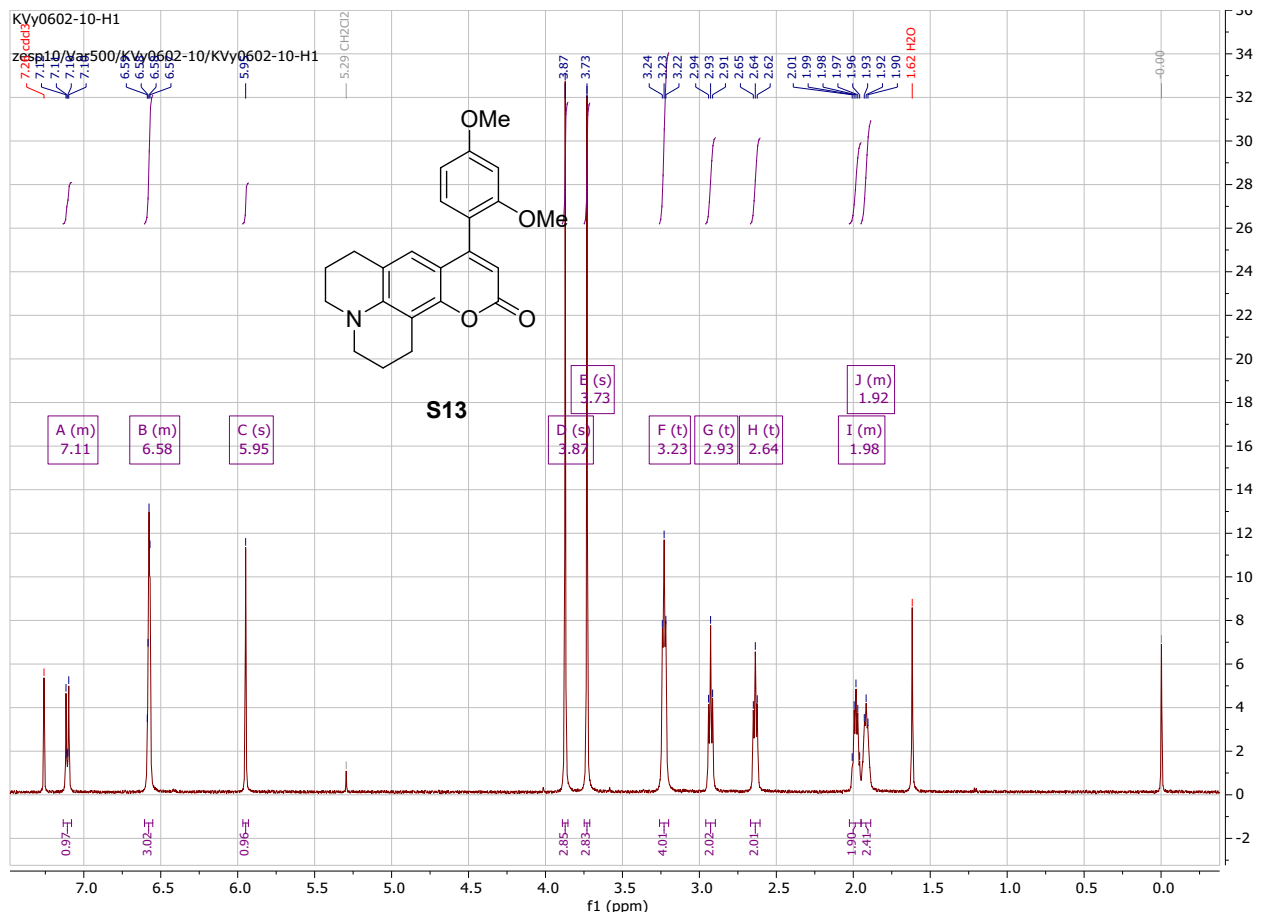


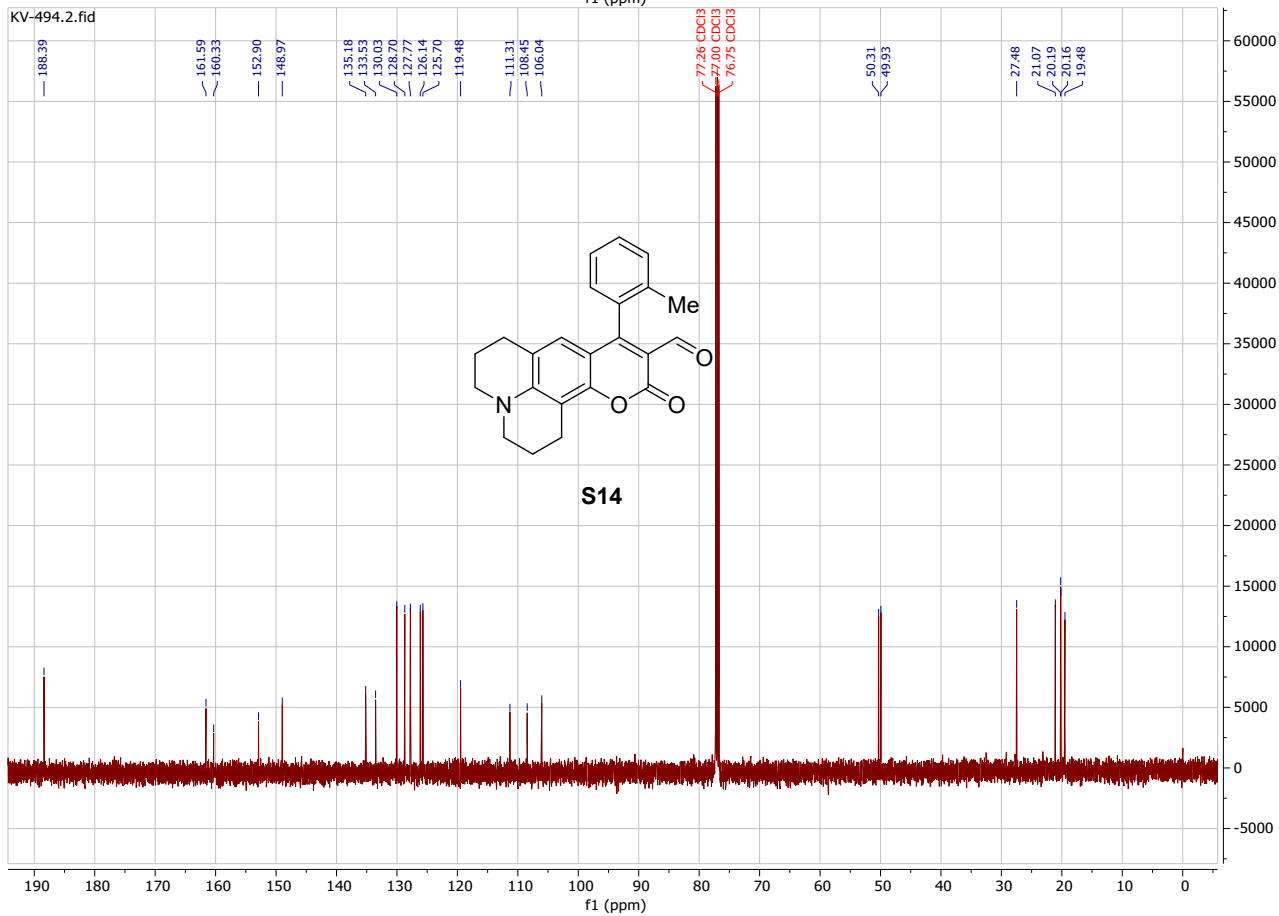
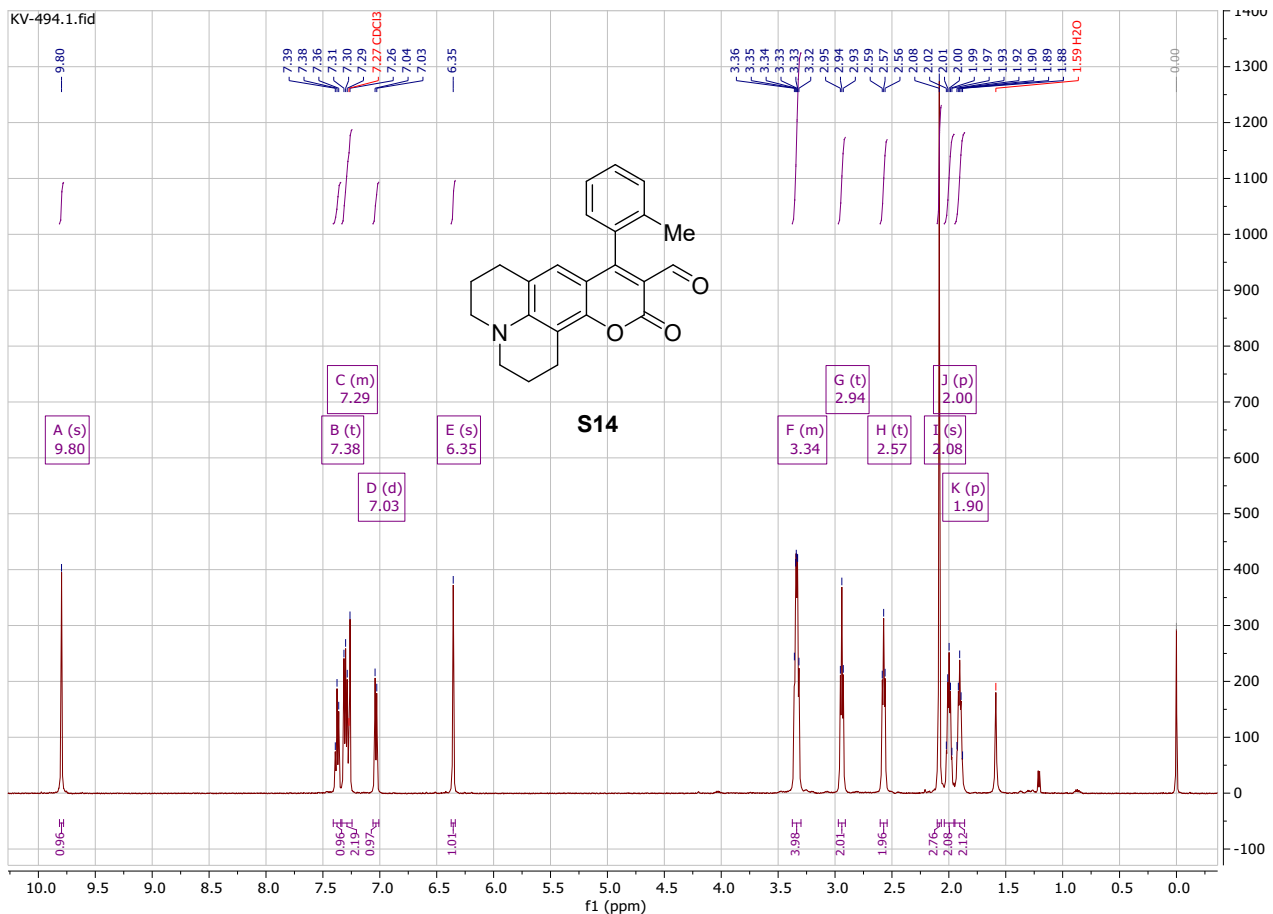


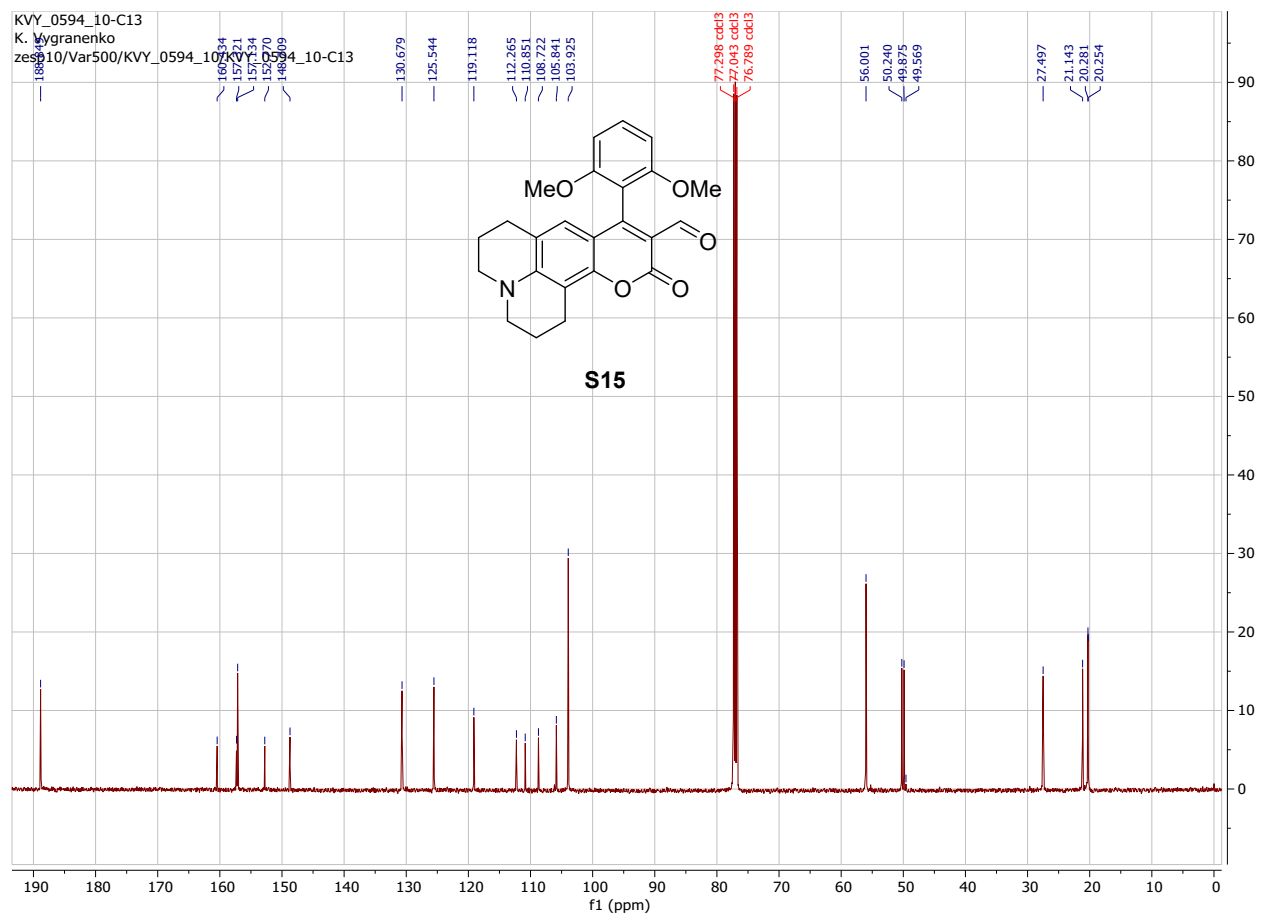
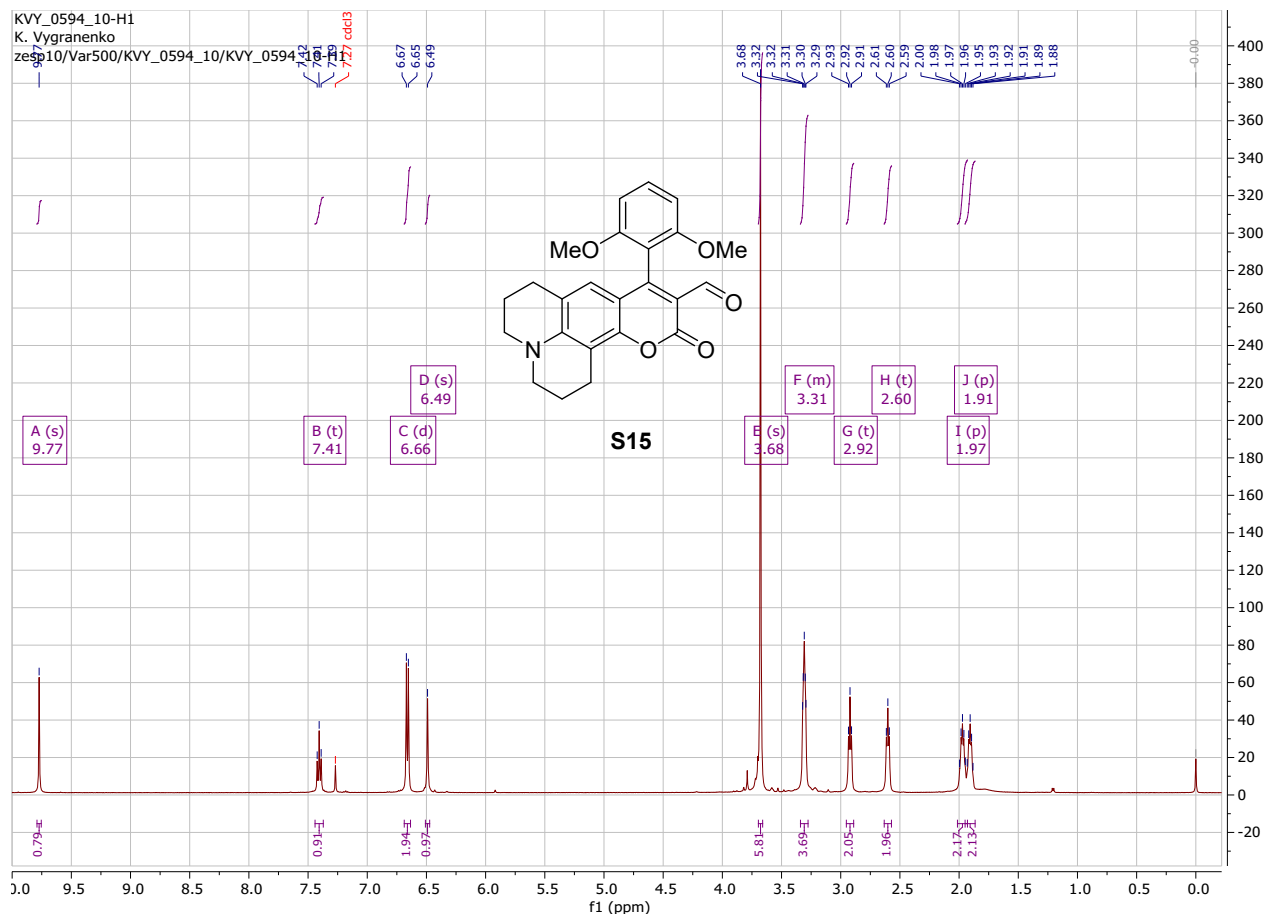


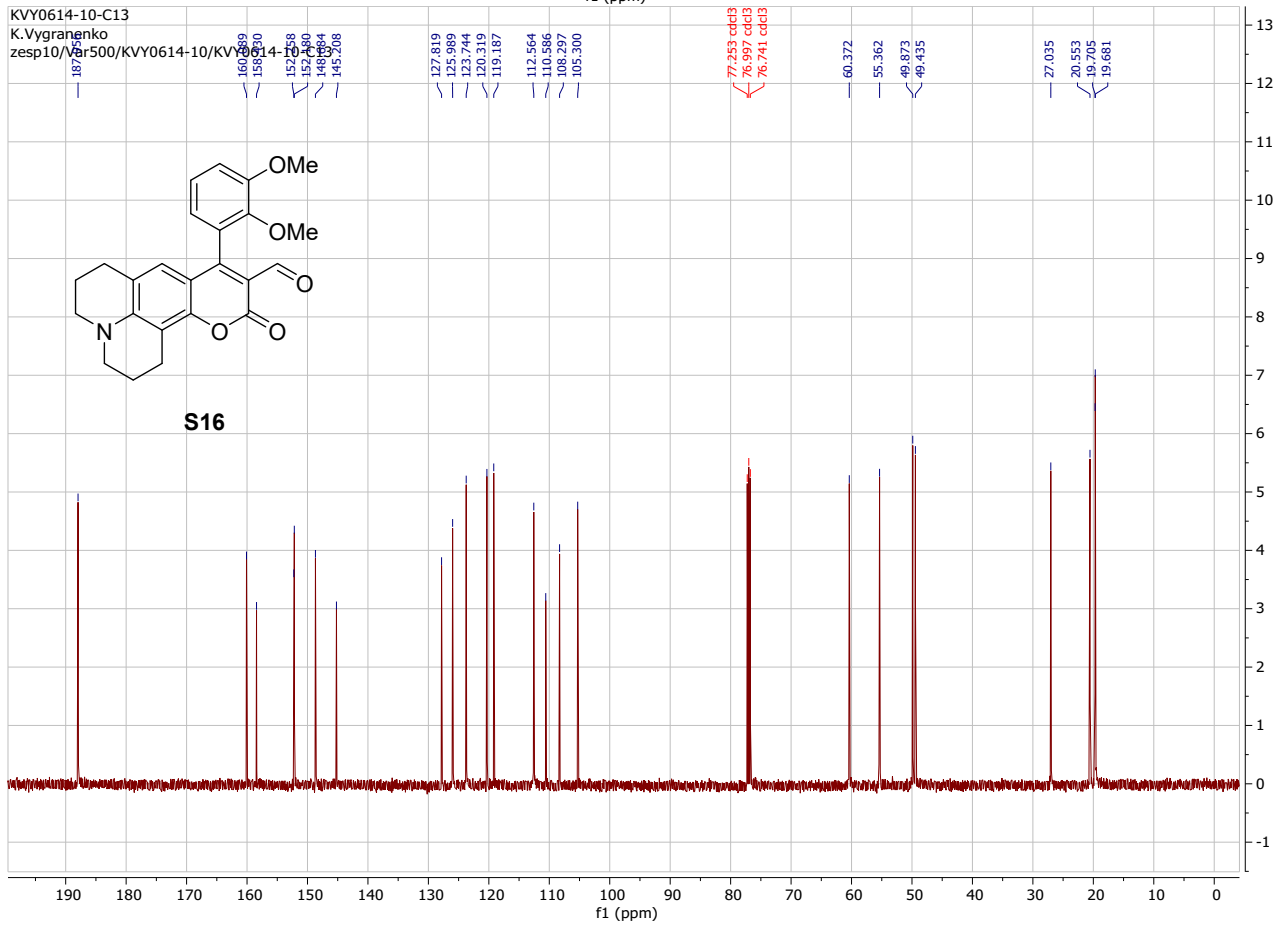
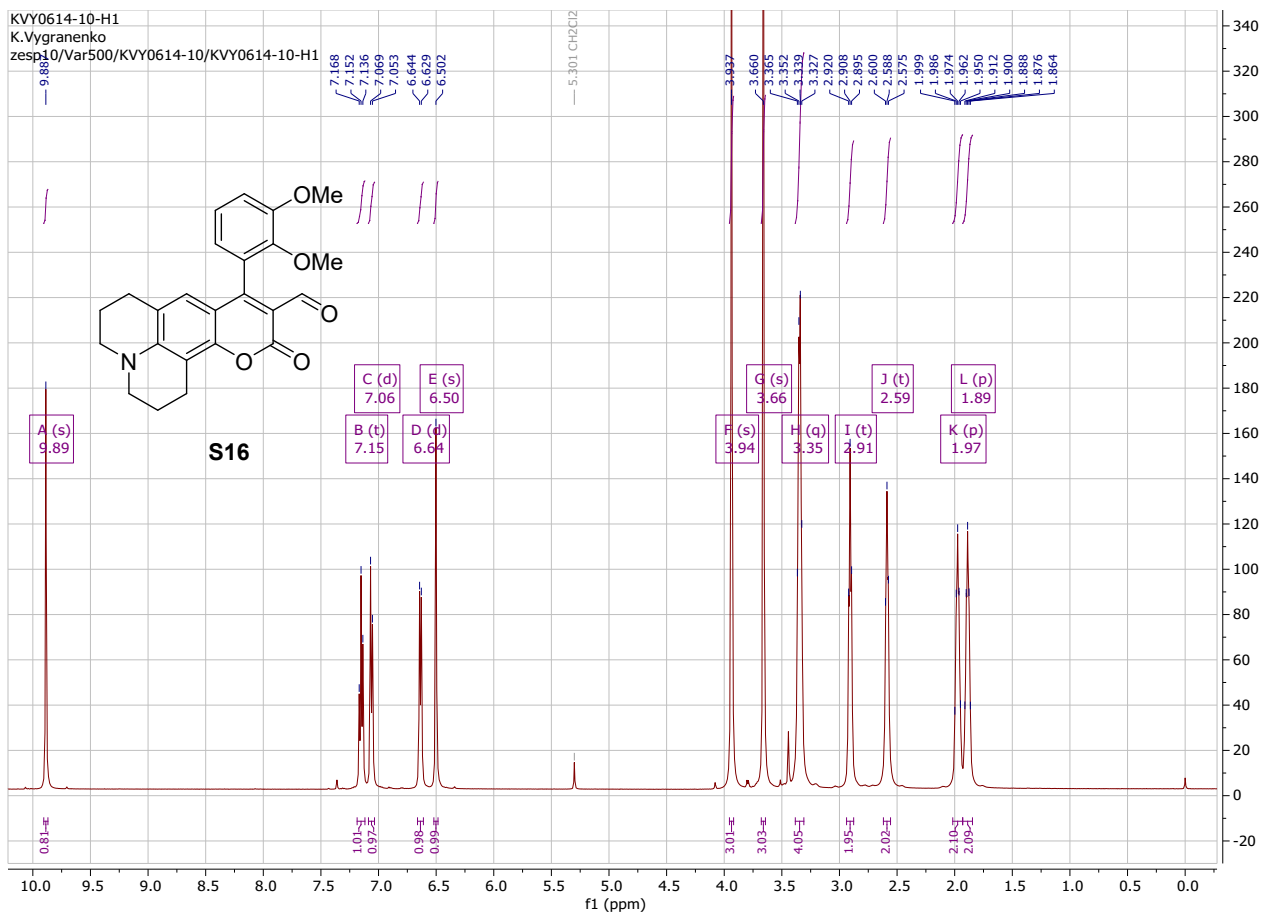


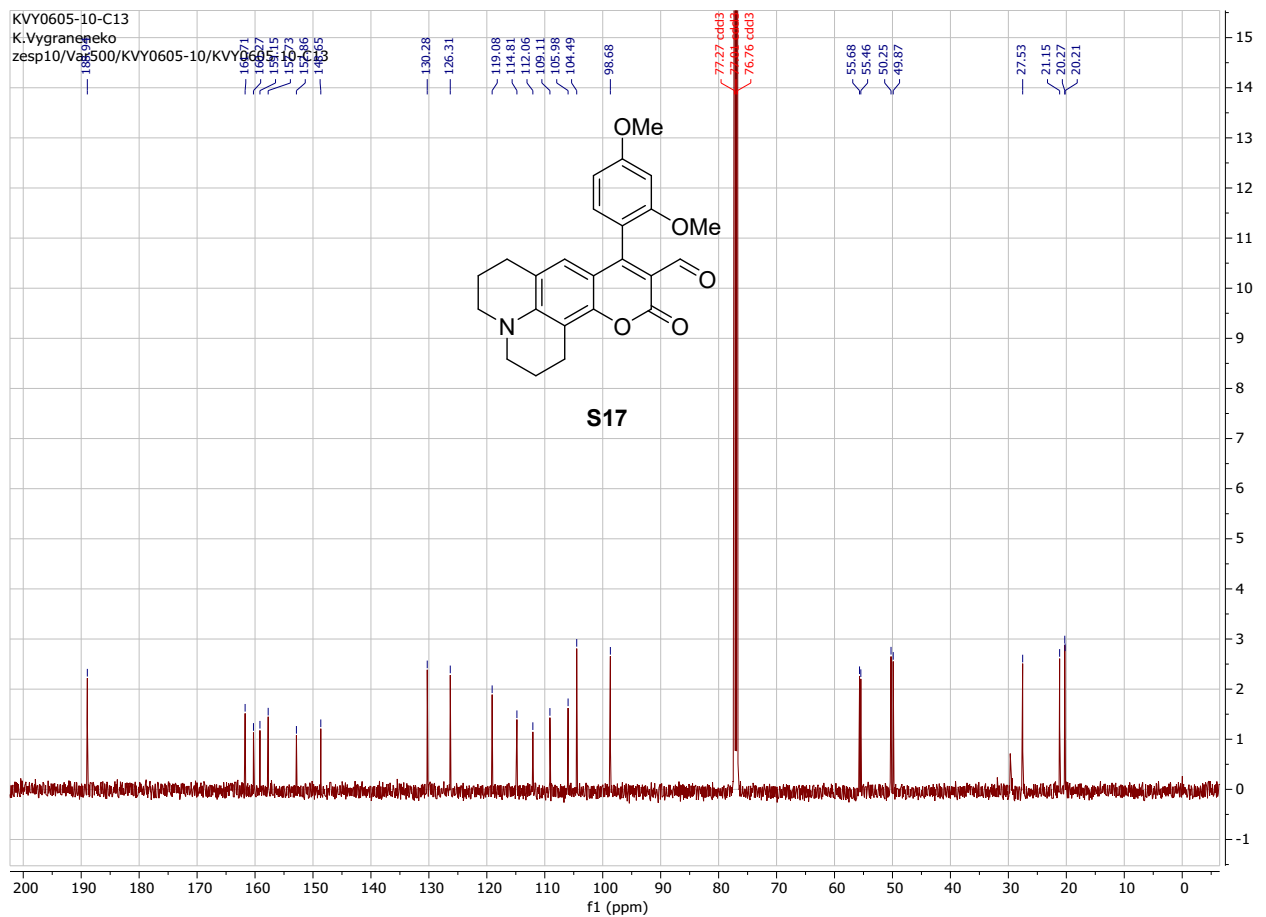
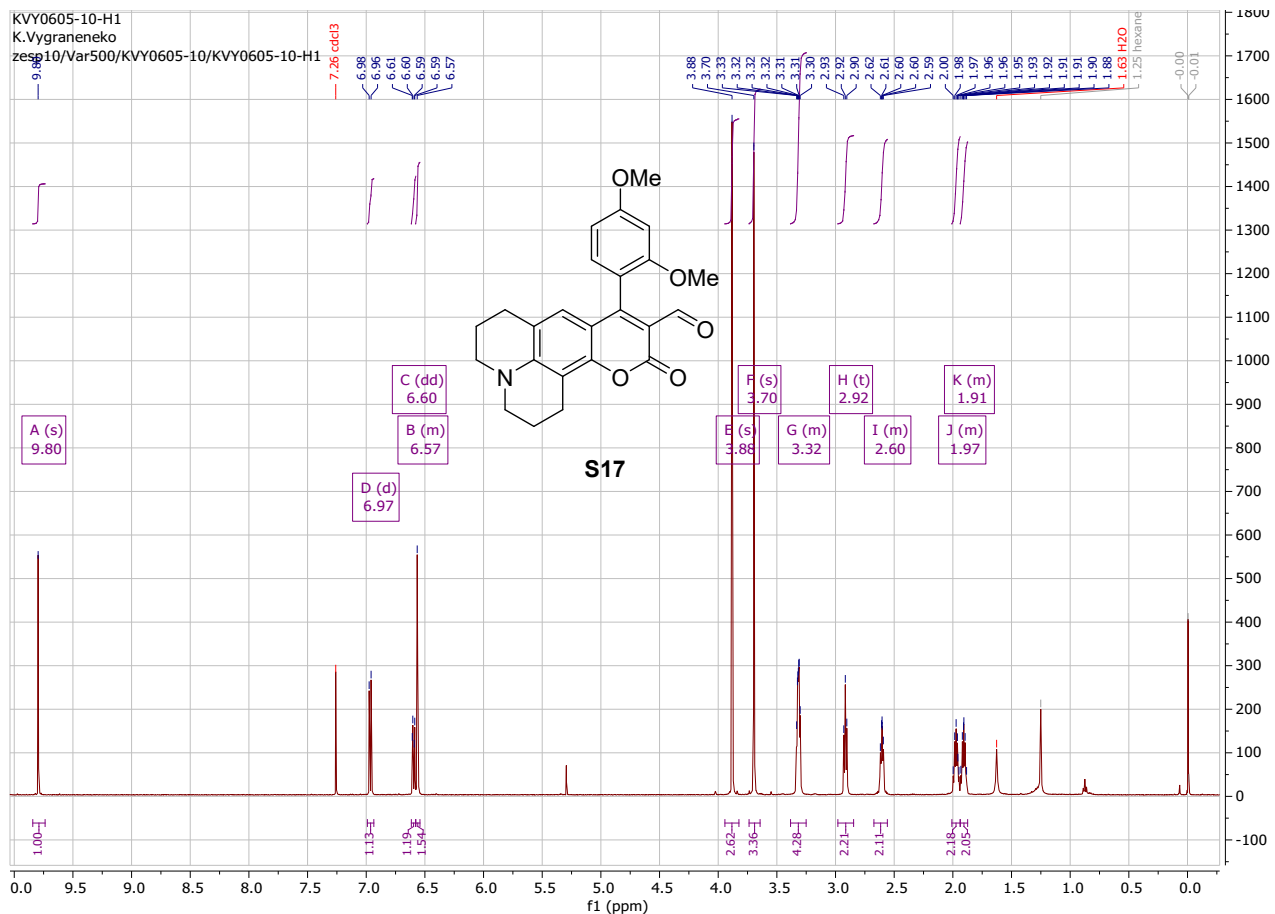


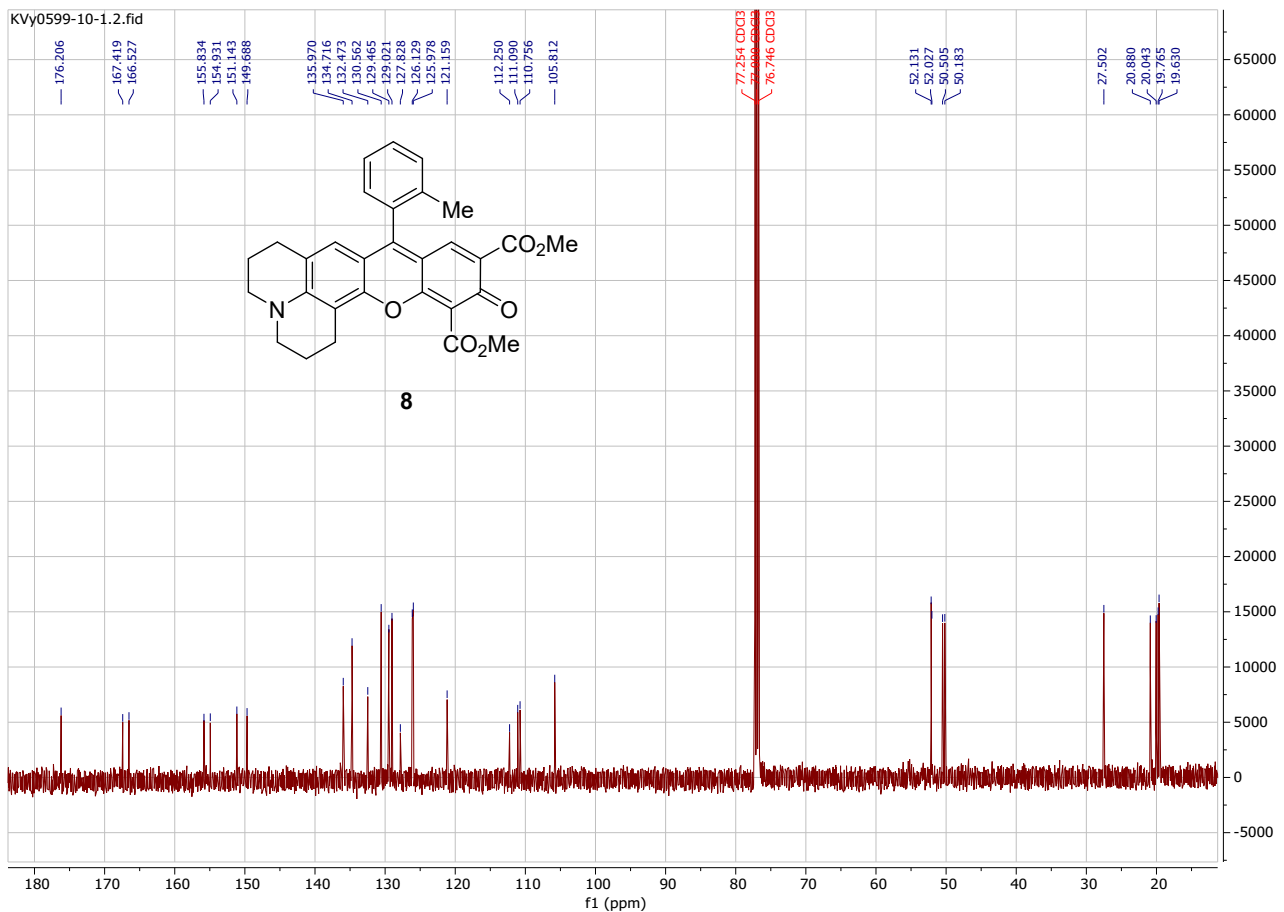
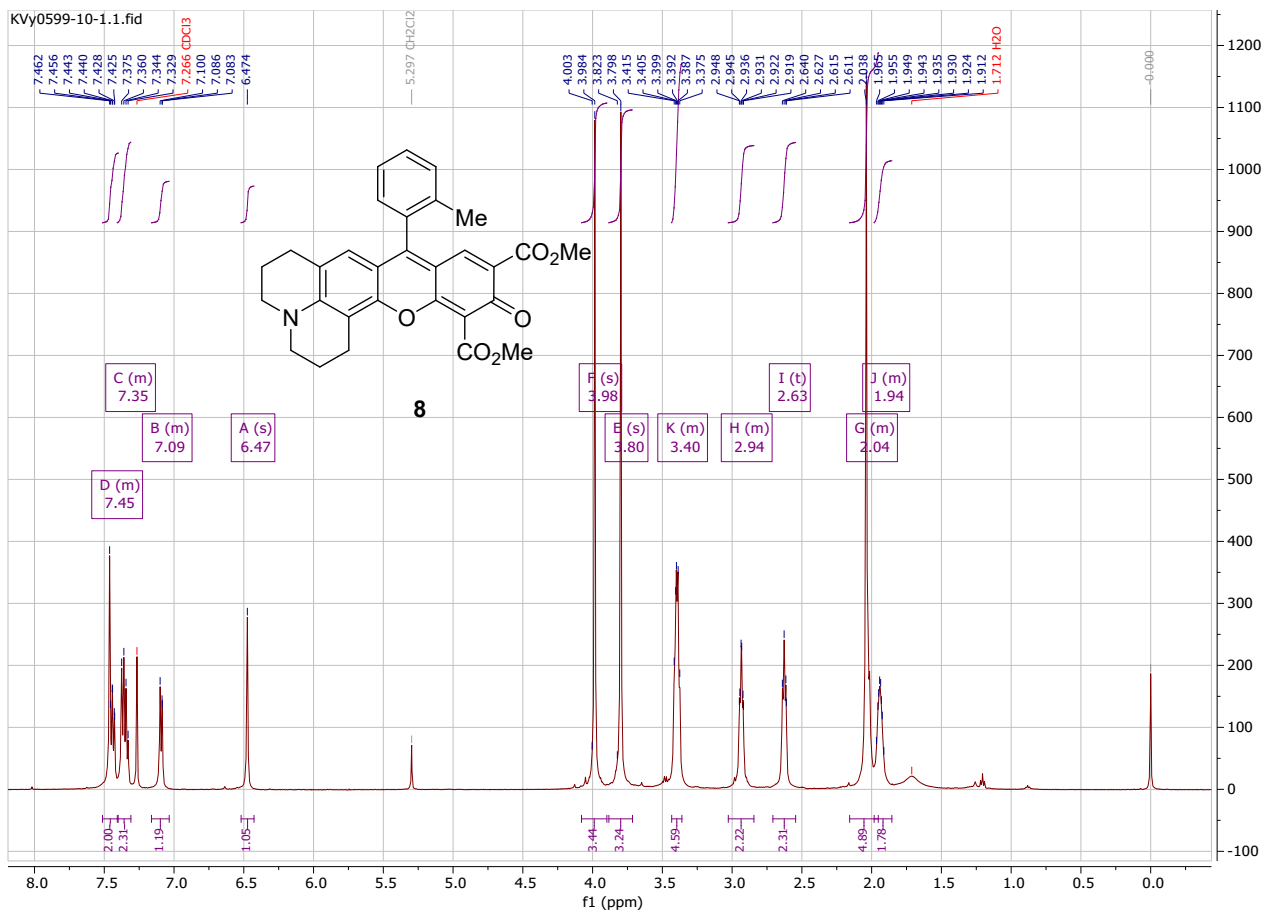


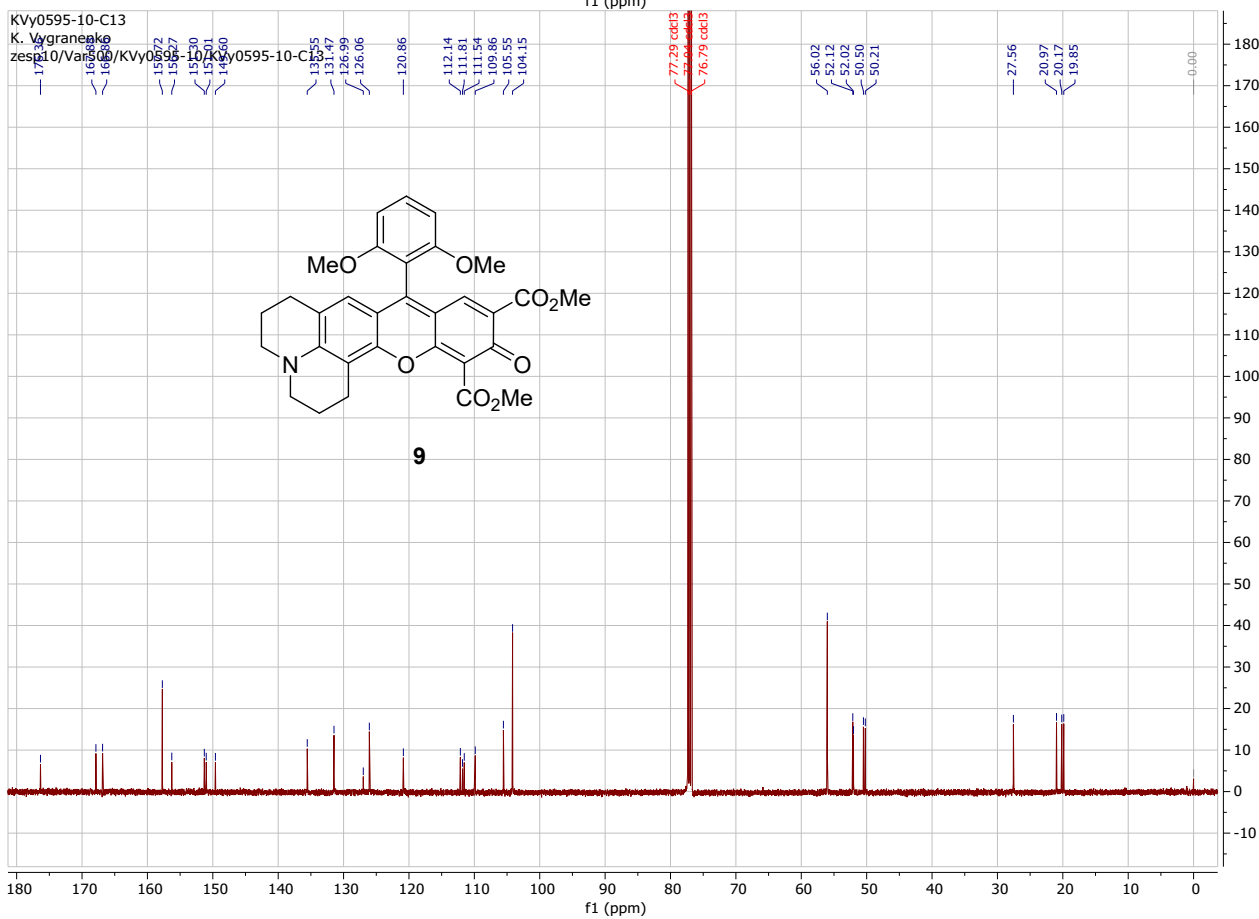
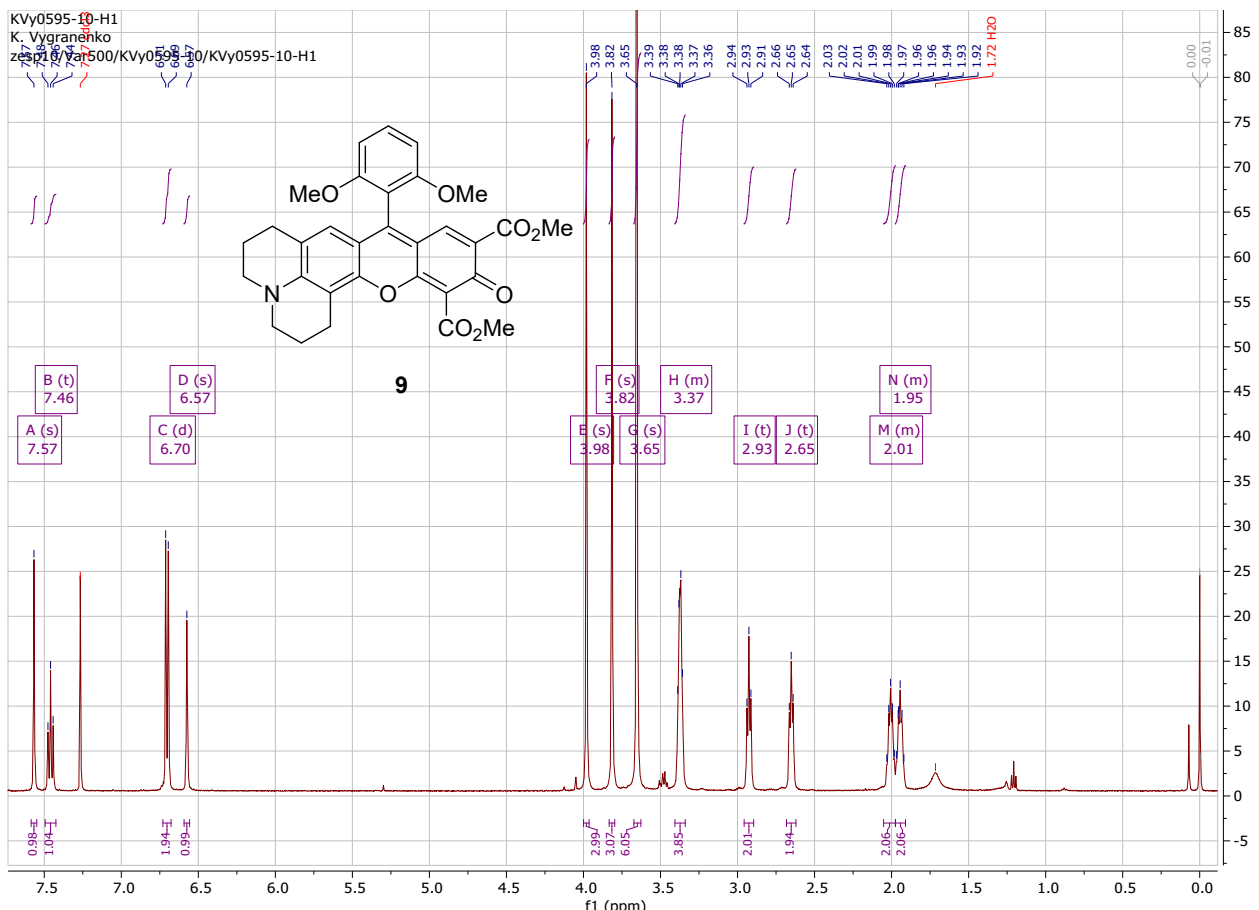


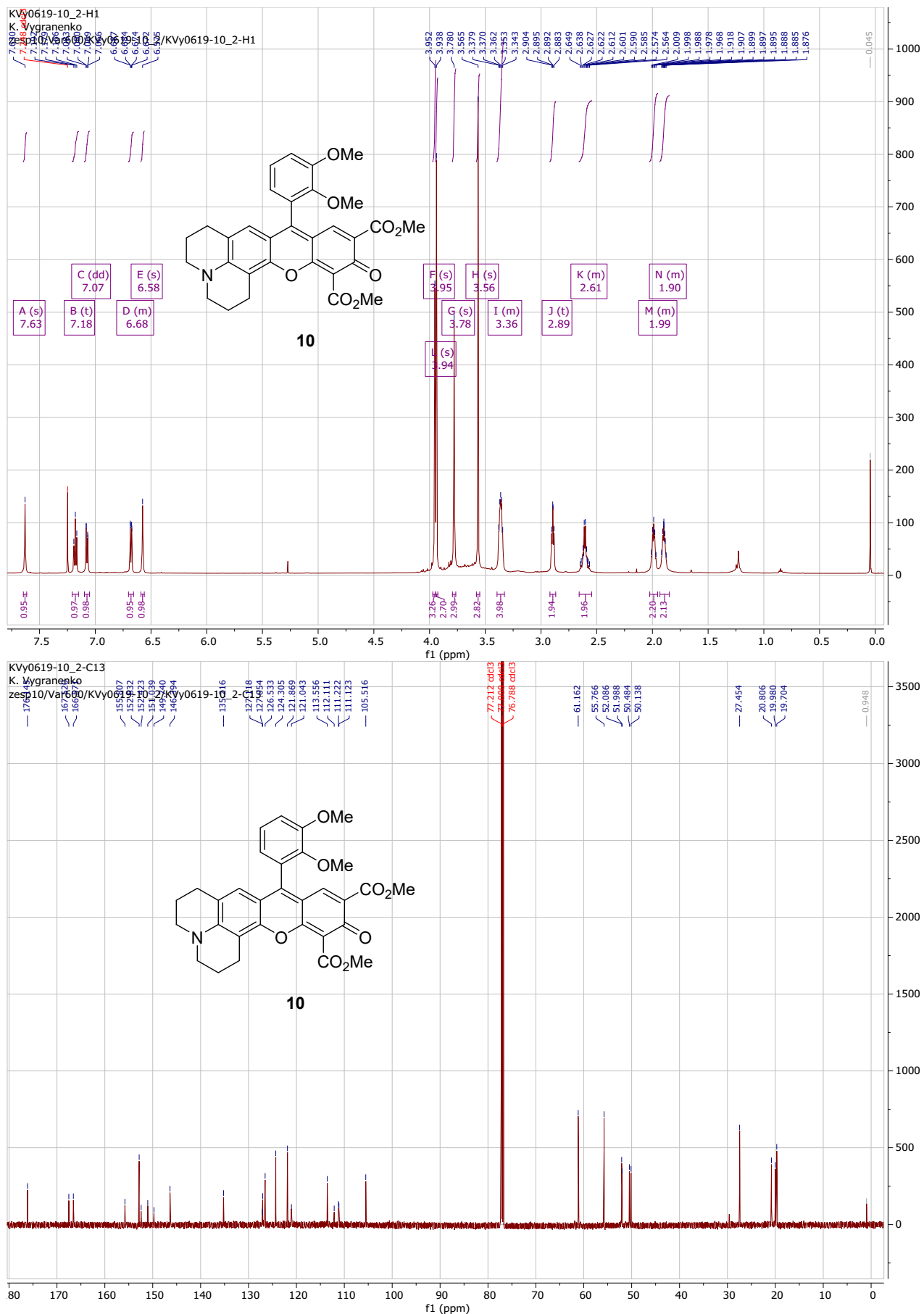


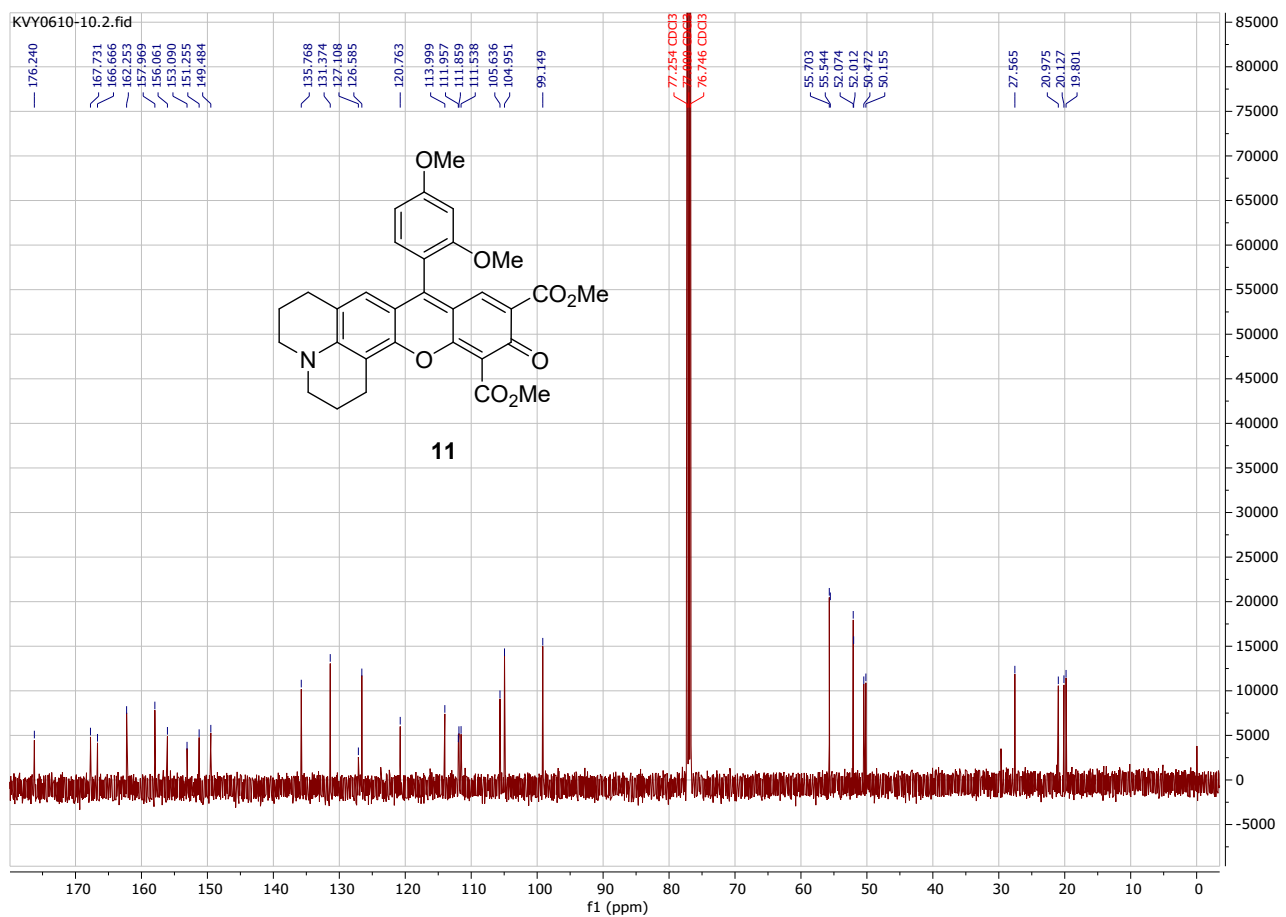
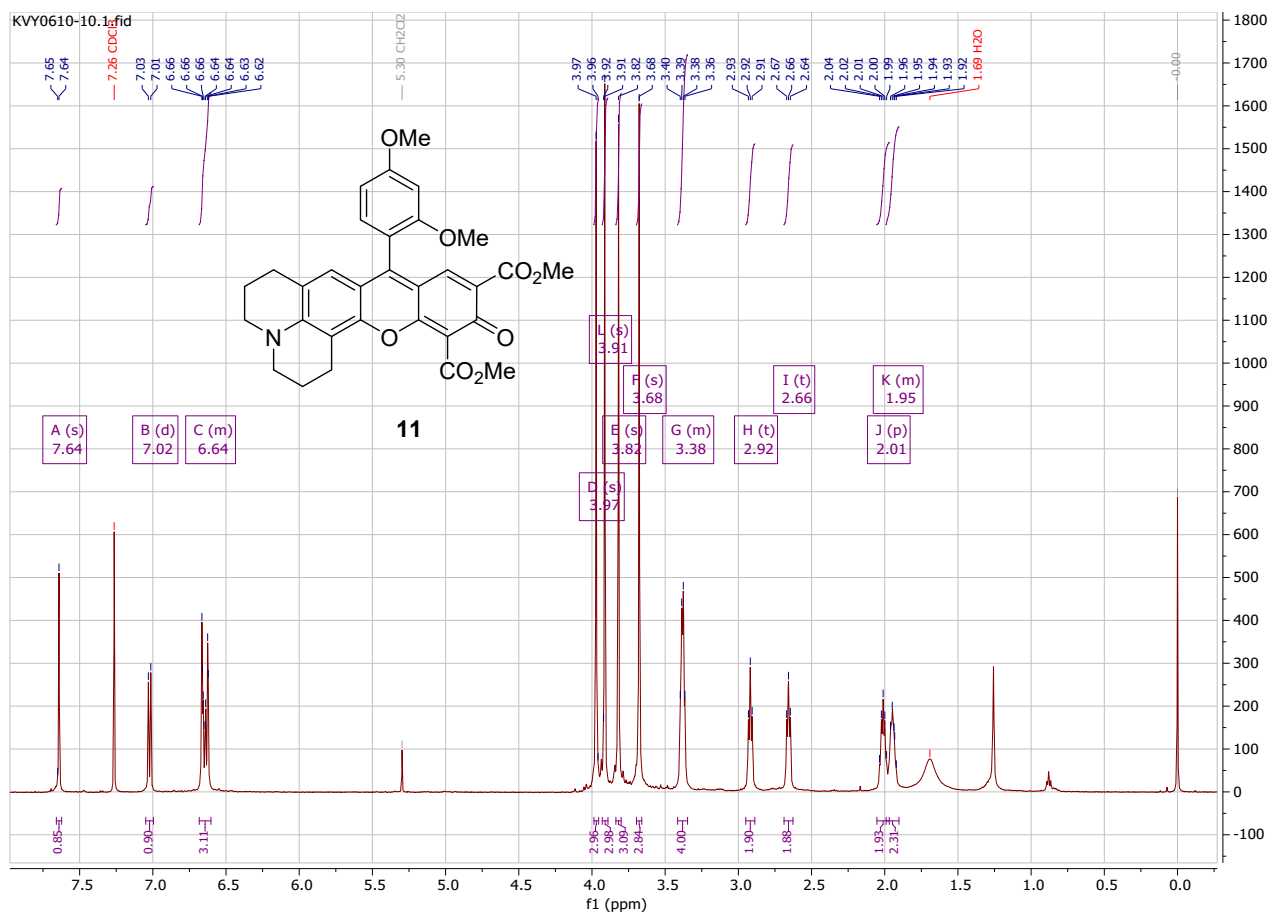


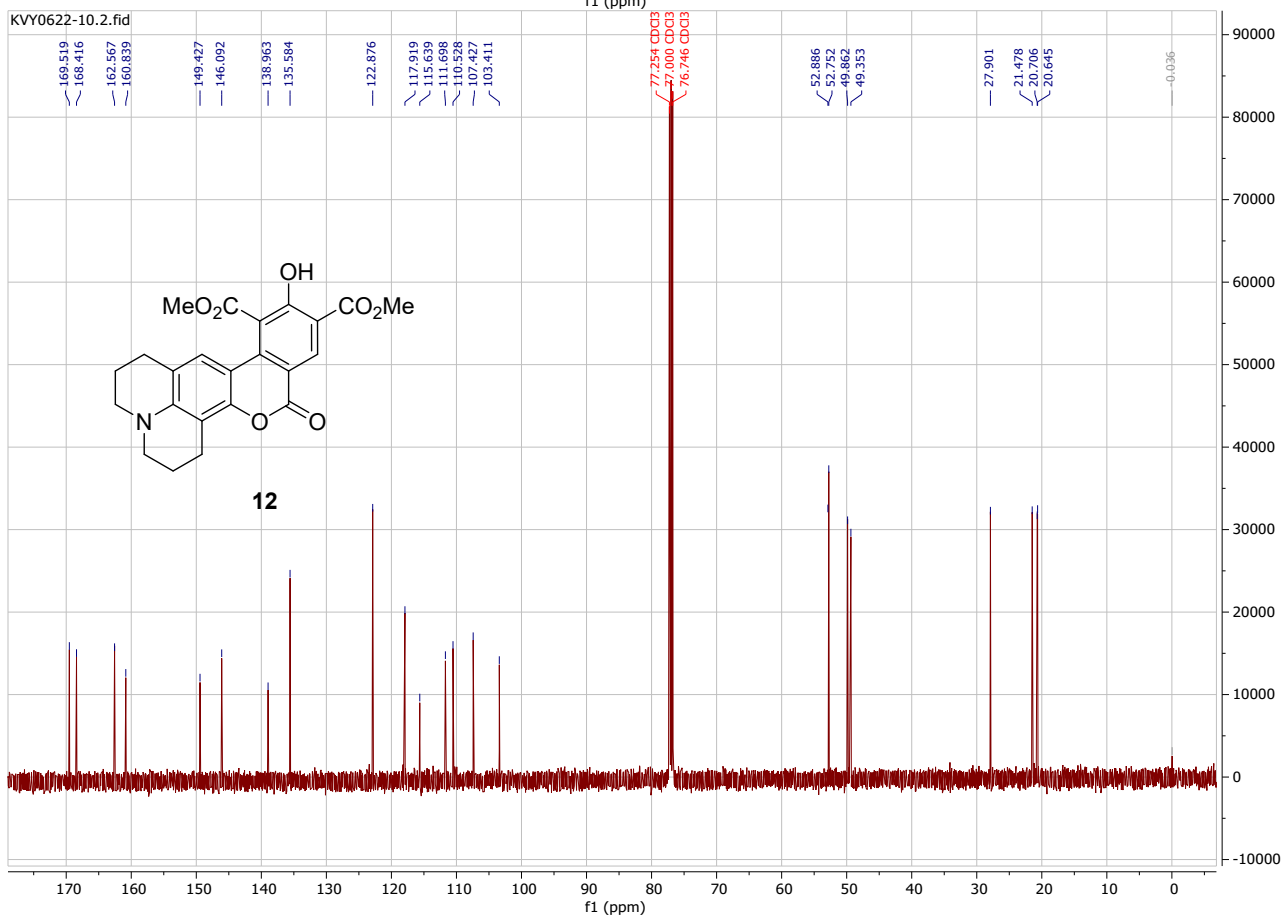
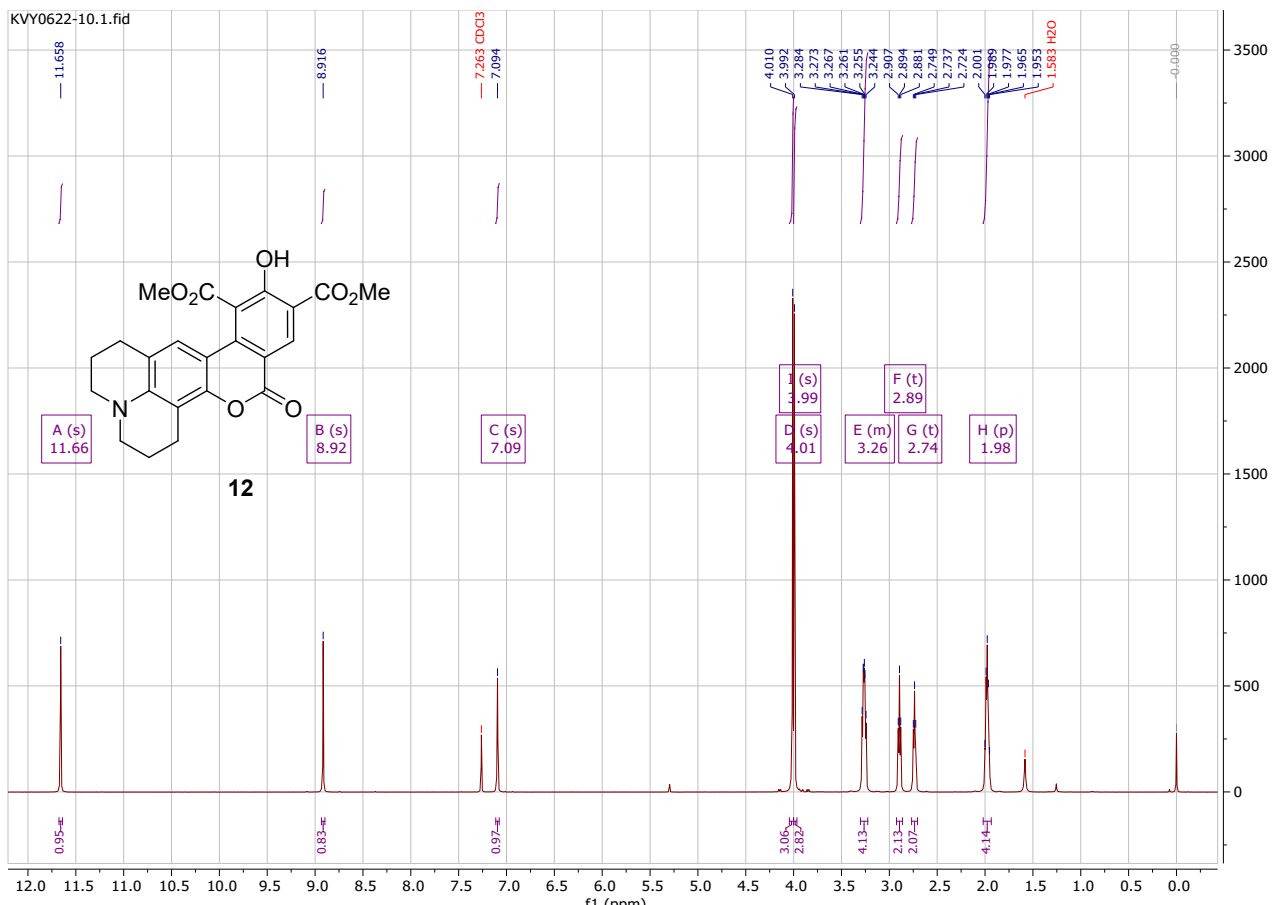


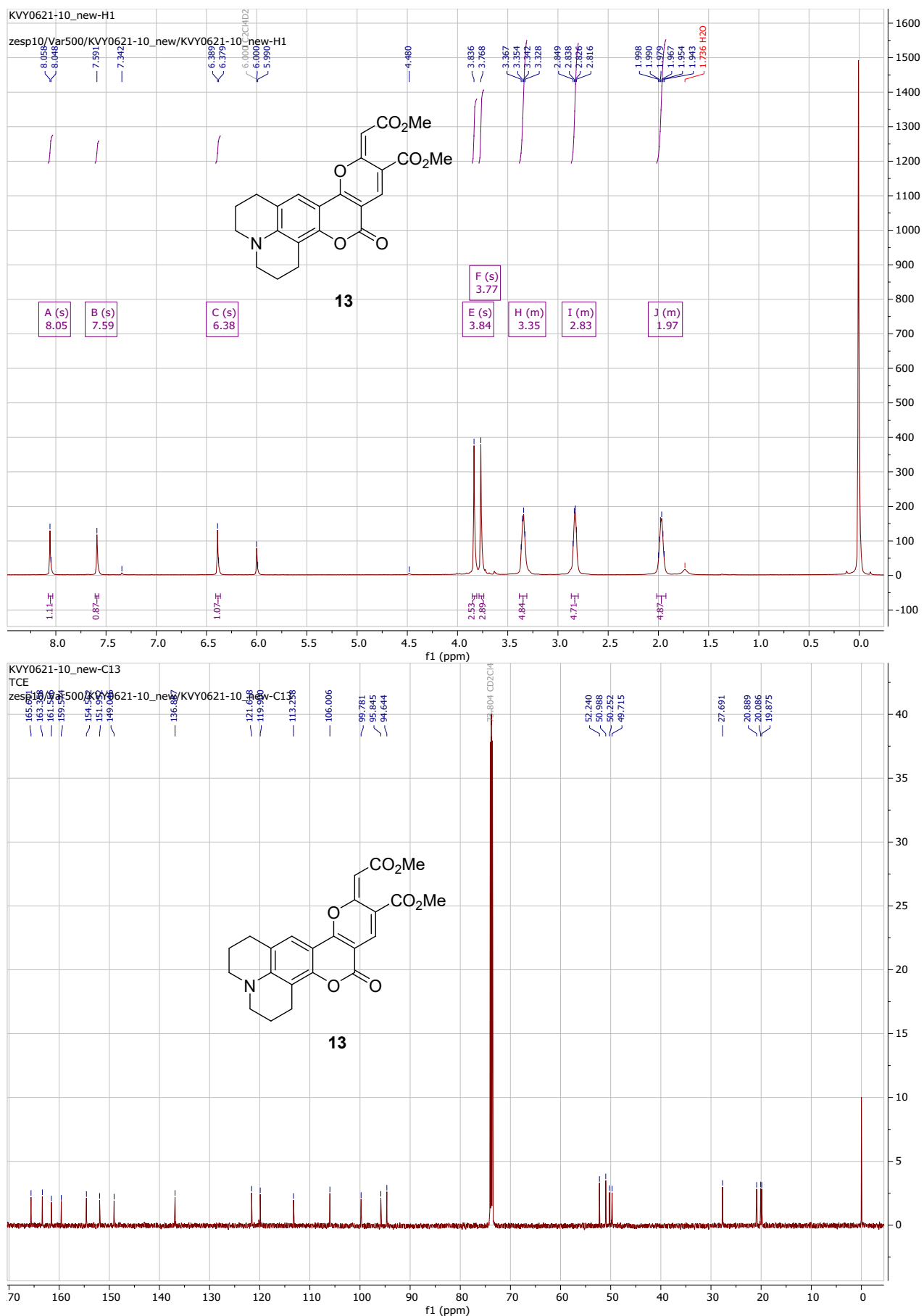


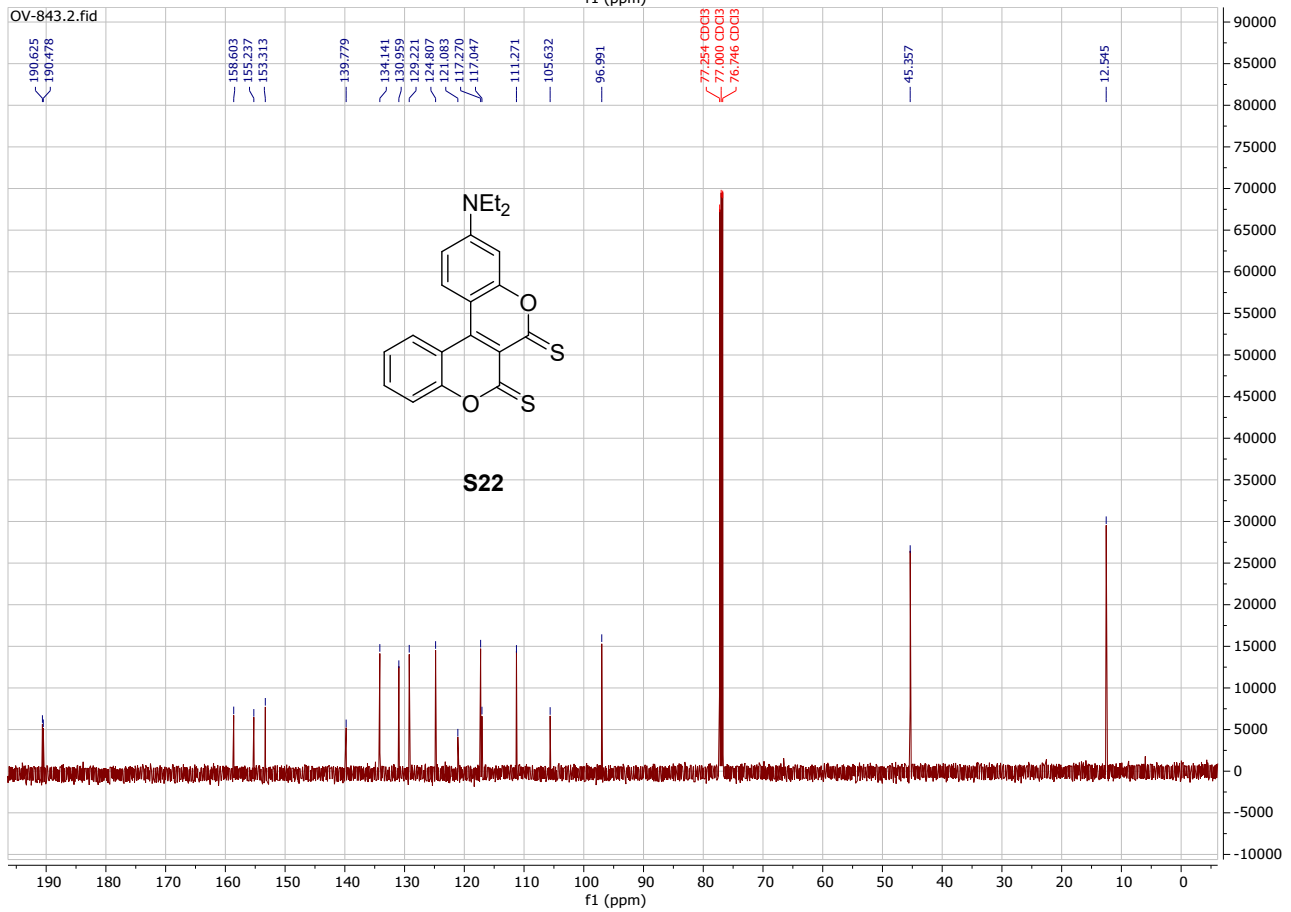
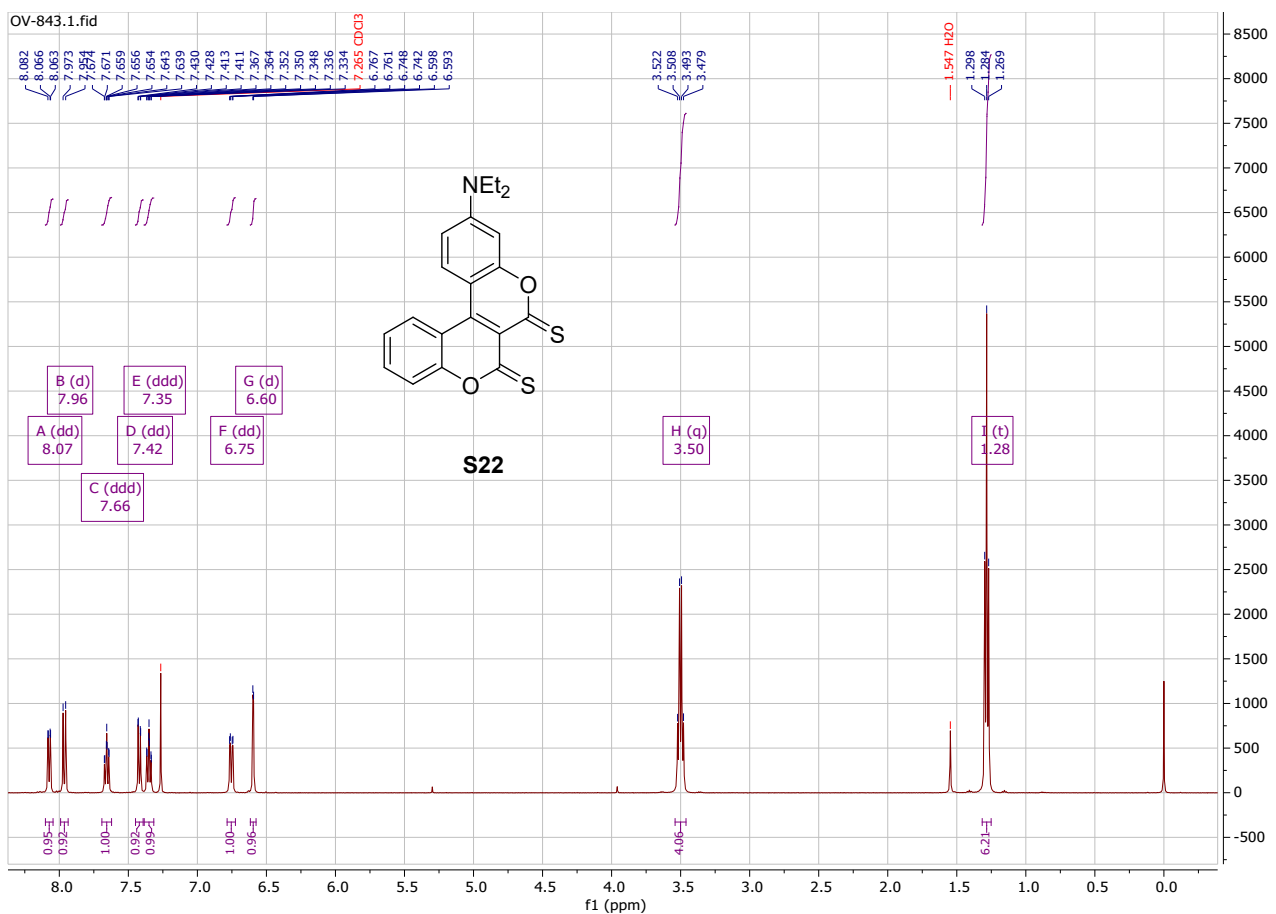


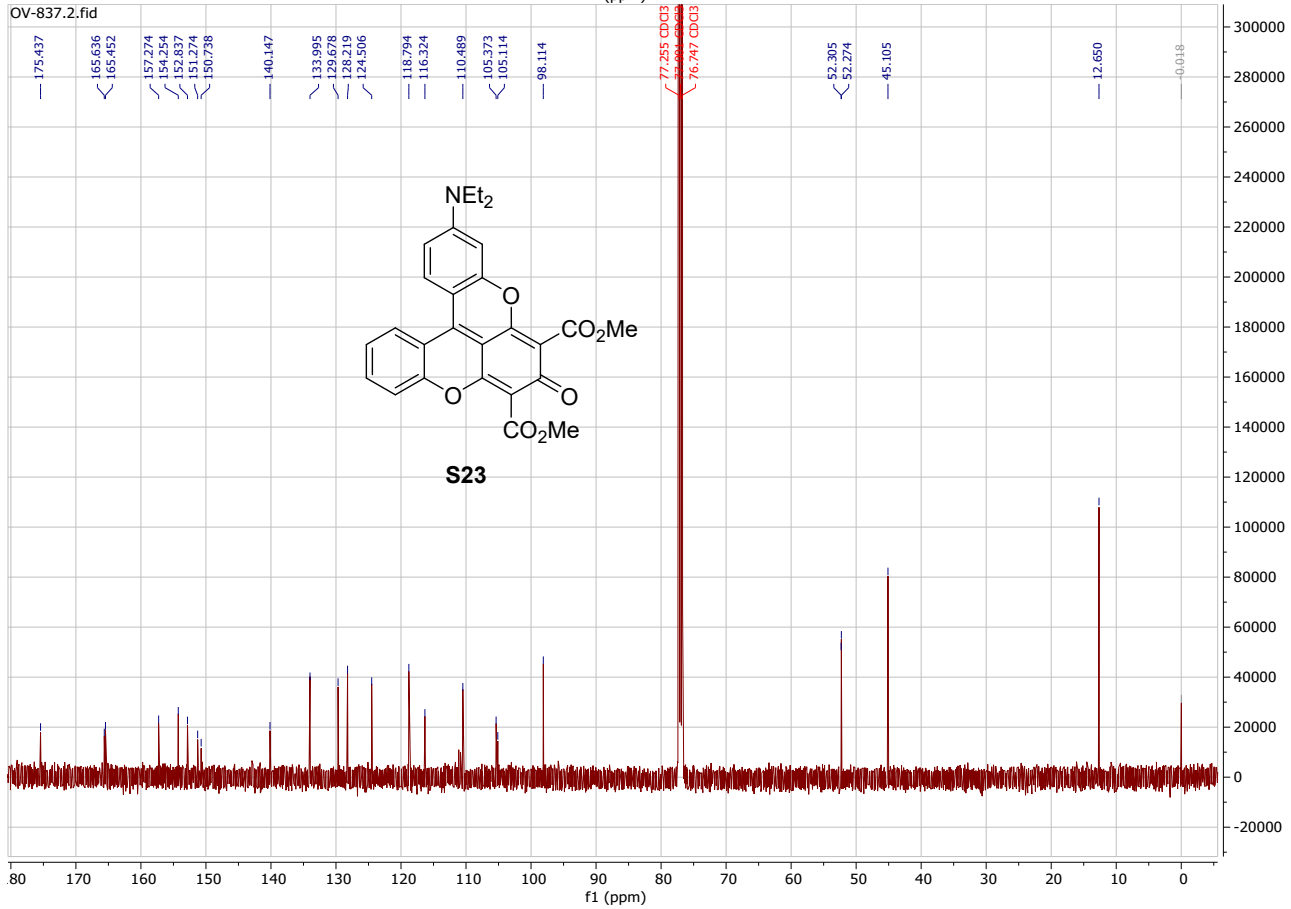
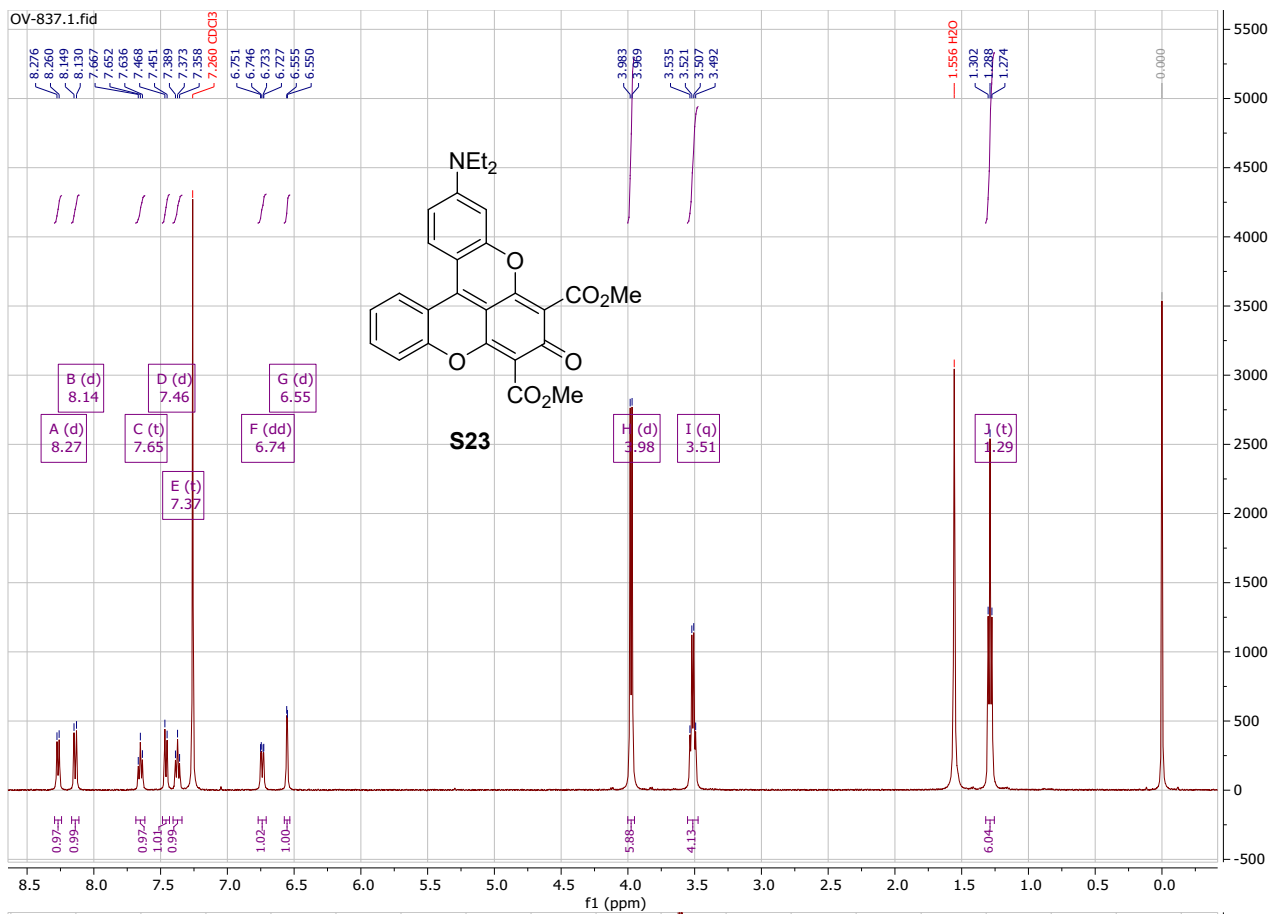












Crystal Structure Report for 12

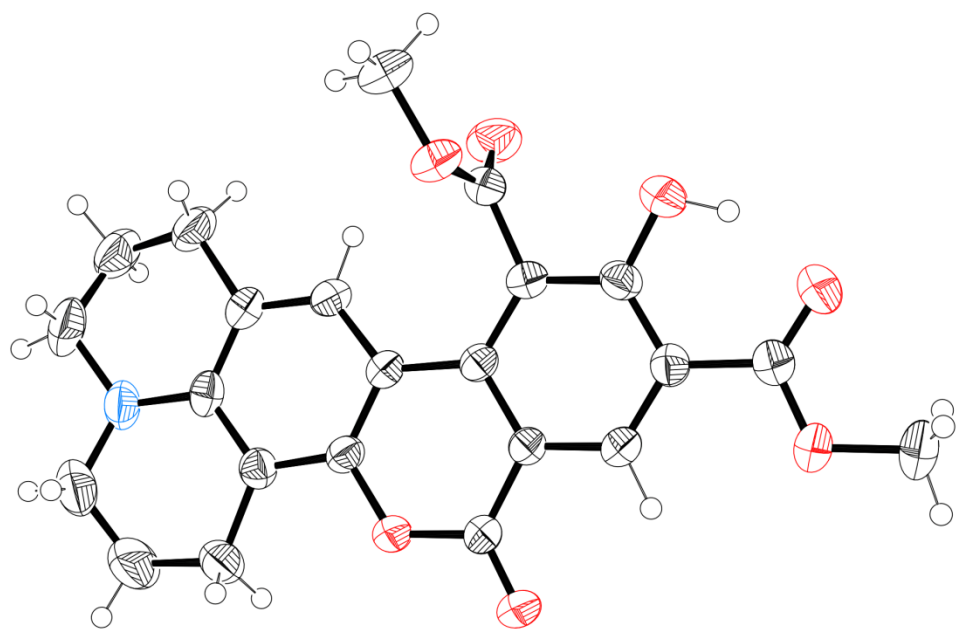


Figure S3. The ORTEP drawing⁴ of X-ray diffraction analysis for compound **12**. CCDC 2125095.

A yellow prisms-like specimen of $C_{23}H_{21}NO_7$, approximate dimensions $0.194\text{ mm} \times 0.244\text{ mm} \times 0.368\text{ mm}$, was used for the X-ray crystallographic analysis. The X-ray intensity data were measured.

Table S1. Data collection details for **12**.

Axis	dx/mm	$2\theta/^\circ$	$\omega/^\circ$	$\phi/^\circ$	$\chi/^\circ$	Width/°	Frames	Time/s	Wavelength/Å	Voltage/kV	Current/mA	Temperature/K
Omega	39.835	-97.72	-192.85	-178.62	24.03	2.00	54	88.00	1.54184	45	30.0	n/a
Omega	39.835	-101.63	-206.31	-24.27	43.23	2.00	56	88.00	1.54184	45	30.0	n/a
Omega	39.835	-101.30	-209.35	-83.58	50.32	2.00	57	88.00	1.54184	45	30.0	n/a
Phi	39.835	-18.13	-3.92	-116.00	23.00	2.00	92	88.00	1.54184	45	30.0	n/a
Omega	39.835	-100.90	-111.03	-90.42	-30.05	2.00	54	88.00	1.54184	45	30.0	n/a
Omega	39.835	-100.79	-203.51	-119.88	40.40	2.00	55	88.00	1.54184	45	30.0	n/a
Omega	39.835	36.11	-52.45	-114.35	52.48	2.00	47	88.00	1.54184	45	30.0	n/a
Phi	39.835	85.61	-280.32	0.00	-58.06	2.00	180	88.00	1.54184	45	30.0	n/a
Omega	39.835	27.38	-337.08	0.00	-54.74	2.00	57	88.00	1.54184	45	30.0	n/a
Omega	39.835	-101.22	-108.86	19.45	-42.31	2.00	56	88.00	1.54184	45	30.0	n/a
Omega	39.835	-100.90	-205.62	22.16	43.34	2.00	56	88.00	1.54184	45	30.0	n/a
Omega	39.835	-100.87	-206.52	-166.47	46.12	2.00	56	88.00	1.54184	45	30.0	n/a
Omega	39.835	-101.30	-204.15	-50.83	40.80	2.00	55	88.00	1.54184	45	30.0	n/a
Omega	39.835	-99.71	-200.88	-223.75	36.03	2.00	55	88.00	1.54184	45	30.0	n/a
Omega	39.835	84.67	-280.79	90.00	-54.74	2.00	58	88.00	1.54184	45	30.0	n/a
Omega	39.835	-101.22	-209.09	-148.00	49.76	2.00	57	88.00	1.54184	45	30.0	n/a
Omega	39.835	84.67	-280.79	180.00	-54.74	2.00	58	88.00	1.54184	45	30.0	n/a
Omega	39.835	84.67	-280.79	0.00	-54.74	2.00	58	88.00	1.54184	45	30.0	n/a
Omega	39.835	-100.35	-109.65	72.81	-32.08	2.00	54	88.00	1.54184	45	30.0	n/a
Omega	39.835	27.38	-337.08	153.00	-54.74	2.00	57	88.00	1.54184	45	30.0	n/a
Phi	39.835	-100.61	-174.76	-44.00	23.00	2.00	28	88.00	1.54184	45	30.0	n/a
Omega	39.835	84.67	-280.79	270.00	-54.74	2.00	58	88.00	1.54184	45	30.0	n/a
Omega	39.835	-101.52	-206.51	57.38	44.15	2.00	56	88.00	1.54184	45	30.0	n/a
Omega	39.835	-100.23	-106.60	-144.54	-49.09	2.00	57	88.00	1.54184	45	30.0	n/a
Omega	39.835	-100.91	-106.03	-34.93	-55.74	2.00	58	88.00	1.54184	45	30.0	n/a
Omega	39.835	-101.15	-205.37	80.53	41.85	2.00	56	88.00	1.54184	45	30.0	n/a
Omega	39.835	12.38	-353.08	270.00	-54.74	2.00	58	88.00	1.54184	45	30.0	n/a

Axis	dx/mm	$2\theta/^\circ$	$\omega/^\circ$	$\phi/^\circ$	$\chi/^\circ$	Width/°	Frames	Time/s	Wavelength/Å	Voltage/kV	Current/mA	Temperature/K
Omega	39.835	-97.67	-64.94	-136.03	-74.84	2.00	46	88.00	1.54184	45	30.0	n/a
Phi	39.835	70.61	-295.32	0.00	-58.06	2.00	180	88.00	1.54184	45	30.0	n/a

A total of 1869 frames were collected. The total exposure time was 45.69 hours. The frames were integrated with the Bruker SAINT software package using a narrow-frame algorithm. The integration of the data using a monoclinic unit cell yielded a total of 20848 reflections to a maximum θ angle of 68.75° (0.83 Å resolution), of which 3496 were independent (average redundancy 5.963, completeness = 97.3%, $R_{\text{int}} = 6.44\%$, $R_{\text{sig}} = 4.22\%$) and 2521 (72.11%) were greater than $2\sigma(F^2)$. The final cell constants of $a = 11.7140(13)$ Å, $b = 9.9926(12)$ Å, $c = 16.775(2)$ Å, $\beta = 98.713(7)$ °, volume = 1940.9(4) Å³, are based upon the refinement of the XYZ-centroids of 7169 reflections above 20 $\sigma(I)$ with $5.329^\circ < 2\theta < 136.6^\circ$. Data were corrected for absorption effects using the numerical method (SADABS). The ratio of minimum to maximum apparent transmission was 0.825. The calculated minimum and maximum transmission coefficients (based on crystal size) are 0.7320 and 0.8440.

The structure was solved and refined using the Bruker SHELXTL Software Package, using the space group P 1 21/n 1, with Z = 4 for the formula unit, C₂₃H₂₁NO₇. The final anisotropic full-matrix least-squares refinement on F² with 326 variables converged at R1 = 4.93%, for the observed data and wR2 = 13.29% for all data. The goodness-of-fit was 1.015. The largest peak in the final difference electron density synthesis was 0.650 e/Å³ and the largest hole was -0.324 e/Å³ with an RMS deviation of 0.044 e/Å³. On the basis of the final model, the calculated density was 1.449 g/cm³ and F(000), 888 e⁻.

Table S2. Sample and crystal data for **12**.

Identification code	KVy0620A	
Chemical formula	C ₂₃ H ₂₁ NO ₇	
Formula weight	423.41 g/mol	
Temperature	296(2) K	
Wavelength	1.54178 Å	
Crystal size	0.194 x 0.244 x 0.368 mm	
Crystal habit	yellow prisms	
Crystal system	monoclinic	
Space group	P 1 21/n 1	
Unit cell dimensions	$a = 11.7140(13)$ Å	$\alpha = 90^\circ$
	$b = 9.9926(12)$ Å	$\beta = 98.713(7)$ °
	$c = 16.775(2)$ Å	$\gamma = 90^\circ$
Volume	1940.9(4) Å ³	
Z	4	
Density (calculated)	1.449 g/cm ³	
Absorption coefficient	0.903 mm ⁻¹	
F(000)	888	

Table S3. Data collection and structure refinement for **12**.

Theta range for data collection	4.31 to 68.75°
Index ranges	-14≤h≤14, -11≤k≤10, -20≤l≤20
Reflections collected	20848
Independent reflections	3496 [R(int) = 0.0644]
Coverage of independent reflections	97.3%
Absorption correction	numerical
Max. and min. transmission	0.8440 and 0.7320
Structure solution technique	direct methods

Structure solution program	SHELXL-2014 (Sheldrick, 2014)				
Refinement method	Full-matrix least-squares on F^2				
Refinement program	SHELXL-2014 (Sheldrick, 2014)				
Function minimized	$\sum w(F_o^2 - F_c^2)^2$				
Data / restraints / parameters	3496 / 0 / 326				
Goodness-of-fit on F^2	1.015				
Final R indices	2521 data; $I > 2\sigma(I)$	R1 = 0.0493, wR2 = 0.1180			
	all data	R1 = 0.0726, wR2 = 0.1329			
Weighting scheme	$w = 1/[\sigma^2(F_o^2) + (0.0563P)^2 + 0.9257P]$ where $P = (F_o^2 + 2F_c^2)/3$				
Largest diff. peak and hole	0.650 and -0.324 e \AA^{-3}				
R.M.S. deviation from mean	0.044 e \AA^{-3}				

Table S4. Atomic coordinates and equivalent isotropic atomic displacement parameters (\AA^2) for **12**. U(eq) is defined as one third of the trace of the orthogonalized U_{ij} tensor.

	x/a	y/b	z/c	U(eq)
N1	0.79545(16)	0.8429(2)	0.96972(13)	0.0496(5)
O1	0.40679(11)	0.73599(15)	0.98848(9)	0.0430(4)
O2	0.22301(12)	0.69230(18)	0.98329(10)	0.0534(5)
O3	0.42098(15)	0.32825(19)	0.27994(10)	0.0564(5)
O4	0.65852(14)	0.33896(17)	0.22349(11)	0.0592(5)
O5	0.63780(12)	0.53689(17)	0.28201(9)	0.0484(4)
O6	0.20390(14)	0.27387(19)	0.26422(11)	0.0596(5)
O7	0.08283(13)	0.38296(18)	0.17120(11)	0.0560(5)
C1	0.9165(2)	0.8403(3)	0.0081(2)	0.0665(8)
C2	0.9551(2)	0.7029(3)	0.0347(2)	0.0626(8)
C3	0.88157(19)	0.6484(3)	0.09211(18)	0.0543(7)
C4	0.75485(17)	0.6737(2)	0.06535(13)	0.0387(5)
C5	0.71712(17)	0.7696(2)	0.00534(14)	0.0383(5)
C6	0.59773(17)	0.7873(2)	0.98031(13)	0.0369(5)
C7	0.5524(2)	0.8849(3)	0.91468(18)	0.0501(6)
C8	0.6456(3)	0.9451(4)	0.8743(2)	0.0893(11)

	x/a	y/b	z/c	U(eq)
)
C9	0.7564(2)	0.9621(3)	0.9255(2)	0.0719(9)
C10	0.67491(17))	0.6033(2)	0.10043(14))	0.0377(5)
C11	0.55527(16))	0.6212(2)	0.08003(13))	0.0335(5)
C12	0.52187(16))	0.7126(2)	0.01808(13))	0.0343(5)
C13	0.31944(16))	0.6681(2)	0.01591(13))	0.0365(5)
C14	0.35030(16))	0.5755(2)	0.08252(12))	0.0316(5)
C15	0.46661(16))	0.5535(2)	0.11724(12))	0.0314(5)
C16	0.48664(17))	0.4678(2)	0.18456(13))	0.0351(5)
C17	0.39510(18))	0.4064(2)	0.21439(13))	0.0381(5)
C18	0.28036(17))	0.4263(2)	0.17743(13))	0.0370(5)
C19	0.26035(17))	0.5115(2)	0.11245(13))	0.0356(5)
C20	0.60377(18))	0.4383(2)	0.23082(14))	0.0394(5)
C21	0.7529(2)	0.5265(3)	0.32706(17))	0.0644(8)
C22	0.18693(19))	0.3537(2)	0.20899(14))	0.0430(6)
C23	0.9883(2)	0.3055(4)	0.1955(2)	0.0831(10))

Table S5. Bond lengths (Å) for **12**.

N1-C5	1.379(3)	N1-C9	1.441(3)
N1-C1	1.466(3)	O1-C13	1.364(2)
O1-C12	1.384(2)	O2-C13	1.203(2)
O3-C17	1.345(3)	O3-H3	0.95(3)
O4-C20	1.198(3)	O5-C20	1.328(3)
O5-C21	1.446(3)	O6-C22	1.216(3)
O7-C22	1.319(3)	O7-C23	1.458(3)
C1-C2	1.492(4)	C1-H1A	0.99(3)
C1-H1B	1.08(4)	C2-C3	1.489(4)
C2-H2A	0.98(3)	C2-H2B	1.06(3)
C3-C4	1.506(3)	C3-H3A	0.99(3)
C3-H3B	1.00(3)	C4-C10	1.373(3)
C4-C5	1.411(3)	C5-C6	1.409(3)
C6-C12	1.385(3)	C6-C7	1.506(3)

C7-C8	1.496(4)	C7-H7A	0.95(3)
C7-H7B	0.95(3)	C8-C9	1.454(4)
C8-H8A	0.97	C8-H8B	0.97
C9-H9A	0.97	C9-H9B	0.97
C10-C11	1.403(3)	C10-H10	0.97(3)
C11-C12	1.395(3)	C11-C15	1.457(3)
C13-C14	1.454(3)	C14-C19	1.390(3)
C14-C15	1.415(3)	C15-C16	1.408(3)
C16-C17	1.393(3)	C16-C20	1.500(3)
C17-C18	1.406(3)	C18-C19	1.375(3)
C18-C22	1.476(3)	C19-H19	0.98(2)
C21-H21A	0.96	C21-H21B	0.96
C21-H21C	0.96	C23-H23A	0.96
C23-H23B	0.96	C23-H23C	0.96

Table S6. Bond angles ($^{\circ}$) for **12**.

C5-N1-C9	118.8(2)	C5-N1-C1	117.6(2)
C9-N1-C1	116.8(2)	C13-O1-C12	122.32(17)
C17-O3-H3	104.4(17)	C20-O5-C21	116.72(19)
C22-O7-C23	115.7(2)	N1-C1-C2	112.1(2)
N1-C1-H1A	102.2(18)	C2-C1-H1A	113.6(18)
N1-C1-H1B	110.9(19)	C2-C1-H1B	108.8(19)
H1A-C1-H1B	109.(3)	C1-C2-C3	110.6(3)
C1-C2-H2A	107.3(16)	C3-C2-H2A	111.0(16)
C1-C2-H2B	108.8(15)	C3-C2-H2B	110.8(15)
H2A-C2-H2B	108.(2)	C2-C3-C4	112.7(2)
C2-C3-H3A	113.8(18)	C4-C3-H3A	107.4(18)
C2-C3-H3B	113.8(19)	C4-C3-H3B	107.4(18)
H3A-C3-H3B	101.(3)	C10-C4-C5	119.56(19)
C10-C4-C3	119.5(2)	C5-C4-C3	121.0(2)
N1-C5-C4	120.84(19)	N1-C5-C6	120.0(2)
C4-C5-C6	119.16(19)	C12-C6-C5	118.2(2)
C12-C6-C7	120.25(19)	C5-C6-C7	121.5(2)
C8-C7-C6	113.0(2)	C8-C7-H7A	108.1(19)
C6-C7-H7A	111.(2)	C8-C7-H7B	109.0(19)
C6-C7-H7B	112.0(19)	H7A-C7-H7B	103.(3)
C9-C8-C7	115.2(3)	C9-C8-H8A	108.5
C7-C8-H8A	108.5	C9-C8-H8B	108.5
C7-C8-H8B	108.5	H8A-C8-H8B	107.5
N1-C9-C8	113.1(2)	N1-C9-H9A	109.0
C8-C9-H9A	109.0	N1-C9-H9B	109.0
C8-C9-H9B	109.0	H9A-C9-H9B	107.8
C4-C10-C11	123.4(2)	C4-C10-H10	115.0(14)
C11-C10-H10	121.5(14)	C12-C11-C10	114.99(19)
C12-C11-C15	119.07(17)	C10-C11-C15	125.9(2)

C6-C12-O1	113.74(18)	C6-C12-C11	124.53(18)
O1-C12-C11	121.73(18)	O2-C13-O1	116.56(19)
O2-C13-C14	125.79(19)	O1-C13-C14	117.63(17)
C19-C14-C15	121.01(19)	C19-C14-C13	117.17(18)
C15-C14-C13	121.80(17)	C16-C15-C14	117.22(18)
C16-C15-C11	125.66(18)	C14-C15-C11	117.12(18)
C17-C16-C15	120.82(18)	C17-C16-C20	114.90(19)
C15-C16-C20	124.26(18)	O3-C17-C16	117.33(19)
O3-C17-C18	121.62(19)	C16-C17-C18	121.0(2)
C19-C18-C17	118.28(19)	C19-C18-C22	122.8(2)
C17-C18-C22	118.9(2)	C18-C19-C14	121.59(19)
C18-C19-H19	122.0(12)	C14-C19-H19	116.4(12)
O4-C20-O5	124.6(2)	O4-C20-C16	124.9(2)
O5-C20-C16	110.47(18)	O5-C21-H21A	109.5
O5-C21-H21B	109.5	H21A-C21-H21B	109.5
O5-C21-H21C	109.5	H21A-C21-H21C	109.5
H21B-C21-H21C	109.5	O6-C22-O7	123.0(2)
O6-C22-C18	123.4(2)	O7-C22-C18	113.6(2)
O7-C23-H23A	109.5	O7-C23-H23B	109.5
H23A-C23-H23B	109.5	O7-C23-H23C	109.5
H23A-C23-H23C	109.5	H23B-C23-H23C	109.5

Table S7. Torsion angles ($^{\circ}$) for **12**.

C5-N1-C1-C2	42.9(4)	C9-N1-C1-C2	-166.2(3)
N1-C1-C2-C3	-58.2(4)	C1-C2-C3-C4	44.2(4)
C2-C3-C4-C10	164.4(3)	C2-C3-C4-C5	-16.2(4)
C9-N1-C5-C4	-163.7(2)	C1-N1-C5-C4	-13.4(3)
C9-N1-C5-C6	18.1(3)	C1-N1-C5-C6	168.3(2)
C10-C4-C5-N1	179.2(2)	C3-C4-C5-N1	-0.1(3)
C10-C4-C5-C6	-2.5(3)	C3-C4-C5-C6	178.1(2)
N1-C5-C6-C12	-179.4(2)	C4-C5-C6-C12	2.3(3)
N1-C5-C6-C7	0.2(3)	C4-C5-C6-C7	-178.0(2)
C12-C6-C7-C8	-173.4(3)	C5-C6-C7-C8	6.9(4)
C6-C7-C8-C9	-31.8(4)	C5-N1-C9-C8	-43.1(4)
C1-N1-C9-C8	166.4(3)	C7-C8-C9-N1	49.8(4)
C5-C4-C10-C11	-0.1(3)	C3-C4-C10-C11	179.3(2)
C4-C10-C11-C12	2.8(3)	C4-C10-C11-C15	-177.4(2)
C5-C6-C12-O1	-179.19(18)	C7-C6-C12-O1	1.1(3)
C5-C6-C12-C11	0.5(3)	C7-C6-C12-C11	-179.1(2)
C13-O1-C12-C6	177.40(19)	C13-O1-C12-C11	-2.3(3)
C10-C11-C12-C6	-3.0(3)	C15-C11-C12-C6	177.2(2)
C10-C11-C12-O1	176.71(19)	C15-C11-C12-O1	-3.1(3)
C12-O1-C13-O2	-176.7(2)	C12-O1-C13-C14	4.5(3)
O2-C13-C14-C19	-1.6(3)	O1-C13-C14-C19	177.10(19)

O2-C13-C14-C15	-179.9(2)	O1-C13-C14-C15	-1.2(3)
C19-C14-C15-C16	-2.0(3)	C13-C14-C15-C16	176.32(19)
C19-C14-C15-C11	177.85(19)	C13-C14-C15-C11	-3.9(3)
C12-C11-C15-C16	-174.23(19)	C10-C11-C15-C16	6.0(3)
C12-C11-C15-C14	6.0(3)	C10-C11-C15-C14	-173.8(2)
C14-C15-C16-C17	0.9(3)	C11-C15-C16-C17	-178.9(2)
C14-C15-C16-C20	-177.24(19)	C11-C15-C16-C20	3.0(3)
C15-C16-C17-O3	-178.59(19)	C20-C16-C17-O3	-0.3(3)
C15-C16-C17-C18	1.1(3)	C20-C16-C17-C18	179.4(2)
O3-C17-C18-C19	177.6(2)	C16-C17-C18-C19	-2.0(3)
O3-C17-C18-C22	-3.3(3)	C16-C17-C18-C22	177.1(2)
C17-C18-C19-C14	1.0(3)	C22-C18-C19-C14	-178.1(2)
C15-C14-C19-C18	1.0(3)	C13-C14-C19-C18	-177.3(2)
C21-O5-C20-O4	4.9(3)	C21-O5-C20-C16	-175.93(19)
C17-C16-C20-O4	81.0(3)	C15-C16-C20-O4	-100.7(3)
C17-C16-C20-O5	-98.1(2)	C15-C16-C20-O5	80.2(3)
C23-O7-C22-O6	-4.6(4)	C23-O7-C22-C18	174.9(2)
C19-C18-C22-O6	176.8(2)	C17-C18-C22-O6	-2.3(4)
C19-C18-C22-O7	-2.7(3)	C17-C18-C22-O7	178.2(2)

Table S8. Anisotropic atomic displacement parameters (\AA^2) for **12**. The anisotropic atomic displacement factor exponent takes the form: $-2\pi^2 [h^2 a^{*2} U_{11} + \dots + 2 h k a^* b^* U_{12}]$

	U_{11}	U_{22}	U_{33}	U_{23}	U_{13}	U_{12}
N1	0.0406(10)	0.0441(12)	0.0659(14)	0.0033(11)	0.0139(9)	-0.0097(8)
O1	0.0297(7)	0.0482(9)	0.0505(10)	0.0159(8)	0.0039(7)	0.0018(6)
O2	0.0299(8)	0.0651(11)	0.0631(11)	0.0227(9)	0.0001(7)	0.0034(7)
O3	0.0484(10)	0.0705(12)	0.0493(10)	0.0254(10)	0.0039(8)	-0.0008(9)
O4	0.0514(10)	0.0502(11)	0.0725(13)	0.0008(10)	-0.0022(9)	0.0149(8)
O5	0.0397(8)	0.0566(10)	0.0448(9)	-0.0050(9)	-0.0068(7)	0.0010(7)
O6	0.0534(10)	0.0658(12)	0.0614(11)	0.0255(10)	0.0142(8)	-0.0031(8)
O7	0.0361(8)	0.0679(12)	0.0637(11)	0.0178(10)	0.0065(8)	-0.0126(8)
C1	0.0414(14)	0.068(2)	0.091(2)	-0.0046(19)	0.0163(14)	-0.0207(13)
C2	0.0343(13)	0.084(2)	0.0692(19)	-0.0005(18)	0.0073(12)	-0.0056(13)
C3	0.0299(11)	0.072(2)	0.0597(18)	0.0020(16)	0.0019(11)	-0.0039(11)
C4	0.0312(10)	0.0423(13)	0.0420(13)	-0.0067(11)	0.0038(9)	-0.0038(9)
C5	0.0355(11)	0.0342(12)	0.0464(13)	-0.0087(11)	0.0102(10)	-0.0077(9)
C6	0.0360(11)	0.0335(12)	0.0420(13)	-0.0006(10)	0.0084(9)	-0.0007(9)
C7	0.0500(14)	0.0473(15)	0.0545(16)	0.0124(14)	0.0124(13)	0.0041(12)
C8	0.0664(19)	0.093(2)	0.111(3)	0.055(2)	0.0226(18)	0.0008(17)
C9	0.0626(17)	0.0553(17)	0.100(2)	0.0191(18)	0.0196(16)	-0.0132(14)
C10	0.0313(10)	0.0439(13)	0.0364(12)	-0.0001(11)	0.0008(9)	0.0016(9)
C11	0.0285(10)	0.0358(12)	0.0357(12)	-0.0021(10)	0.0034(8)	-0.0001(8)
C12	0.0286(10)	0.0350(12)	0.0386(12)	-0.0013(10)	0.0026(9)	0.0014(8)
C13	0.0296(10)	0.0380(12)	0.0417(12)	0.0037(11)	0.0052(9)	0.0003(9)
C14	0.0303(10)	0.0324(11)	0.0318(11)	-0.0016(10)	0.0036(8)	-0.0007(8)

	U_{11}	U_{22}	U_{33}	U_{23}	U_{13}	U_{12}
C15	0.0295(10)	0.0328(11)	0.0315(11)	-0.0048(10)	0.0029(8)	0.0001(8)
C16	0.0336(10)	0.0372(12)	0.0334(11)	-0.0011(10)	0.0012(9)	0.0020(9)
C17	0.0418(11)	0.0400(12)	0.0322(12)	0.0047(11)	0.0049(9)	0.0009(9)
C18	0.0363(11)	0.0379(12)	0.0373(12)	0.0004(11)	0.0076(9)	-0.0026(9)
C19	0.0304(10)	0.0375(12)	0.0379(12)	-0.0028(10)	0.0022(9)	-0.0001(9)
C20	0.0379(11)	0.0413(13)	0.0385(12)	0.0068(11)	0.0038(9)	0.0008(10)
C21	0.0457(14)	0.080(2)	0.0594(17)	0.0042(16)	-0.0169(12)	-0.0061(13)
C22	0.0425(12)	0.0440(13)	0.0432(14)	0.0039(12)	0.0086(10)	-0.0035(10)
C23	0.0462(15)	0.108(3)	0.094(2)	0.034(2)	0.0067(15)	-0.0303(16)

Table S9. Hydrogen atomic coordinates and isotropic atomic displacement parameters (\AA^2) for **12**.

	x/a	y/b	z/c	$U(\text{eq})$
H8A	0.6568	0.8888	-0.1710	0.107
H8B	0.6195	1.0319	-0.1471	0.107
H9A	0.8136	0.9883	-0.1077	0.086
H9B	0.7501	1.0341	-0.0366	0.086
H21A	0.7632	0.4395	0.3513	0.097
H21B	0.7633	0.5937	0.3685	0.097
H21C	0.8087	0.5396	0.2913	0.097
H23A	0.0067	0.2119	0.1949	0.125
H23B	-0.0812	0.3223	0.1586	0.125
H23C	-0.0227	0.3313	0.2489	0.125
H10	0.707(2)	0.539(3)	0.1413(15)	0.054(7)
H19	0.1821(18)	0.532(2)	0.0856(12)	0.036(6)
H1A	0.957(3)	0.877(3)	-0.0349(18)	0.083(10)
H2A	1.036(2)	0.709(3)	0.0601(16)	0.064(8)
H3A	0.901(3)	0.684(3)	0.148(2)	0.087(10)
H3B	0.891(3)	0.550(4)	0.102(2)	0.091(11)
H7A	0.511(3)	0.956(3)	-0.0652(19)	0.086(10)
H2B	0.951(2)	0.641(3)	-0.0168(18)	0.070(9)
H7B	0.496(3)	0.846(3)	-0.1249(19)	0.080(10)
H1B	0.930(3)	0.906(4)	0.060(2)	0.110(12)
H3	0.349(3)	0.292(3)	0.2888(17)	0.074(9)

Table S10. Hydrogen bond distances (\AA) and angles ($^\circ$) for **12**.

	Donor-H	Acceptor-H	Donor-Acceptor	Angle
O3-H3···O6	0.95(3)	1.69(3)	2.574(2)	152.(3)
C2-H2B···O7	1.06(3)	2.57(3)	3.521(4)	149.(2)
C23-H23A···O5	0.96	2.5	3.115(3)	121.4

Crystal Structure Report for 13

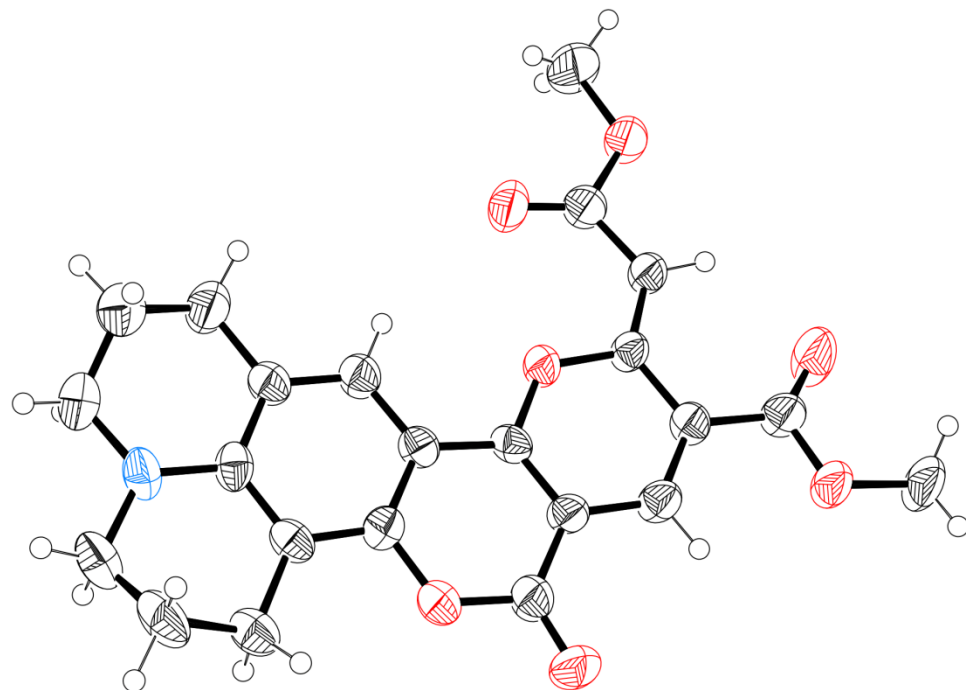


Figure S4. The ORTEP drawing⁴ of X-ray diffraction analysis for compound **13**. CCDC 2125096.

A red needle-like specimen of $C_{23}H_{21}NO_7$, approximate dimensions $0.093\text{ mm} \times 0.118\text{ mm} \times 0.654\text{ mm}$, was used for the X-ray crystallographic analysis. The X-ray intensity data were measured.

Table S11. Data collection details for **13**.

Axis	dx/mm	$2\theta/^\circ$	$\omega/^\circ$	$\phi/^\circ$	$\chi/^\circ$	Width/°	Fra-mes	Time/s	Wave-length/ \AA	Volta-ge/kV	Current/mA	Tempe- rature/K
Omega	39.875	-99.52	-196.16	0.05	26.30	1.60	68	24.00	1.54184	45	30.0	n/a
Omega	39.875	-100.83	-210.20	-187.67	52.45	1.60	72	24.00	1.54184	45	30.0	n/a
Omega	39.875	-100.46	-106.07	105.38	-57.83	1.60	74	24.00	1.54184	45	30.0	n/a

Axis	dx/mm	2θ/°	ω/°	ϕ/°	χ/°	Width/°	Fra-mes	Time/s	Wave-length/Å	Volta-ge/kV	Current/mA	Tempe-rature/K
Omega	39.875	-100.80	-200.04	-257.00	32.48	1.60	68	24.00	1.54184	45	30.0	n/a
Omega	39.875	-101.00	-203.00	-126.64	37.78	1.60	69	24.00	1.54184	45	30.0	n/a
Omega	39.875	39.67	-326.19	270.00	-54.74	1.60	73	24.00	1.54184	45	30.0	n/a
Omega	39.875	-99.90	-197.24	-57.68	27.86	1.60	68	24.00	1.54184	45	30.0	n/a
Omega	39.875	44.78	-38.43	75.16	69.29	1.60	55	24.00	1.54184	45	30.0	n/a
Phi	39.875	85.61	-280.32	0.00	-58.06	1.60	225	24.00	1.54184	45	30.0	n/a
Omega	39.875	-97.67	-103.69	-113.67	-56.62	1.60	74	24.00	1.54184	45	30.0	n/a
Omega	39.875	39.67	-326.19	90.00	-54.74	1.60	73	24.00	1.54184	45	30.0	n/a
Omega	39.875	-94.23	-62.72	37.64	-80.63	1.60	62	24.00	1.54184	45	30.0	n/a
Omega	39.875	39.67	-326.19	0.00	-54.74	1.60	73	24.00	1.54184	45	30.0	n/a
Omega	39.875	-100.72	-200.75	42.15	34.55	1.60	68	24.00	1.54184	45	30.0	n/a
Omega	39.875	39.67	-326.19	180.00	-54.74	1.60	73	24.00	1.54184	45	30.0	n/a
Omega	39.875	-96.19	-196.73	-227.77	35.95	1.60	68	24.00	1.54184	45	30.0	n/a
Omega	39.875	-100.83	-106.04	47.01	-58.93	1.60	74	24.00	1.54184	45	30.0	n/a
Omega	39.875	82.64	-36.62	-58.22	77.11	1.60	63	24.00	1.54184	45	30.0	n/a
Omega	39.875	-100.85	-110.62	134.78	-31.95	1.60	68	24.00	1.54184	45	30.0	n/a
Omega	39.875	-99.90	-202.81	-86.05	40.42	1.60	69	24.00	1.54184	45	30.0	n/a
Omega	39.875	-101.52	-208.03	75.65	46.31	1.60	71	24.00	1.54184	45	30.0	n/a
Omega	39.875	-100.86	-210.38	-164.63	52.92	1.60	72	24.00	1.54184	45	30.0	n/a
Omega	39.875	69.67	-296.19	0.00	-54.74	1.60	73	24.00	1.54184	45	30.0	n/a
Omega	39.875	-100.21	-75.75	-33.75	-65.22	1.60	58	24.00	1.54184	45	30.0	n/a
Omega	39.875	69.67	-296.19	90.00	-54.74	1.60	73	24.00	1.54184	45	30.0	n/a
Phi	39.875	70.61	-295.32	0.00	-58.06	1.60	225	24.00	1.54184	45	30.0	n/a
Omega	39.875	-91.39	-190.44	-37.93	31.98	1.60	68	24.00	1.54184	45	30.0	n/a
Omega	39.875	93.00	-382.07	7.02	62.00	1.60	75	24.00	1.54184	45	30.0	n/a
Omega	39.875	-98.85	-106.83	44.61	-38.97	1.60	69	24.00	1.54184	45	30.0	n/a
Omega	39.875	-2.62	-113.72	270.00	54.74	1.60	73	24.00	1.54184	45	30.0	n/a

Axis	dx/mm	2θ/°	ω/°	ϕ/°	χ/°	Width/°	Fra-mes	Time/s	Wave-length/Å	Volta-ge/kV	Current/mA	Tempe-rature/K
Omega	39.875	84.67	-281.19	180.00	-54.74	1.60	73	24.00	1.54184	45	30.0	n/a
Omega	39.875	84.67	-281.19	0.00	-54.74	1.60	73	24.00	1.54184	45	30.0	n/a
Omega	39.875	54.67	-311.19	270.00	-54.74	1.60	73	24.00	1.54184	45	30.0	n/a
Omega	39.875	-99.76	-110.47	-109.53	-29.62	1.60	68	24.00	1.54184	45	30.0	n/a
Omega	39.875	54.67	-311.19	90.00	-54.74	1.60	73	24.00	1.54184	45	30.0	n/a
Omega	39.875	54.67	-311.19	180.00	-54.74	1.60	73	24.00	1.54184	45	30.0	n/a
Omega	39.875	54.67	-311.19	0.00	-54.74	1.60	73	24.00	1.54184	45	30.0	n/a
Omega	39.875	84.67	-281.19	90.00	-54.74	1.60	73	24.00	1.54184	45	30.0	n/a
Omega	39.875	87.22	-37.01	-42.42	81.01	1.60	62	24.00	1.54184	45	30.0	n/a
Omega	39.875	84.67	-281.19	270.00	-54.74	1.60	73	24.00	1.54184	45	30.0	n/a
Phi	39.875	55.61	49.69	0.00	-58.06	1.60	225	24.00	1.54184	45	30.0	n/a
Omega	39.875	27.38	-337.68	-105.00	-54.74	1.60	72	24.00	1.54184	45	30.0	n/a
Phi	39.875	-18.13	-3.92	0.00	23.00	1.60	225	24.00	1.54184	45	30.0	n/a
Omega	39.875	69.67	-296.19	270.00	-54.74	1.60	73	24.00	1.54184	45	30.0	n/a
Omega	39.875	91.50	-381.45	-46.60	58.28	1.60	74	24.00	1.54184	45	30.0	n/a
Phi	39.875	43.16	28.95	0.00	-23.00	1.60	225	24.00	1.54184	45	30.0	n/a
Phi	39.875	-18.13	-12.20	0.00	58.06	1.60	225	24.00	1.54184	45	30.0	n/a
Omega	39.875	27.38	-337.68	-156.00	-54.74	1.60	72	24.00	1.54184	45	30.0	n/a
Omega	39.875	27.38	-337.68	-54.00	-54.74	1.60	72	24.00	1.54184	45	30.0	n/a
Omega	39.875	91.71	-373.51	-178.35	44.85	1.60	70	24.00	1.54184	45	30.0	n/a
Omega	39.875	69.67	-296.19	180.00	-54.74	1.60	73	24.00	1.54184	45	30.0	n/a
Omega	39.875	93.00	-366.21	62.22	32.38	1.60	68	24.00	1.54184	45	30.0	n/a
Phi	39.875	40.61	34.69	0.00	-58.06	1.60	225	24.00	1.54184	45	30.0	n/a
Omega	39.875	27.38	-337.68	0.00	-54.74	1.60	72	24.00	1.54184	45	30.0	n/a
Omega	39.875	27.38	-337.68	153.00	-54.74	1.60	72	24.00	1.54184	45	30.0	n/a
Phi	39.875	43.16	37.23	0.00	-58.06	1.60	225	24.00	1.54184	45	30.0	n/a
Omega	39.875	-81.15	-181.41	-167.12	35.16	1.60	68	24.00	1.54184	45	30.0	n/a

Axis	dx/mm	2θ/°	ω/°	ϕ/°	χ/°	Width/°	Fra-mes	Time/s	Wave-length/Å	Volta-ge/kV	Current/mA	Tempe-rature/K
Omega	39.875	27.38	-337.68	51.00	-54.74	1.60	72	24.00	1.54184	45	30.0	n/a
Omega	39.875	-2.62	-113.72	0.00	54.74	1.60	73	24.00	1.54184	45	30.0	n/a
Omega	39.875	27.38	-337.68	102.00	-54.74	1.60	72	24.00	1.54184	45	30.0	n/a
Omega	39.875	-2.62	-113.72	90.00	54.74	1.60	73	24.00	1.54184	45	30.0	n/a
Omega	39.875	-2.62	-113.72	180.00	54.74	1.60	73	24.00	1.54184	45	30.0	n/a
Omega	39.875	12.38	-353.48	0.00	-54.74	1.60	73	24.00	1.54184	45	30.0	n/a

A total of 5680 frames were collected. The total exposure time was 37.87 hours. The frames were integrated with the Bruker SAINT software package using a narrow-frame algorithm. The integration of the data using a monoclinic unit cell yielded a total of 45603 reflections to a maximum θ angle of 66.19° (0.84 Å resolution), of which 3201 were independent (average redundancy 14.246, completeness = 91.9%, Rint = 14.21%, Rsig = 12.25%) and 1257 (39.27%) were greater than $2\sigma(F_2)$. The final cell constants of $a = 11.3428(5)$ Å, $b = 20.3876(9)$ Å, $c = 8.5895(4)$ Å, $\beta = 93.145(3)$ °, volume = 1983.35(15) Å³, are based upon the refinement of the XYZ-centroids of 7323 reflections above 20 $\sigma(I)$ with $7.806^\circ < 2\theta < 111.6^\circ$. Data were corrected for absorption effects using the multi-scan method (SADABS). The ratio of minimum to maximum apparent transmission was 0.772. The calculated minimum and maximum transmission coefficients (based on crystal size) are 0.5960 and 0.9220.

The structure was solved and refined using the Bruker SHELXTL Software Package, using the space group P 1 21/c 1, with Z = 4 for the formula unit, C₂₃H₂₁NO₇. The final anisotropic full-matrix least-squares refinement on F₂ with 283 variables converged at R1 = 7.38%, for the observed data and wR2 = 23.70% for all data. The goodness-of-fit was 0.989. The largest peak in the final difference electron density synthesis was 0.273 e-/Å³ and the largest hole was -0.257 e-/Å³ with an RMS deviation of 0.060 e-/Å³. On the basis of the final model, the calculated density was 1.418 g/cm³ and F(000), 888 e-.

Table S12. Sample and crystal data for **13**.

Identification code	KVy0615_10	
Chemical formula	C ₂₃ H ₂₁ NO ₇	
Formula weight	423.41 g/mol	
Temperature	296(2) K	
Wavelength	1.54178 Å	
Crystal size	0.093 x 0.118 x 0.654 mm	
Crystal habit	red needle	
Crystal system	monoclinic	
Space group	P 1 21/c 1	
Unit cell dimensions	$a = 11.3428(5)$ Å	$\alpha = 90^\circ$
	$b = 20.3876(9)$ Å	$\beta = 93.145(3)$ °
	$c = 8.5895(4)$ Å	$\gamma = 90^\circ$
Volume	1983.35(15) Å ³	
Z	4	
Density (calculated)	1.418 g/cm ³	
Absorption coefficient	0.884 mm ⁻¹	
F(000)	888	

Table S13. Data collection and structure refinement for **13**.

Theta range for data collection	3.90 to 66.19°
Index ranges	-12≤h≤12, -22≤k≤23, -9≤l≤9
Reflections collected	45603
Independent reflections	3201 [R(int) = 0.1421]
Coverage of independent reflections	91.9%

Absorption correction	multi-scan		
Max. and min. transmission	0.9220 and 0.5960		
Structure solution technique	direct methods		
Structure solution program	SHELXL-2014 (Sheldrick, 2014)		
Refinement method	Full-matrix least-squares on F2		
Refinement program	SHELXL-2014 (Sheldrick, 2014)		
Function minimized	$\Sigma w(Fo^2 - Fc^2)^2$		
Data / restraints / parameters	3201 / 0 / 283		
Goodness-of-fit on F2	0.989		
$\Delta/\sigma_{\text{max}}$	0.006		
Final R indices	1257 data; $I > 2\sigma(I)$	R1 = 0.0738, wR2 = 0.1727	
	all data	R1 = 0.2244, wR2 = 0.2370	
Weighting scheme	$w = 1/[\sigma^2(Fo^2) + (0.0977P)^2 + 1.3622P]$ where $P = (Fo^2 + 2Fc^2)/3$		
Extinction coefficient	0.0002(1)		
Largest diff. peak and hole	0.273 and -0.257 e \AA^{-3}		
R.M.S. deviation from mean	0.060 e \AA^{-3}		

Table S14. Atomic coordinates and equivalent isotropic atomic displacement parameters (\AA^2) for **13**. U(eq) is defined as one third of the trace of the orthogonalized U_{ij} tensor.

	x/a	y/b	z/c	U(eq)
N1	0.0470(4)	0.3526(2)	0.3296(5)	0.0535(13)
O1	0.8548(3)	0.15605(17)	0.1646(4)	0.0513(10)
O2	0.7813(3)	0.06119(18)	0.0827(4)	0.0723(13)
O3	0.6111(3)	0.25900(14)	0.8953(4)	0.0442(9)
O4	0.5256(3)	0.37712(17)	0.8099(5)	0.0805(14)
O5	0.3723(3)	0.37069(16)	0.6370(4)	0.0668(12)
O6	0.3440(4)	0.15007(18)	0.6299(5)	0.0871(15)
O7	0.4453(3)	0.06125(17)	0.6947(4)	0.0679(12)
C1	0.0523(5)	0.4238(3)	0.3430(7)	0.0765(19)
C2	0.9991(6)	0.4567(3)	0.2021(8)	0.097(2)
C3	0.8758(5)	0.4335(3)	0.1653(7)	0.0699(18)
C4	0.8695(4)	0.3599(2)	0.1623(6)	0.0457(14)
C5	0.9545(4)	0.3217(3)	0.2509(6)	0.0421(13)
C6	0.9487(4)	0.2528(3)	0.2506(6)	0.0413(13)
C7	0.0401(4)	0.2123(2)	0.3416(6)	0.0513(15)
C8	0.1558(4)	0.2492(3)	0.3616(7)	0.0655(17)
C9	0.1351(5)	0.3165(3)	0.4257(7)	0.0669(18)
C10	0.7817(4)	0.3281(2)	0.0759(6)	0.0458(14)
C11	0.7731(4)	0.2596(2)	0.0732(6)	0.0390(13)
C12	0.8576(4)	0.2240(2)	0.1620(6)	0.0423(14)
C13	0.6902(4)	0.2230(3)	0.9827(5)	0.0373(13)
C14	0.6871(4)	0.1562(2)	0.9792(6)	0.0420(14)

	x/a	y/b	z/c	U(eq)
C15	0.7727(4)	0.1203(3)	0.0748(6)	0.0493(15)
C16	0.5999(4)	0.1252(2)	0.8818(6)	0.0462(14)
C17	0.5200(4)	0.1599(2)	0.7928(6)	0.0410(13)
C18	0.5235(4)	0.2310(2)	0.7979(6)	0.0386(14)
C19	0.4527(4)	0.2732(2)	0.7190(6)	0.0436(14)
C20	0.4593(5)	0.3437(3)	0.7318(6)	0.0500(15)
C21	0.3689(5)	0.4415(3)	0.6327(7)	0.089(2)
C22	0.4273(5)	0.1257(3)	0.6972(7)	0.0514(15)
C23	0.3583(5)	0.0224(2)	0.6063(7)	0.0743(19)

Table S15. Bond lengths (Å) for **13**.

N1-C5	1.369(6)	N1-C1	1.457(6)
N1-C9	1.460(6)	O1-C15	1.384(5)
O1-C12	1.385(5)	O2-C15	1.210(5)
O3-C13	1.354(5)	O3-C18	1.387(5)
O4-C20	1.194(5)	O5-C20	1.360(5)
O5-C21	1.444(6)	O6-C22	1.190(5)
O7-C22	1.330(5)	O7-C23	1.447(5)
C1-C2	1.483(7)	C1-H1A	0.97
C1-H1B	0.97	C2-C3	1.494(7)
C2-H2A	0.97	C2-H2B	0.97
C3-C4	1.504(6)	C3-H3A	0.97
C3-H3B	0.97	C4-C10	1.372(6)
C4-C5	1.426(6)	C5-C6	1.406(6)
C6-C12	1.381(6)	C6-C7	1.509(6)
C7-C8	1.514(6)	C7-H7A	0.97
C7-H7B	0.97	C8-C9	1.502(7)
C8-H8A	0.97	C8-H8B	0.97
C9-H9A	0.97	C9-H9B	0.97
C10-C11	1.400(6)	C10-H10	0.93
C11-C12	1.396(6)	C11-C13	1.402(6)
C13-C14	1.363(6)	C14-C16	1.409(6)
C14-C15	1.437(6)	C16-C17	1.353(6)
C16-H16	0.93	C17-C18	1.450(6)
C17-C22	1.474(7)	C18-C19	1.336(6)
C19-C20	1.443(6)	C19-H19	0.93
C21-H21A	0.96	C21-H21B	0.96
C21-H21C	0.96	C23-H23A	0.96
C23-H23B	0.96	C23-H23C	0.96

Table S16. Bond angles (°) for **13**.

C5-N1-C1	121.6(5)	C5-N1-C9	122.0(5)
C1-N1-C9	115.7(5)	C15-O1-C12	122.2(4)

C13-O3-C18	122.8(4)	C20-O5-C21	115.9(4)
C22-O7-C23	116.7(4)	N1-C1-C2	111.9(5)
N1-C1-H1A	109.2	C2-C1-H1A	109.2
N1-C1-H1B	109.2	C2-C1-H1B	109.2
H1A-C1-H1B	107.9	C1-C2-C3	111.3(5)
C1-C2-H2A	109.4	C3-C2-H2A	109.4
C1-C2-H2B	109.4	C3-C2-H2B	109.4
H2A-C2-H2B	108.0	C2-C3-C4	111.2(5)
C2-C3-H3A	109.4	C4-C3-H3A	109.4
C2-C3-H3B	109.4	C4-C3-H3B	109.4
H3A-C3-H3B	108.0	C10-C4-C5	118.8(5)
C10-C4-C3	120.8(5)	C5-C4-C3	120.4(5)
N1-C5-C6	119.6(5)	N1-C5-C4	119.3(5)
C6-C5-C4	120.9(5)	C12-C6-C5	117.4(5)
C12-C6-C7	121.6(5)	C5-C6-C7	121.0(5)
C6-C7-C8	110.7(4)	C6-C7-H7A	109.5
C8-C7-H7A	109.5	C6-C7-H7B	109.5
C8-C7-H7B	109.5	H7A-C7-H7B	108.1
C9-C8-C7	110.0(5)	C9-C8-H8A	109.7
C7-C8-H8A	109.7	C9-C8-H8B	109.7
C7-C8-H8B	109.7	H8A-C8-H8B	108.2
N1-C9-C8	111.7(4)	N1-C9-H9A	109.3
C8-C9-H9A	109.3	N1-C9-H9B	109.3
C8-C9-H9B	109.3	H9A-C9-H9B	107.9
C4-C10-C11	121.8(5)	C4-C10-H10	119.1
C11-C10-H10	119.1	C12-C11-C10	117.7(5)
C12-C11-C13	116.4(5)	C10-C11-C13	125.8(5)
C6-C12-O1	115.7(5)	C6-C12-C11	123.3(5)
O1-C12-C11	120.9(5)	O3-C13-C14	121.0(4)
O3-C13-C11	114.9(5)	C14-C13-C11	124.1(5)
C13-C14-C16	118.5(4)	C13-C14-C15	118.7(5)
C16-C14-C15	122.8(5)	O2-C15-O1	116.3(5)
O2-C15-C14	126.1(5)	O1-C15-C14	117.6(5)
C17-C16-C14	121.8(4)	C17-C16-H16	119.1
C14-C16-H16	119.1	C16-C17-C18	119.3(5)
C16-C17-C22	120.1(5)	C18-C17-C22	120.5(5)
C19-C18-O3	115.6(4)	C19-C18-C17	127.8(5)
O3-C18-C17	116.6(4)	C18-C19-C20	125.2(5)
C18-C19-H19	117.4	C20-C19-H19	117.4
O4-C20-O5	121.3(5)	O4-C20-C19	129.8(5)
O5-C20-C19	109.0(5)	O5-C21-H21A	109.5
O5-C21-H21B	109.5	H21A-C21-H21B	109.5
O5-C21-H21C	109.5	H21A-C21-H21C	109.5
H21B-C21-H21C	109.5	O6-C22-O7	121.5(5)
O6-C22-C17	126.7(5)	O7-C22-C17	111.8(5)

O7-C23-H23A	109.5	O7-C23-H23B	109.5
H23A-C23-H23B	109.5	O7-C23-H23C	109.5
H23A-C23-H23C	109.5	H23B-C23-H23C	109.5

Table S17. Torsion angles ($^{\circ}$) for **13**.

C5-N1-C1-C2	-33.8(7)	C9-N1-C1-C2	155.8(5)
N1-C1-C2-C3	54.5(7)	C1-C2-C3-C4	-50.5(7)
C2-C3-C4-C10	-154.4(5)	C2-C3-C4-C5	26.2(7)
C1-N1-C5-C6	-175.3(5)	C9-N1-C5-C6	-5.6(7)
C1-N1-C5-C4	8.6(7)	C9-N1-C5-C4	178.3(5)
C10-C4-C5-N1	175.8(4)	C3-C4-C5-N1	-4.8(7)
C10-C4-C5-C6	-0.2(7)	C3-C4-C5-C6	179.1(5)
N1-C5-C6-C12	-176.2(4)	C4-C5-C6-C12	-0.2(7)
N1-C5-C6-C7	2.6(7)	C4-C5-C6-C7	178.7(4)
C12-C6-C7-C8	152.5(5)	C5-C6-C7-C8	-26.3(6)
C6-C7-C8-C9	51.4(6)	C5-N1-C9-C8	32.4(7)
C1-N1-C9-C8	-157.3(5)	C7-C8-C9-N1	-54.8(6)
C5-C4-C10-C11	0.4(7)	C3-C4-C10-C11	-179.0(5)
C4-C10-C11-C12	-0.1(7)	C4-C10-C11-C13	-176.7(5)
C5-C6-C12-O1	179.9(4)	C7-C6-C12-O1	1.1(7)
C5-C6-C12-C11	0.5(7)	C7-C6-C12-C11	-178.3(4)
C15-O1-C12-C6	-176.4(4)	C15-O1-C12-C11	3.1(7)
C10-C11-C12-C6	-0.4(7)	C13-C11-C12-C6	176.5(4)
C10-C11-C12-O1	-179.8(4)	C13-C11-C12-O1	-2.9(7)
C18-O3-C13-C14	-0.2(7)	C18-O3-C13-C11	179.4(4)
C12-C11-C13-O3	-178.6(4)	C10-C11-C13-O3	-1.9(7)
C12-C11-C13-C14	1.0(7)	C10-C11-C13-C14	177.7(5)
O3-C13-C14-C16	0.3(7)	C11-C13-C14-C16	-179.3(4)
O3-C13-C14-C15	-179.7(4)	C11-C13-C14-C15	0.7(8)
C12-O1-C15-O2	177.6(4)	C12-O1-C15-C14	-1.2(7)
C13-C14-C15-O2	-179.3(5)	C16-C14-C15-O2	0.7(8)
C13-C14-C15-O1	-0.6(7)	C16-C14-C15-O1	179.4(4)
C13-C14-C16-C17	0.0(7)	C15-C14-C16-C17	180.0(5)
C14-C16-C17-C18	-0.3(7)	C14-C16-C17-C22	-177.6(5)
C13-O3-C18-C19	-179.8(4)	C13-O3-C18-C17	-0.1(6)
C16-C17-C18-C19	180.0(5)	C22-C17-C18-C19	-2.7(8)
C16-C17-C18-O3	0.4(7)	C22-C17-C18-O3	177.7(4)
O3-C18-C19-C20	-1.8(7)	C17-C18-C19-C20	178.6(5)
C21-O5-C20-O4	2.4(8)	C21-O5-C20-C19	-178.2(4)
C18-C19-C20-O4	0.5(9)	C18-C19-C20-O5	-178.9(5)
C23-O7-C22-O6	-0.1(8)	C23-O7-C22-C17	178.9(4)
C16-C17-C22-O6	169.9(6)	C18-C17-C22-O6	-7.4(9)
C16-C17-C22-O7	-9.1(7)	C18-C17-C22-O7	173.6(4)

Table S18. Anisotropic atomic displacement parameters (\AA^2) for **13**. The anisotropic atomic displacement factor exponent takes the form: $-2\pi^2 [h^2 a^*{}^2 U_{11} + \dots + 2 h k a^* b^* U_{12}]$

	U11	U22	U33	U23	U13	U12
N1	0.042(3)	0.062(3)	0.055(3)	-0.005(3)	-0.012(2)	-0.009(3)
O1	0.044(2)	0.051(2)	0.057(2)	0.002(2)	-0.0133(19)	0.0024(19)
O2	0.071(3)	0.039(2)	0.104(3)	0.006(2)	-0.028(2)	0.007(2)
O3	0.036(2)	0.039(2)	0.055(2)	-0.0009(18)	-0.0126(18)	-0.0015(18)
O4	0.082(3)	0.044(3)	0.110(4)	-0.004(2)	-0.047(3)	-0.005(2)
O5	0.061(3)	0.041(2)	0.093(3)	-0.001(2)	-0.035(2)	0.009(2)
O6	0.063(3)	0.053(3)	0.140(4)	-0.019(2)	-0.052(3)	0.008(2)
O7	0.061(3)	0.040(2)	0.098(3)	-0.001(2)	-0.038(2)	-0.007(2)
C1	0.077(5)	0.063(5)	0.086(5)	-0.003(4)	-0.022(4)	-0.024(4)
C2	0.093(5)	0.072(5)	0.119(6)	0.023(4)	-0.048(5)	-0.026(4)
C3	0.061(4)	0.048(4)	0.098(5)	-0.001(3)	-0.020(4)	-0.007(3)
C4	0.038(3)	0.048(3)	0.051(4)	0.001(3)	-0.006(3)	0.004(3)
C5	0.033(3)	0.051(4)	0.043(3)	-0.006(3)	0.005(3)	-0.010(3)
C6	0.031(3)	0.055(4)	0.038(3)	0.003(3)	0.001(3)	0.005(3)
C7	0.040(3)	0.066(4)	0.048(4)	0.007(3)	-0.001(3)	0.004(3)
C8	0.031(3)	0.099(5)	0.065(4)	0.011(4)	-0.014(3)	0.000(3)
C9	0.051(4)	0.086(5)	0.060(4)	-0.003(4)	-0.020(3)	0.001(3)
C10	0.037(3)	0.046(4)	0.053(4)	-0.002(3)	-0.004(3)	0.003(3)
C11	0.028(3)	0.044(3)	0.045(3)	0.001(3)	-0.001(3)	0.003(3)
C12	0.041(4)	0.039(3)	0.047(4)	-0.002(3)	0.004(3)	-0.003(3)
C13	0.025(3)	0.044(3)	0.042(4)	0.005(3)	-0.002(3)	0.004(3)
C14	0.034(3)	0.037(3)	0.054(4)	0.005(3)	-0.004(3)	0.000(3)
C15	0.039(4)	0.048(4)	0.059(4)	-0.002(3)	-0.007(3)	0.001(3)
C16	0.037(3)	0.037(3)	0.064(4)	0.002(3)	-0.001(3)	0.000(3)
C17	0.029(3)	0.042(3)	0.052(4)	-0.002(3)	-0.003(3)	0.002(3)
C18	0.030(3)	0.035(3)	0.050(4)	0.000(3)	-0.001(3)	-0.003(3)
C19	0.035(3)	0.038(3)	0.057(4)	0.000(3)	-0.009(3)	0.000(3)
C20	0.042(4)	0.046(4)	0.061(4)	0.002(3)	-0.007(3)	0.004(3)
C21	0.112(6)	0.039(4)	0.112(6)	-0.003(4)	-0.034(4)	0.022(4)
C22	0.039(4)	0.042(4)	0.072(4)	0.001(3)	-0.008(3)	0.005(3)
C23	0.063(4)	0.044(3)	0.112(5)	-0.010(3)	-0.030(4)	-0.016(3)

Table S19. Hydrogen atomic coordinates and isotropic atomic displacement parameters (\AA^2) for **13**.

	x/a	y/b	z/c	U(eq)
H1A	1.1340	0.4373	0.3590	0.092
H1B	1.0107	0.4374	0.4333	0.092
H2A	1.0468	0.4478	0.1141	0.116
H2B	0.9987	0.5038	0.2188	0.116
H3A	0.8477	0.4507	0.0647	0.084

	x/a	y/b	z/c	U(eq)
H3B	0.8247	0.4501	0.2432	0.084
H7A	1.0524	0.1715	0.2870	0.062
H7B	1.0118	0.2019	0.4432	0.062
H8A	1.2099	0.2253	0.4322	0.079
H8B	1.1913	0.2528	0.2618	0.079
H9A	1.1087	0.3126	0.5308	0.08
H9B	1.2088	0.3407	0.4308	0.08
H10	0.7263	0.3528	0.0174	0.055
H16	0.5971	0.0796	-0.1213	0.055
H19	0.3946	0.2558	-0.3496	0.052
H21A	0.4479	0.4583	-0.3695	0.134
H21B	0.3329	0.4576	-0.2762	0.134
H21C	0.3237	0.4556	-0.4589	0.134
H23A	0.2900	0.0166	-0.3339	0.112
H23B	0.3913	-0.0197	-0.4163	0.112
H23C	0.3359	0.0445	-0.4895	0.112

Table S20. Hydrogen bond distances (Å) and angles (°) for **13**.

	Donor-H	Acceptor-H	Donor-Acceptor	Angle
C23-H23B...O4	0.96	2.46	3.305(6)	146.6
C19-H19...O6	0.93	2.24	2.882(6)	126.1
C9-H9B...O5	0.97	2.57	3.350(6)	137.8

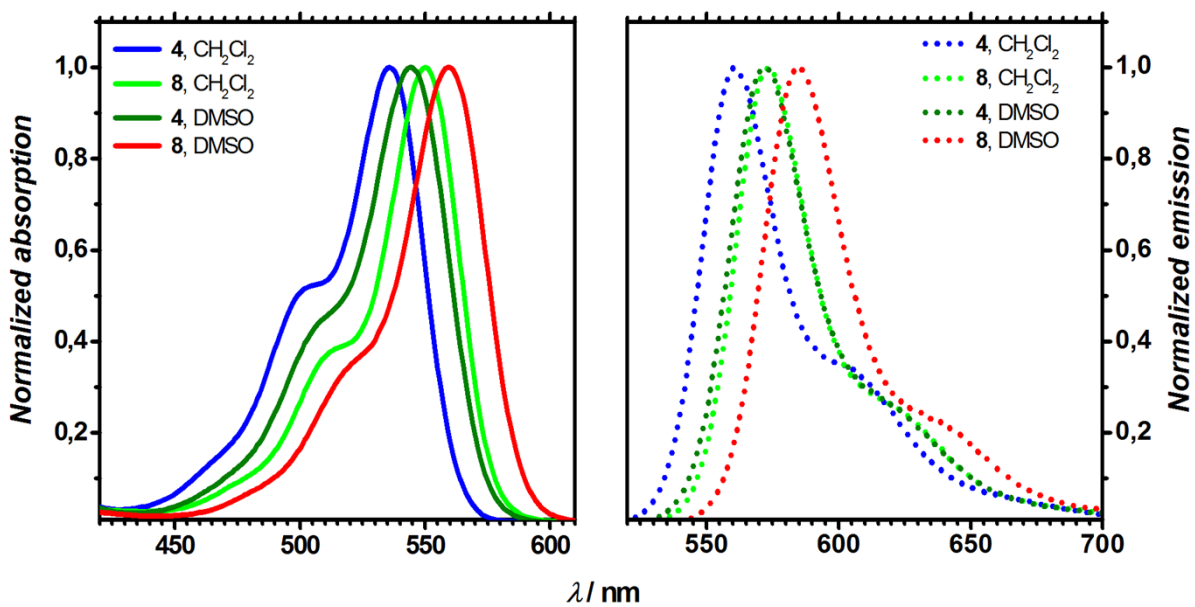


Figure S5. Absorption (solid) and emission (dotted) of compounds **4** and **23** in CH_2Cl_2 and DMSO.

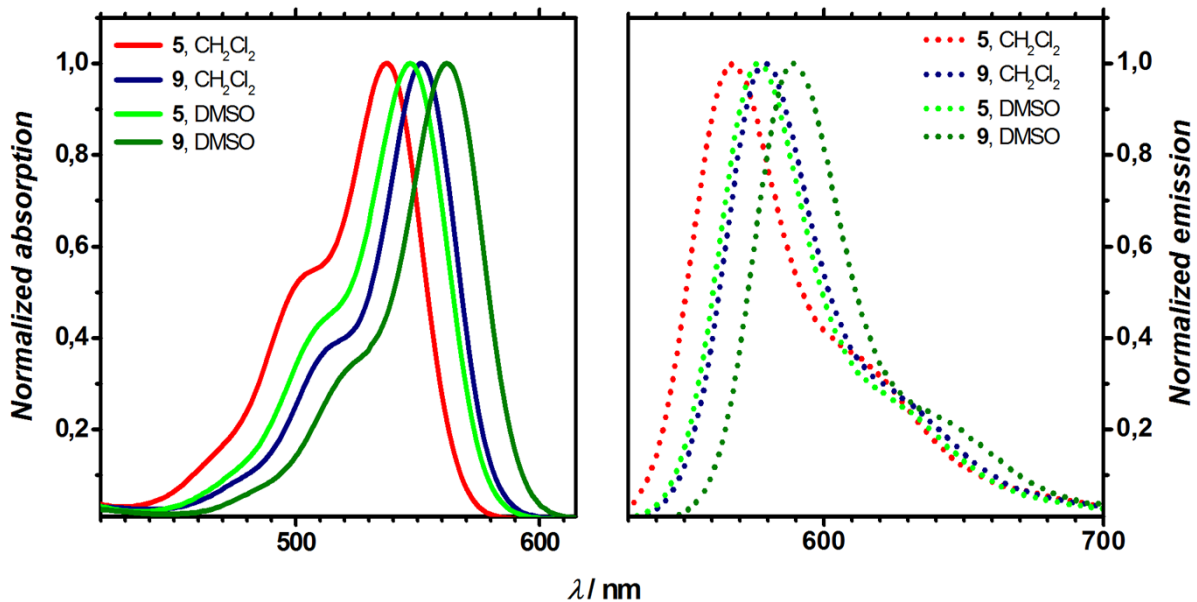


Figure S6. Absorption (solid) and emission (dotted) of compounds **5** and **9** in CH_2Cl_2 and DMSO.

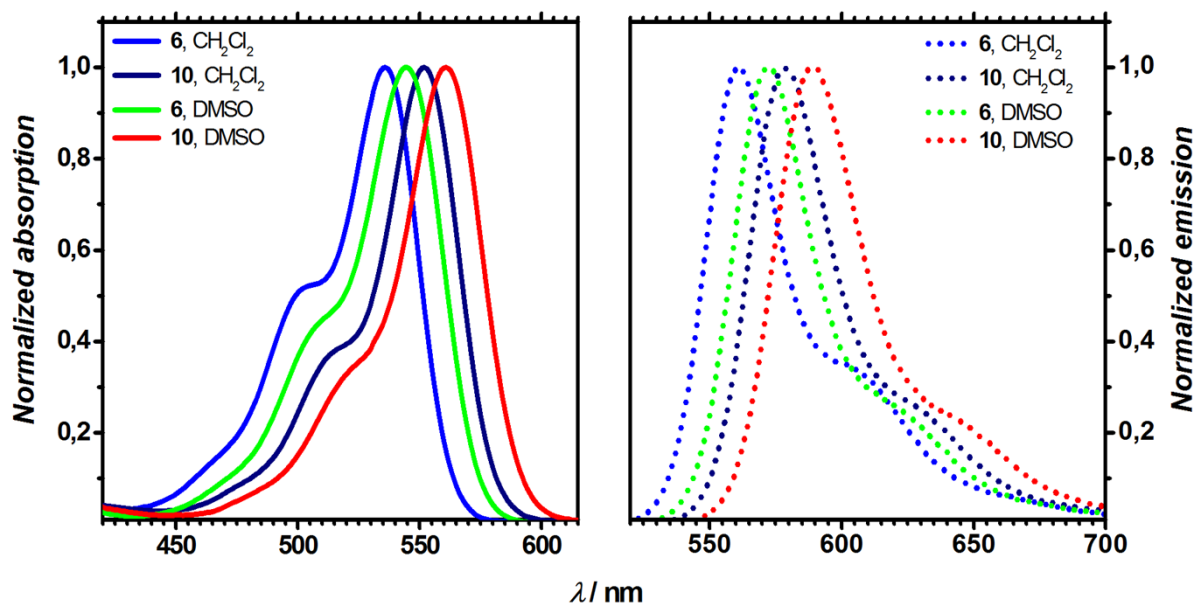


Figure S7. Absorption (solid) and emission (dotted) of compounds **6** and **10** in CH₂Cl₂ and DMSO.

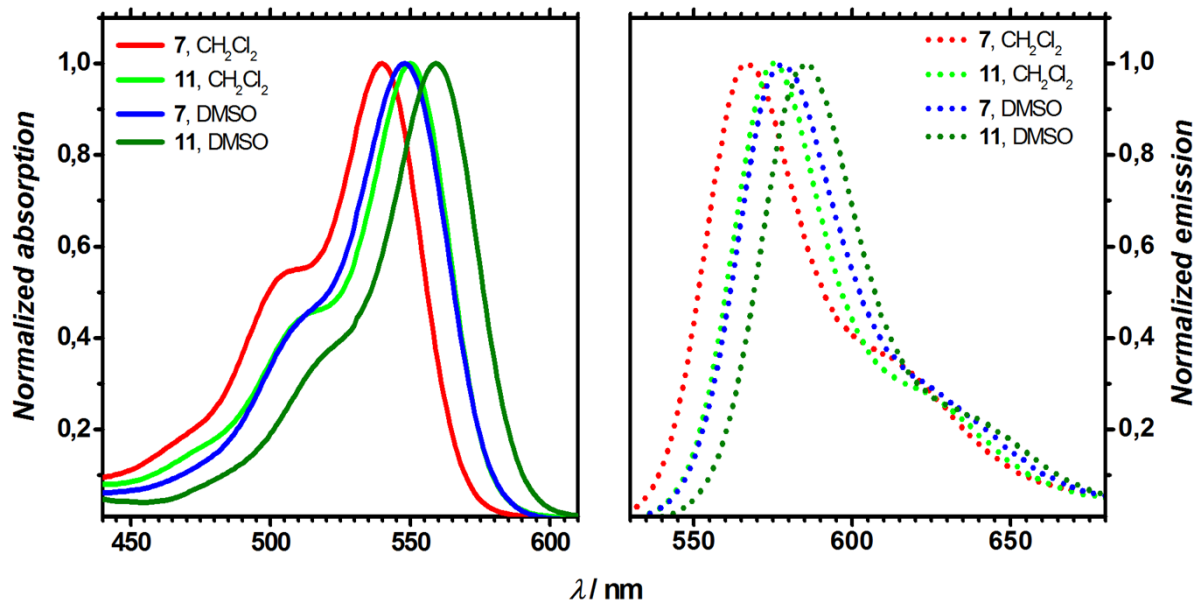


Figure S8. Absorption (solid) and emission (dotted) of compounds **7** and **11** in CH₂Cl₂ and DMSO.

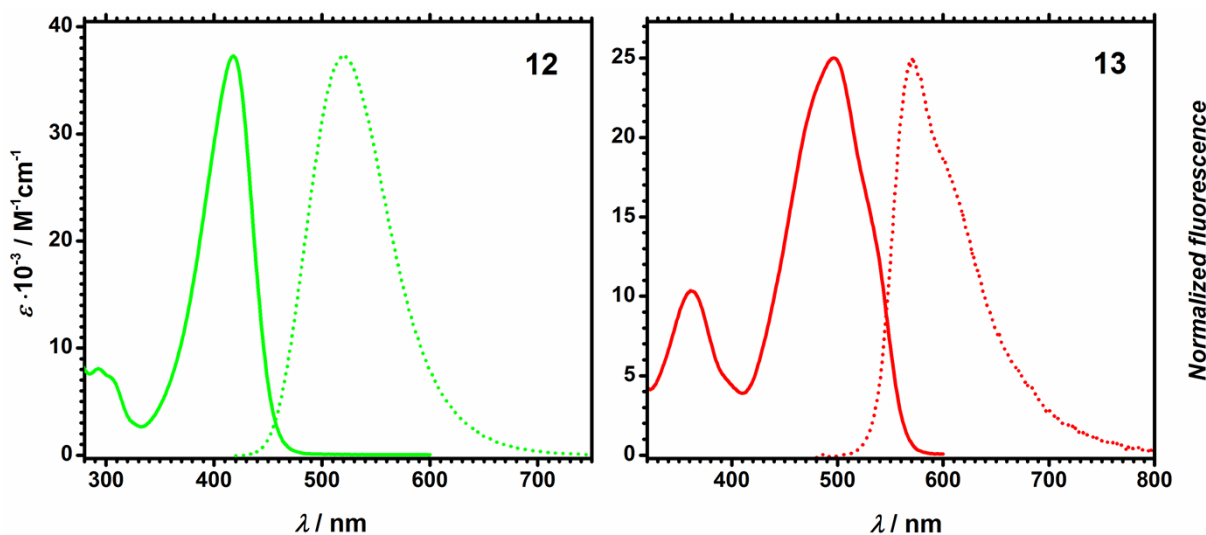


Figure S9. Absorption (solid) and emission (dotted) spectra for compounds **12** (in CH_2Cl_2) and **13** (in DMSO).

Table S21. The spectroscopic properties for compounds **12** and **13**.

Dye	Solvent	$\lambda_{\text{abs}}^{\text{max}}$ [nm]	$\varepsilon \cdot 10^{-3}$ [$\text{M}^{-1}\text{cm}^{-1}$]	$\lambda_{\text{em}}^{\text{max}}$ [nm]	$\bar{\Delta\nu}$ [cm^{-1}]	Φ_{fl}
12^a	CH_2Cl_2	418	37	520	4700	0.73
13	CH_2Cl_2	491	32	— ^b	—	—
	DMSO	497	25	571	2600	0.037

^a – Compound **12** in DMSO does not show linear dependence of the absorption vs. concentration.

^b – In the fluorescence spectrum compound **13** in CH_2Cl_2 shows emission from two forms.

Photostability measurements

Photostability was determined through the variation in absorption of each sample at the appropriate absorption maximum wavelength (λ_{abs}) with respect to irradiation time. Ethanol was selected as the solvent. Concentrations giving similar optical densities ($A \approx 1$) were used. Quartz cells of samples were irradiated with a 300 W Xe lamp (Asahi spectra MAX-350) for 120 min (for compounds **4-7** in DMSO), 50 min (for compounds **8-11** in DMSO) and 30 min for all dyes in DCM at 25 °C equipped with a UV/vis mirror module through a glass fiber. The absorption spectra were measured at appropriate times during the irradiation. **Rhodamine 6G**, **Fluorescein** and **Rdl12⁵** in appropriate solvents were used as references.

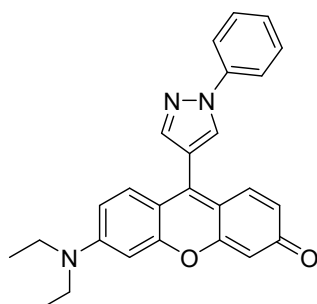


Figure S10. The structure of **Rdl12**.

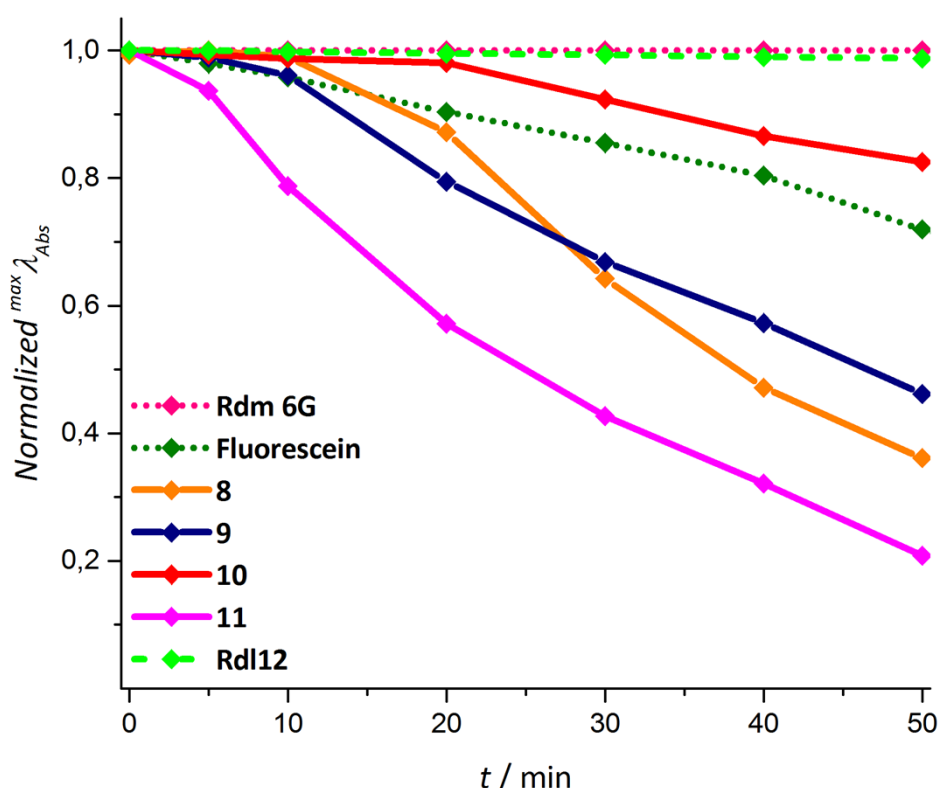


Figure S11. Photostability of rhodols **8-11** compared to the Rhodamine 6G in EtOH, fluorescein in 0,1M NaOH aqueous solution and **Rdl12** measured in DMSO using a collimated light source from a 300W Xe lamp.

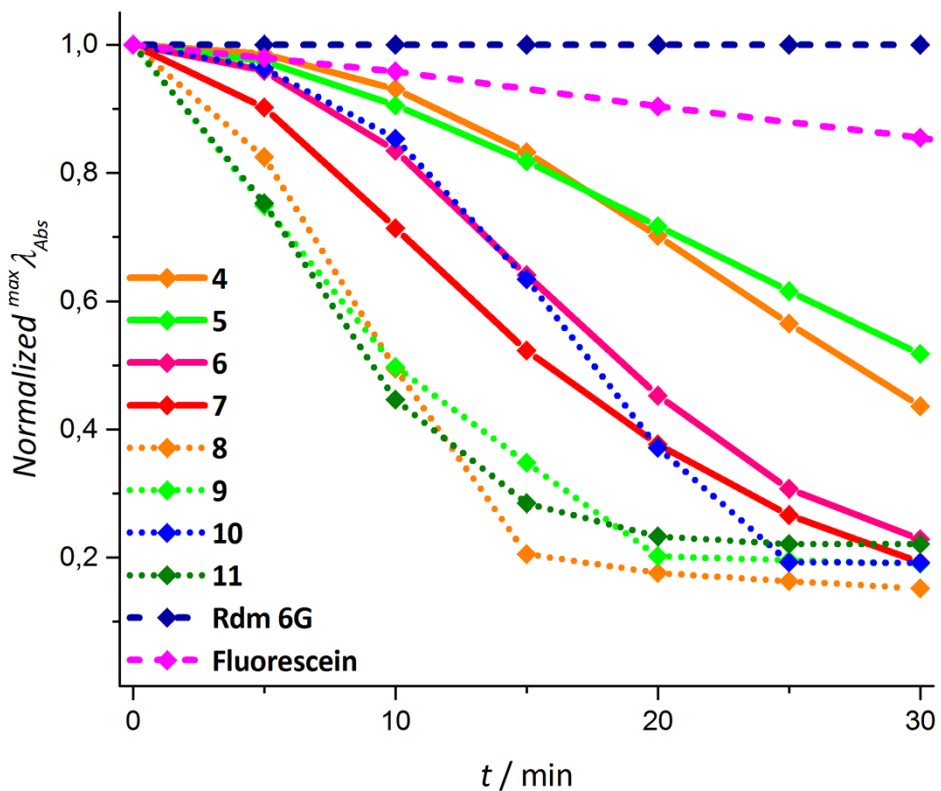


Figure S12. Photostability of rhodols **4-11** compared to the **Rhodamine 6G** in EtOH and **Fluorescein** in 0,1M NaOH aqueous solution measured in CH_2Cl_2 using a collimated light source from a 300W Xe lamp.

Theoretical methods

We have performed the DFT and TD-DFT calculations with the Gaussian 16 code⁶ on all dyes. For **4**, we performed a conformational search on the side esters groups and only the most stables ones were latter used. Default Gaussian16 thresholds and algorithms were used but for an improved optimization threshold (10^{-5} au on average residual forces), a stricter self-consistent field convergence criterion (10^{-10} a.u.) and the use of the *ultrafine* DFT integration grid.

Firstly, the S_0 geometries have been optimized with DFT and the vibrational frequencies have been analytically determined, using the M06-2X *meta*-GGA hybrid exchange-correlation functional.⁷ These calculations were performed with the 6-311G(d,p) atomic basis set and account for solvent effects through the linear-response PCM approach considering DCM as solvent.⁸ Secondly, starting from the optimal ground-state geometries, we have used TD-DFT with the same functional and basis set to optimize the S_1 geometry and compute the vibrational frequencies. All optimized structures correspond to true minima of the potential energy surface. Thirdly, the vertical transition energies were determined with TD-DFT and the same functional, but a larger basis set, namely 6-311+G(2d,p), in gas-phase as well as in solution using the cLR² variant of the PCM,⁹ in its *non-equilibrium* limit.

As the shortcomings of TD-DFT for cyanine derivatives¹⁰ are known, the obtained transition energies were also computed using COSMO-ADC(2)¹¹ with the Turbomole 7.3 code.¹² These ADC(2) energies were calculated in gas phase applying the resolution of identity scheme, and using the *aug-cc-pVDZ* atomic basis set.

The vibrationally resolved spectrum were determined with the FCClasses 3 program.^{13,14} We used a time-dependent formulation, applied the FC approximation (HT effects were neglected), and selected the so-called *Vertical Gradient*¹⁵ vibronic model for the band topologies on the basis of the TD-DFT data only. We used a simulation temperature of 298K. The obtained stick spectrum were convoluted with Gaussian having HWHM of 300 cm^{-1} . The radiative and internal conversion rates have been obtained using the TVCF formalism.¹⁶ These calculations were made within the time-dependent formulation, the same FC approach and the *Vertical Gradient* model.¹⁵ For the radiative part, we used the same broadening as for the band shapes, i.e., a 300 cm^{-1} Gaussian, but this is known to be not important for the radiative rate.¹⁷ For the IC part, we used a 10 cm^{-1} broadening Lorentzian, which is a typical value in the literature.^{17,18}

Additional theoretical data

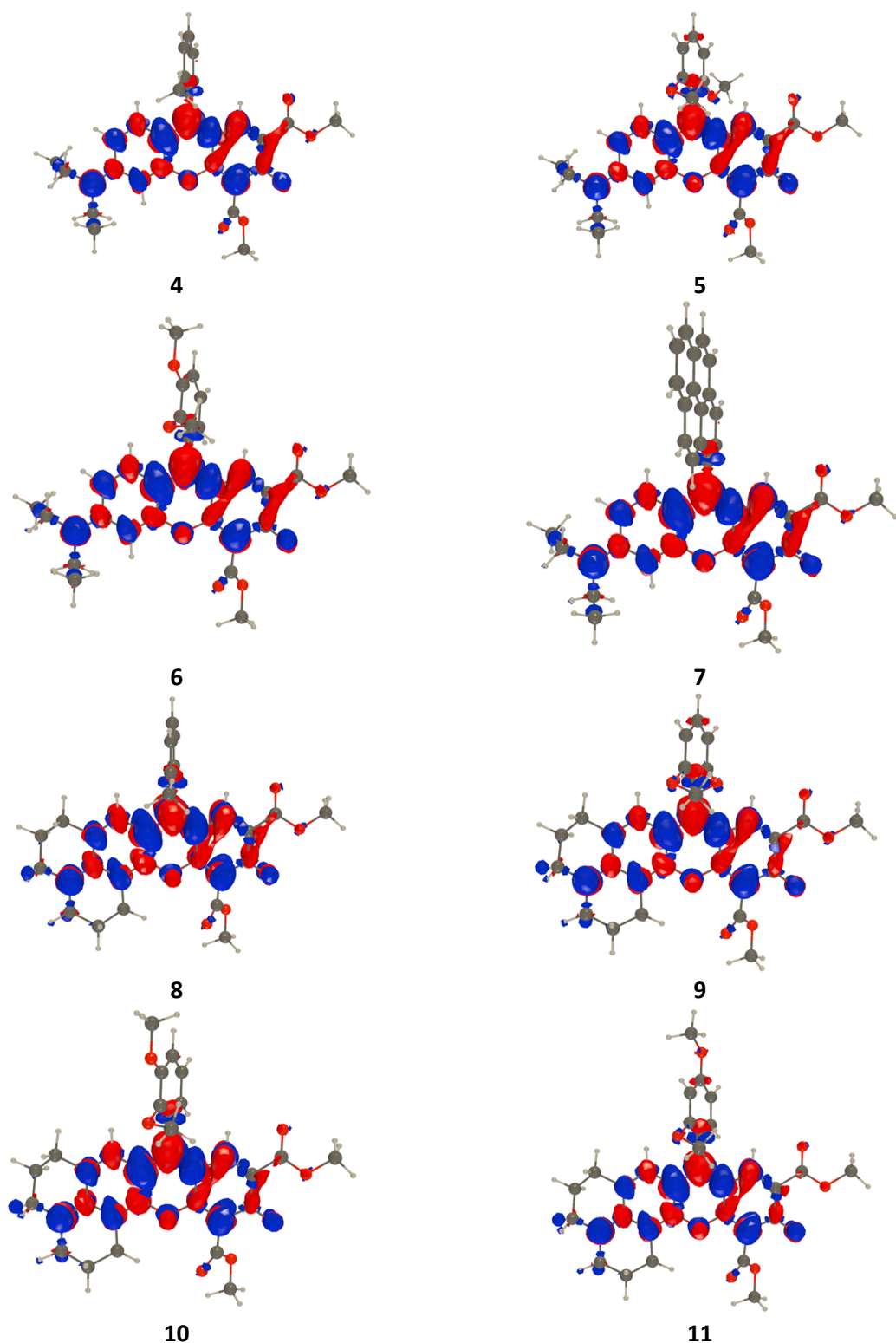


Figure S13. Electron density difference (EDD) plots for the lowest excited states of compounds **4-11**, as obtained with TD-DFT. The blue and red lobes correspond to regions of decrease and increase of electron density respectively. Contour threshold: 0.001 au.

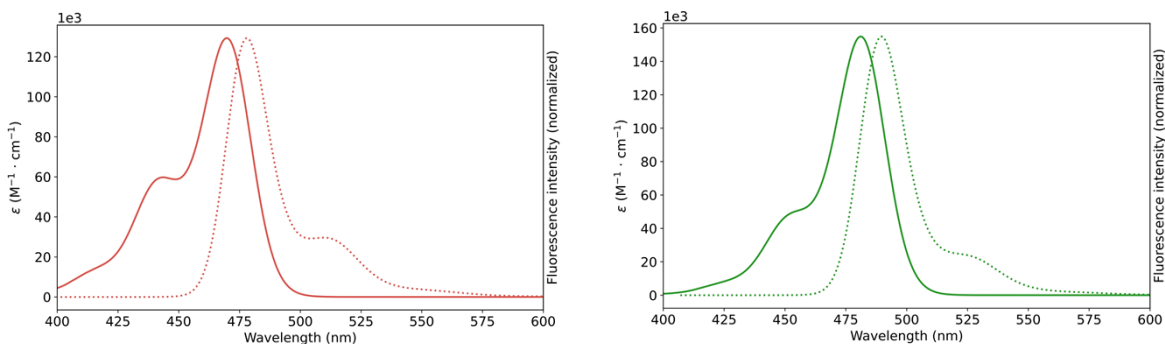


Figure S14. Computed vibrationally-resolved absorption and emission spectra for **4** (left) and **8** (right). The presence of the typical ‘‘cyanine shoulder’’ is clear in all cases.

Table S22. Computed vertical absorption, vertical emission, and 0-0 wavelengths with TD-DFT and ADC(2) for rhodols **4-11**. All values are given in nm. We recall here that vertical transition energies cannot be directly compared to experimental λ_{\max} , and that, in contrast, 0-0 values can be rigorously related to the experimental crossing point between the absorption and fluorescence curves. It can be noted that the experimental values are bracketed by the TD-DFT and ADC(2) estimates, but closer from the latter.

	cLR ² -PCM-TD-DFT			COSMO-ADC(2)		
	$\lambda_{\text{vert-abso}}$	$\lambda_{\text{vert-fluo}}$	λ_{0-0}	$\lambda_{\text{vert-abso}}$	$\lambda_{\text{vert-fluo}}$	λ_{0-0}
4	440	471	466	562	625	603
5	452	491	479	585	665	640
6	445	480	472	573	643	620
7	443	478	472	570	640	617
8	452	478	477	592	641	622
9	467	496	492	621	681	663
10	456	487	482	601	660	642
11	460	486	485	607	659	640

Table S23. Computed radiative and international conversion rates (10^8 s^{-1}) and deduced quantum yield of emission.

	k_r	k_{ic}	ϕ_f
8	3.44	1.48	0.70
9	2.97	1.65	0.64
10	3.23	1.56	0.67
11	3.22	1.54	0.68

Notes and references

- 1 L. Yuan, W. Lin, J. Song and Y. Yang, *Chem. Commun.*, 2011, **47**, 12691–12693.
- 2 G. Yin, T. Niu, T. Yu, Y. Gan, X. Sun, P. Yin, H. Chen, Y. Zhang, H. Li and S. Yao, *Angew. Chem. Int. Ed.*, 2019, **58**, 4557–4561.
- 3 M. Tasior, Y. M. Poronik, O. Vakuliuk, B. Sadowski, M. Karczewski and D. T. Gryko, *J. Org. Chem.*, 2014, **79**, 8723–8732.
- 4 L. J. Farrugia, *J. Appl. Crystallogr.*, 2012, **45**, 849–854.
- 5 Y. M. Poronik, G. Clermont, M. Blanchard-Desce and D. T. Gryko, *J. Org. Chem.*, 2013, **78**, 11721–11732.
- 6 M. J. Frisch, G. W. Trucks, H. B. Schlegel, G. E. Scuseria, M. A. Robb, J. R. Cheeseman, G. Scalmani, V. Barone, G. A. Petersson, H. Nakatsuji, X. Li, M. Caricato, A. V. Marenich, J. Bloino, B. G. Janesko, R. Gomperts, B. Mennucci, H. P. Hratchian, J. V. Ortiz, A. F. Izmaylov, J. L. Sonnenberg, D. Williams-Young, F. Ding, F. Lipparini, F. Egidi, J. Goings, B. Peng, A. Petrone, T. Henderson, D. Ranasinghe, V. G. Zakrzewski, J. Gao, N. Rega, G. Zheng, W. Liang, M. Hada, M. Ehara, K. Toyota, R. Fukuda, J. Hasegawa, M. Ishida, T. Nakajima, Y. Honda, O. Kitao, H. Nakai, T. Vreven, K. Throssell, J. A. Montgomery Jr., J. E. Peralta, F. Ogliaro, M. J. Bearpark, J. J. Heyd, E. N. Brothers, K. N. Kudin, V. N. Staroverov, T. A. Keith, R. Kobayashi, J. Normand, K. Raghavachari, A. P. Rendell, J. C. Burant, S. S. Iyengar, J. Tomasi, M. Cossi, J. M. Millam, M. Klene, C. Adamo, R. Cammi, J. W. Ochterski, R. L. Martin, K. Morokuma, O. Farkas, J. B. Foresman and D. J. Fox, *Gaussian 16 Revision A.03*, Gaussian, Inc., Wallingford CT, 2016.
- 7 Y. Zhao and D. G. Truhlar, *Theor. Chem. Acc.*, 2008, **120**, 215–241.
- 8 J. Tomasi, B. Mennucci and R. Cammi, *Chem. Rev.*, 2005, **105**, 2999–3093.
- 9 C. A. Guido, A. Chrayteh, G. Scalmani, B. Mennucci and D. Jacquemin, *J. Chem. Theory Comput.*, 2021, **17**, 5155–5164.
- 10 B. Le Guennic and D. Jacquemin, *Acc. Chem. Res.*, 2015, **48**, 530–537.
- 11 A. Dreuw and M. Wormit, *Wiley Interdiscip. Rev. Comput. Mol. Sci.*, 2015, **5**, 82–95.
- 12 *TURBOMOLE V7.3*, A development of University of Karlsruhe and Forschungszentrum Karlsruhe GmbH, 1989–2007, TURBOMOLE GmbH. <http://www.turbomole.com>, 2007.
- 13 J. Cerezo and F. Santoro, *FCClasses 3.0*, <http://www.pi.iccom.cnr.it/fcclasses>.
- 14 F. Santoro, R. Improta, A. Lami, J. Bloino and V. Barone, *J. Chem. Phys.*, 2007, **126**, 084509.
- 15 F. Santoro and D. Jacquemin, *Wiley Interdiscip. Rev. Comput. Mol. Sci.*, 2016, **6**, 460–486.
- 16 Q. Peng, Y. Yi, Z. Shuai and J. Shao, *J. Chem. Phys.*, 2007, **126**, 114302.
- 17 A. Humeniuk, M. Bužančić, J. Hoche, J. Cerezo, R. Mitrić, F. Santoro and V. Bonačić-Koutecký, *J. Chem. Phys.*, 2020, **152**, 054107.
- 18 Q. Ou, Q. Peng and Z. Shuai, *J. Phys. Chem. Lett.*, 2020, **11**, 7790–7797.